

**Complex Interactions Between Skeletal Muscle Ryanodine  
Receptor and Dihydropyridine Receptor Proteins**

**By**

**Peng Khun Leong**

**A thesis submitted in conformity with the requirements  
for the degree of Doctor of Philosophy,  
Graduate Department of Biochemistry,  
University of Toronto**

**©Copyright by Peng K. Leong, 1999**



**National Library  
of Canada**

**Acquisitions and  
Bibliographic Services**

**395 Wellington Street  
Ottawa ON K1A 0N4  
Canada**

**Bibliothèque nationale  
du Canada**

**Acquisitions et  
services bibliographiques**

**395, rue Wellington  
Ottawa ON K1A 0N4  
Canada**

*Your file Votre référence*

*Our file Notre référence*

**The author has granted a non-exclusive licence allowing the National Library of Canada to reproduce, loan, distribute or sell copies of this thesis in microform, paper or electronic formats.**

**The author retains ownership of the copyright in this thesis. Neither the thesis nor substantial extracts from it may be printed or otherwise reproduced without the author's permission.**

**L'auteur a accordé une licence non exclusive permettant à la Bibliothèque nationale du Canada de reproduire, prêter, distribuer ou vendre des copies de cette thèse sous la forme de microfiche/film, de reproduction sur papier ou sur format électronique.**

**L'auteur conserve la propriété du droit d'auteur qui protège cette thèse. Ni la thèse ni des extraits substantiels de celle-ci ne doivent être imprimés ou autrement reproduits sans son autorisation.**

**0-612-41206-7**

## **ABSTRACT**

**Complex Interactions Between Skeletal Muscle Ryanodine Receptor and Dihydropyridine Receptor Proteins.**

**Doctor of Philosophy, 1998**

**Peng Khun Leong**

**Department of Biochemistry**

**University of Toronto**

Excitation-contraction coupling refers to the linkage between depolarization of the sarcolemma and muscle contraction which is manifested through the interaction between the  $\text{Ca}^{2+}$  release channel (ryanodine receptor) of skeletal muscle sarcoplasmic reticulum and the L-type  $\text{Ca}^{2+}$  channel on the sarcolemma (dihydropyridine receptor). Attempts to express a functional recombinant  $\text{Ca}^{2+}$  release channel in HEK 293 cells and to characterize the single channel properties of the channel in a planar lipid bilayer provided the starting point for the studies presented in this thesis. The recombinant channel was demonstrated to have conductance, kinetics of opening, current-voltage relationship,  $\text{Ca}^{2+}$  permeability, and modulation by physiological ligands identical to those of the native rabbit skeletal muscle  $\text{Ca}^{2+}$  release channel. Understanding of the complex interactions between the  $\text{Ca}^{2+}$  release

channel and the L-type  $\text{Ca}^{2+}$  channel that result in excitation-contraction coupling required the identification of sites in the ryanodine receptor which interact with sites in the dihydropyridine receptor. To locate these sites of interaction, the amino acid sequences that form links between domains II and III (II-III loop) and domains III and IV (III-IV loop) of the dihydropyridine receptor were fused to glutathione S-transferase or poly His-peptide and used as protein affinity columns for binding of fragments of the ryanodine receptor synthesized by *in vitro* transcription and translation and labeled with [ $^{35}\text{S}$ ]-methionine. A 37 amino acid sequence in the ryanodine receptor, Arg<sup>1076</sup>. Asp<sup>1112</sup>, was shown to interact with the amino acids linking the dihydropyridine receptor II-III loop and to form part of a linear sequence that interacts with the dihydropyridine receptor III-IV loop. Thus, dihydropyridine receptor II-III and III-IV loops interact with a contiguous sequence on RyR1 which could participate in both opening and closing of the  $\text{Ca}^{2+}$  release channel.



## ACKNOWLEDGEMENTS

I would like to thank Dr. David H. MacLennan for providing an environment that was very conducive to learning. I am grateful for his eagerness to pass on to his students an understanding of the scientific method that has been successful in his endeavours. My tutelage under Dr. MacLennan has taught me a rational approach to science that will be appreciated by granting committees, peer reviewers of journal submissions, and students that I will encounter in my career.

I am grateful to my supervisory committee members, Dr. Charles Deber and Dr. Annelise Jorgensen for being supportive through all of the challenges which I faced, and further thanks to Dr. Annelise Jorgensen for many inspiring discussions.

The members of the laboratory have been indispensable for their willingness to help and their sense of humour. Dr. Wayne Chen, a former post-doctoral fellow played a key role in my early training. I am grateful to Vijay Khanna, Stella De Leon, Kaz Kurzydowski, Lin Zhang and Claire Bartlett for their expert technical assistance.

My fellow graduate students have been a source of technical and moral support. Dr. William Rice was present pipetting at the most opportune moments for asking questions and for therapeutic beverages. I thank Michael

Phillips for required and additional information. Kimby Barton has provided much needed comic relief Monday mornings, and most other times.

Finally, I am grateful to family and friends for blindly believing that there would be an end to my studies. I appreciate the opportunities that my parents ensured were available to me throughout my life, and hope that I take full advantage of that gift. I thank my best friend and housemate, Paul Wikkerink, for taking care of my sanity.

# **TABLE OF CONTENTS**

<b>ABSTRACT</b>	<b>ii</b>
<b>ACKNOWLEDGMENTS</b>	<b>iv</b>
<b>TABLE OF CONTENTS</b>	<b>vi</b>
<b>LIST OF FIGURES</b>	<b>ix</b>
<b>LIST OF ABBREVIATIONS</b>	<b>xi</b>
<b>CHAPTER 1: INTRODUCTION</b>	<b>1</b>
<b>Excitation-Contraction Coupling in Skeletal Muscle</b>	<b>2</b>
<b>Protein Components of Excitation-Contraction Coupling</b>	<b>6</b>
<b>Role of <math>\text{Ca}^{2+}</math>-induced <math>\text{Ca}^{2+}</math> Release and <math>\text{Ca}^{2+}</math>-inactivation of <math>\text{Ca}^{2+}</math>-Release in Skeletal Muscle Excitation-Contraction Coupling</b>	<b>39</b>
<b>Evidence that Protein-Protein Interactions Are Important for Activating <math>\text{Ca}^{2+}</math> Channel Opening and Closing</b>	<b>41</b>
<b>Spatial Relationships Between Dihydropyridine Receptors and Ryanodine Receptors Define the Mode of E-C Coupling</b>	<b>46</b>
<b>Identification of Regions of Skeletal Muscle RyR1 and DHPR Involved in Activation of Sarcoplasmic Reticulum <math>\text{Ca}^{2+}</math> Release</b>	<b>51</b>
<b>The Role of the DHPR III-IV Loop in Malignant Hyperthermia and in Channel Activation and Inactivation</b>	<b>56</b>
<b>Thesis Objectives</b>	<b>58</b>

<b>CHAPTER 2: A 37 AMINO ACID SEQUENCE IN THE SKELETAL MUSCLE RYANODINE RECEPTOR INTERACTS WITH THE CYTOPLASMIC LOOP BETWEEN DOMAINS II AND III IN THE SKELETAL MUSCLE DIHYDROPYRIDINE RECEPTOR</b>	<b>62</b>
Chapter Summary	63
Introduction	64
Methods	67
Results	73
Discussion	82
 <b>CHAPTER 3: THE CYTOPLASMIC LOOPS BETWEEN DOMAINS II AND III AND DOMAINS III AND IV IN THE SKELETAL MUSCLE DIHYDROPYRIDINE RECEPTOR BIND TO A CONTIGUOUS SITE IN THE SKELETAL MUSCLE RYANODINE RECEPTOR</b>	 <b>87</b>
Chapter Summary	88
Introduction	90
Methods	93
Results	100
Discussion	117

<b>CHAPTER 4: SINGLE CHANNEL PROPERTIES OF THE RECOMBINANT SKELETAL MUSCLE <math>Ca^{2+}</math> RELEASE CHANNEL (RYANODINE RECEPTOR)</b>	<b>125</b>
Chapter Summary	126
Introduction	127
Methods	130
Results	136
Discussion	158
 <b>CHAPTER 5: SUMMARY AND FUTURE DIRECTIONS</b>	 <b>163</b>
Summary	164
Future Directions	168
 <b>REFERENCES</b>	 <b>178</b>

## LIST OF FIGURES

Fig. 1.1	Activation of $\text{Ca}^{2+}$ release through the $\text{Ca}^{2+}$ Release Channel During Excitation-Contraction Coupling	3
Fig 1.2	Schematic of RyR1 illustrating functional domains and regulatory sites.	16
Fig 1.3	Schematic of the $\alpha 1$ -subunit of L-type $\text{Ca}^{2+}$ Channels illustrating functional domains and regulatory sites.	33
Fig. 2.1	Affinity of RyR1 fragments for the skeletal DHPR II-III loop.	74
Fig. 2.2	Affinity of chimeric RyR1/RyR2 constructs for the skeletal DHPR II-III loop.	76
Fig. 2.3	Affinity of chimeric RyR1/RyR2 constructs for skeletal and cardiac $\text{Ca}^{2+}$ and $\text{Na}^{+}$ channel II-III loop-GST fusion proteins.	79
Fig. 3.1	Binding of RyR1 fragments to the skeletal DHPR III-IV loop.	101
Fig. 3.2	Binding of chimeric RyR1/RyR2 constructs to the skeletal DHPR III-IV loop.	103
Fig. 3.3	Co-purification of RyR1 fragments with DHPR loops.	107
Fig. 3.4	Saturation co-purification of RyR1 (922-1112) by DHPR II-III loop GST fusion protein and of RyR1 (922-1112) by DHPR III-IV loop His-peptide fusion proteins.	109
Fig. 3.5	Competitive Inhibition of RyR1 (922-1112) binding to DHPR loops.	112
Fig 3.6	Binding of RyR1 (922-1112) constructs to skeletal and cardiac $\text{Ca}^{2+}$ and N-type $\text{Ca}^{2+}$ channel III-IV loop-GST fusion proteins.	114
Fig. 4.1	Immunocytochemical staining of control and transfected HEK-293 cells.	137
Fig, 4.2	Comparison of single channel properties of recombinant and native single $\text{Ca}^{2+}$ release channels.	141

Fig. 4.3	Ca <sup>2+</sup> permeability and Ca <sup>2+</sup> conductance of recombinant single Ca <sup>2+</sup> release channels.	145
Fig. 4.4	The response to cytoplasmic Ca <sup>2+</sup> of recombinant single Ca <sup>2+</sup> release channels.	147
Fig. 4.5	Ligand gating properties of recombinant single Ca <sup>2+</sup> release channels.	152
Fig. 4.6	Asymmetrical blockade of recombinant single Ca <sup>2+</sup> release channels.	155
Fig 5.1	Model of Interactions Between Ryanodine and Dihydropyridine Receptors During Excitation-Contraction Coupling	173

## LIST OF ABBREVIATIONS

Ala or A	Alanine
ADP	adenosine diphosphate
AMP	adenosine monophosphate
Arg or R	Arginine
Asn or N	Asparagine
Asp or D	Aspartate
ATP	adenosine triphosphate
BSA	Bovine serum albumin
C-terminus	Carboxyl-terminus
CCD	Central core disease
CHAPS	(3-[(3-Cholamidopropyl)dimethylammonio]-1-propanesulfonate)
Cys or C	Cysteine
DNA	Deoxyribonucleic acid
DHPR	Dihydropyridine receptor
DMEM	Dulbecco's modified Eagle's medium
DTT	dithiothreitol
E. coli	Escherichia coli
EDTA	Ethylene diamine tetraacetic acid
EGTA	Ethylene glycol bis(2-aminoethyl ether)-N, N, N', N'-tetraacetic acid
ELISA	Enzyme-linked immunosorbent assay
E-C	excitation-contraction
FKBP	FK506 binding protein
Gly or G	Glycine
Glu or E	Glutamate
GST	Glutathione-S-transferase
HEPES	(N-[2-Hydroxyethyl]piperazine-N'-[2-ethanesulfonic acid])



His or H	Histidine
Ile or I	Isoleucine
IP3	Inositol triphosphate
Leu or L	Leucine
LIS	Low ionic strength buffer
Lys or K	Lysine
MH	malignant hyperthermia
Met or M	methionine
Ni-NTA	nickel nitrilo-tri-acetic acid
N-terminal	amino-terminus
PAGE	polyacrylamide gel electrophoresis
PBS	phosphate buffered saline
PCR	polymerase chain reaction
Po	open probability
Pro or P	proline
rskM1	cDNA encoding the $\alpha$ -subunit of the skeletal muscle sodium channel
Rt-PCR	reverse transcriptase polymerase chain reaction
RyR1, RyR2, RyR3	ryanodine receptor or calcium release channel protein
RYR1, RYR2, RYR3	genes encoding RyR1, RyR2, and RyR3
SDS	sodium dodecyl sulfate
Ser or S	serine
SERCA	Sarco(Endo)plasmic Reticulum Calcium ATPase
TRIS	Tris(hydroxymethyl)aminomethane
T-tubule	Transverse tubule
Thr or T	Threonine
Val or V	Valine

## **CHAPTER 1**

### **Introduction**

# **1 Excitation-Contraction Coupling**

## **1.1 Physiology of Excitation-Contraction Coupling in Skeletal Muscle**

The events linking electrical stimulation of muscle and muscle contraction are referred to as excitation-contraction coupling. The entry of  $\text{Na}^+$  following stimulatory events at the neuromuscular junction initiates a wave of depolarization across the membranes of the sarcolemma and invaginations of the sarcolemma referred to as transverse tubules or T-tubules. Depolarization leads to a change in conformation of L-type  $\text{Ca}^{2+}$  channel proteins or dihydropyridine receptors (DHPR) (Schneider and Chandler, 1973) which are highly concentrated in the T-tubule (Curtis and Catterall, 1986; Jorgensen et al., 1989). A "mechanical coupling" mechanism involving protein-protein interactions between the  $\text{Ca}^{2+}$  release channel of the skeletal muscle sarcoplasmic reticulum or ryanodine receptor (RyR1) and the DHPR is proposed to lead to  $\text{Ca}^{2+}$  release from the sarcoplasmic reticulum (Meissner and Lu, 1995). It has been proposed that elevated intracellular  $\text{Ca}^{2+}$  can amplify further  $\text{Ca}^{2+}$  release by activating RyR1 channels which are not linked to the DHPR (Endo et al., 1970).  $\text{Ca}^{2+}$  released into the sarcoplasm binds to troponin C, resulting in a conformational change which alters the position of the troponin-tropomyosin complex in the thin filament to permit actin and myosin to interact, leading to muscle contraction (Zot and Potter, 1987). Upon repolarization, the DHPR interacts with RyR1 to terminate  $\text{Ca}^{2+}$

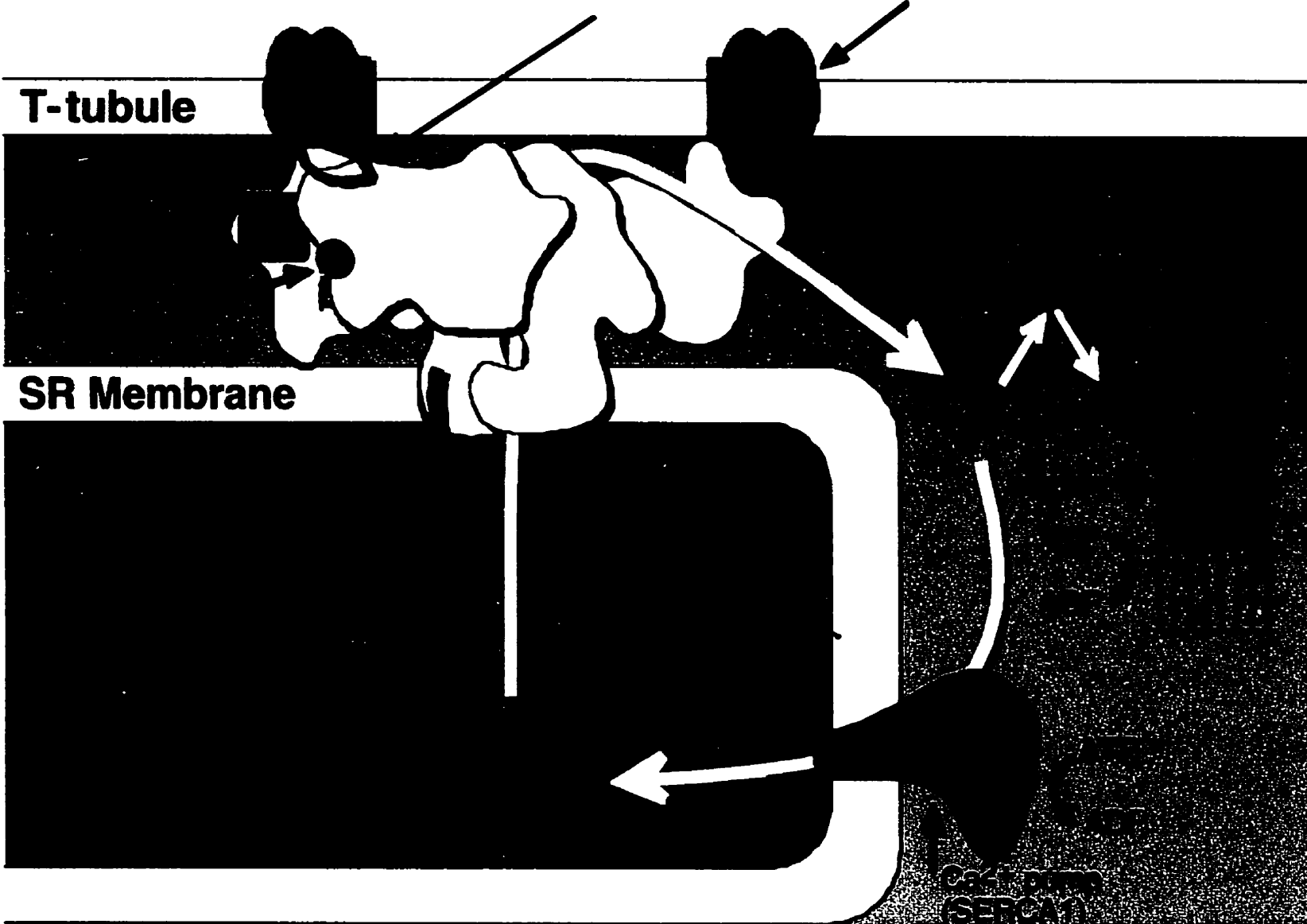
**Fig 1.1 Activation of  $\text{Ca}^{2+}$  release through the  $\text{Ca}^{2+}$  Release Channel During Excitation-Contraction Coupling.** The  $\text{Ca}^{2+}$  release channels of skeletal muscle sarcoplasmic reticulum and the L-type  $\text{Ca}^{2+}$  channels of the transverse tubule (the dihydropyridine receptor or DHPR) appear to be in physical contact (Block et al., 1988). In the relaxed muscle,  $\text{Ca}^{2+}$  release channels are closed. The entry of  $\text{Na}^{+}$  following stimulatory events at the neuromuscular junction initiates a wave of depolarization across the transverse tubular membrane. Depolarization is proposed to result in the change in conformation of the DHPR (Schneider and Chandler, 1973), and the DHPR II-III loop is proposed to activate the  $\text{Ca}^{2+}$  release channel to release  $\text{Ca}^{2+}$  (Tanabe et al., 1990a).  $\text{Ca}^{2+}$  released into the sarcoplasm binds to troponin C, resulting in a conformational change which alters the position of the troponin-tropomyosin complex in the thin filament to permit actin and myosin to interact, leading to muscle contraction (Zot and Potter, 1987). Upon repolarization,  $\text{Ca}^{2+}$  release is terminated (Suda, 1995) and the  $\text{Ca}^{2+}$  pump returns cytoplasmic  $\text{Ca}^{2+}$  to resting levels (Lytton and MacLennan, 1992).

DHPR loops activate opening and closing of the  $\text{Ca}^{2+}$  release channel

L-type  $\text{Ca}^{2+}$ ,  $\alpha 1$ ,  $\alpha 2/\delta$ ,  $\beta$ ,  $\gamma$  subunits (DHP Receptor)

T-tubule

SR Membrane



release through RyR1 (Suda, 1995). RyR1 has also been shown to enhance DHPR channel activity during E-C coupling (Nakai et al., 1996; Yamazawa et al., 1996).

Evidence is accumulating to support a direct interaction between the DHPR and RyR that is essential for the E-C coupling process. The evidence presented in this thesis for specific sites of interaction between sub-domains of DHPR with one or more sub-domains of RyR strongly supports the postulate that direct interaction occurs between these two proteins. Based upon the results presented in Chapters 2 and 3 of this thesis, I propose a more detailed model of the mechanism of excitation-contraction coupling which I describe in Chapter 5.

## **1.2 Functional Interactions Between $\text{Ca}^{2+}$ Channels and Ryanodine Receptor in Non-Muscle Cells**

Although the primary endoplasmic reticulum  $\text{Ca}^{2+}$  release channel in non-muscle cells is the homologous inositol-1,4,5-triphosphate ( $\text{IP}_3$ )- receptor, RyR2 and RyR3 are often present in non-muscle cells, where their physiological function is likely to be concerned with the regulation of cytosolic  $\text{Ca}^{2+}$  concentrations (Franzini-Armstrong and Protasi, 1997).  $\text{Ca}^{2+}$  is released from intracellular  $\text{Ca}^{2+}$  stores through RyR by  $\text{Ca}^{2+}$ -induced  $\text{Ca}^{2+}$  release and activation by ligands such as cyclic ADP ribose (Empson and Galione, 1997; Mothet et al., 1998).

In the cerebellum, RyR has been observed to enhance L-type  $\text{Ca}^{2+}$  channel activity (Chavis et al., 1996). In cerebellar granule cells, activation of the type-1 metabotropic glutamate receptor induced a large, oscillating increase of an L-type  $\text{Ba}^{2+}$  current or  $\text{Ca}^{2+}$  current that was blocked by ryanodine. Caffeine could also trigger large  $\text{Ba}^{2+}$  or  $\text{Ca}^{2+}$  current oscillations. Since ryanodine and caffeine act specifically on RyR, the blockage of L-type channel  $\text{Ca}^{2+}$  currents by ryanodine, and the activation of  $\text{Ca}^{2+}$  oscillations by caffeine suggests that functional coupling between RyR and L-type  $\text{Ca}^{2+}$  channels in the cerebellum leads to the enhancement of L-type  $\text{Ca}^{2+}$  channel function. Thus RyRs are involved in the regulation of activation of  $\text{Ca}^{2+}$  entry through L-type  $\text{Ca}^{2+}$  channels by type-1 metabotropic glutamate receptors. Since metabotropic glutamate receptors regulate transmitter release at mammalian central synapses (Nakanishi, 1994; Schoepp and Johnson, 1993), RyRs may be important in regulating neuronal electrical activity and synaptic plasticity.

## **2. Protein Components of Excitation-Contraction Coupling**

### **2.1 The Ryanodine Receptor or Calcium Release Channel**

Ryanodine receptors (RyR) are a family of intracellular  $\text{Ca}^{2+}$  release channels that play a critical role in regulation of intracellular  $\text{Ca}^{2+}$  levels (Coronado et al., 1994; Franzini-Armstrong and Protasi, 1997).  $\text{Ca}^{2+}$  signaling

is crucial to the regulation of cellular functions in a wide variety of cell types (Berridge, 1993). Three genes encoding RyR isoforms have been identified in mammalian tissues, *RYR1*, *RYR2*, and *RYR3*. All have been cloned and sequenced (Takeshima et al., 1989; Zorzato et al., 1990; Otsu et al., 1990; Nakai et al., 1990; Hakamata et al., 1992; Giannini et al., 1992). Functional RyRs exist as homotetramers of about 565 kDa subunits located in the junctional terminal cisternae of the sarcoplasmic reticulum membrane in striated muscle and in the endoplasmic reticulum membrane of non-muscle cells (Henkart et al., 1976; Block et al., 1988).

RyR1 is the major isoform expressed in mammalian skeletal muscle, and RyR2 is the major isoform in cardiac muscle. All three isoforms are expressed in the brain (Franzini-Armstrong and Protasi, 1997). In avian and amphibian skeletal muscles, RYR1 and RyR3 are expressed in approximately equal amounts (Bull and Marengo, 1993; Murayama and Ogawa, 1992; Percival et al., 1994). RyR1 and RyR2 are important for  $\text{Ca}^{2+}$  release during E-C coupling (Meissner and Lu, 1995; Franzini-Armstrong and Protasi, 1997), but the importance of RyR3 in mammalian tissue is not known, since mice with a targeted mutation in RYR3 do not exhibit any gross skeletal muscle abnormalities (Takeshima et al., 1996). All three RyRs are likely to play an important role in  $\text{Ca}^{2+}$  mobilization in the brain, since RyR1 is coupled to L-type  $\text{Ca}^{2+}$  channels in cerebellar granule cells, RyR2 is widely distributed in the brain, and RyR3 deficient mice have abnormal locomotor



activity, (Franzini-Armstrong and Protasi, 1997; Takeshima et al., 1996; Chavis et al., 1996). Since locomotor activity is controlled in the frontoparietal cortex, basal ganglia, and thalamus where RyR3 predominates (Furuichi et al., 1994; Giannini et al., 1995), abnormalities in  $\text{Ca}^{2+}$  signaling in these neurons caused by a lack of RyR3 activity may result in locomotor hyperactivity.

### **2.1.1 Modulation of Ryanodine Receptors**

The modulation of  $\text{Ca}^{2+}$  release channels by a variety of agents has been studied indirectly through measurements of tension development in skinned fibres or directly by measurements of  $\text{Ca}^{2+}$  efflux from heavy sarcoplasmic reticulum vesicles or of  $\text{Ca}^{2+}$  flux through single channels following their incorporation into planar lipid bilayers from sarcoplasmic reticulum vesicles or purified RyR channels. All three approaches have yielded corroboratory results (Endo et al., 1970; Kirino et al., 1983; Meissner et al., 1986; Moutin and Dupont, 1988; Smith et al., 1986a; Chen et al., 1997b).

All three RyR channels display a biphasic response to  $\text{Ca}^{2+}$ . They are activated by submicromolar  $\text{Ca}^{2+}$  and inactivated by millimolar  $\text{Ca}^{2+}$  (Coronado et al., 1994; Chen et al., 1997b). They are activated by caffeine and ATP, inhibited by  $\text{Mg}^{2+}$  and ruthenium red, and modified by ryanodine, but the three isoforms differ in their gating kinetics, sensitivity to activation and inactivation by  $\text{Ca}^{2+}$ , and inhibition by  $\text{Mg}^{2+}$ . Differences in responses to cyclic

ADP-ribose, inorganic phosphate and perchlorate have also been observed. These differences among RyR isoforms may account for their tissue-specific functions.

Most important is the difference in  $\text{Ca}^{2+}$  sensitivity. RyR2 has the highest  $\text{Ca}^{2+}$  sensitivity (Fabiato, 1982; Coronado et al., 1994; Takeshima et al., 1995), in line with the importance of  $\text{Ca}^{2+}$ -induced  $\text{Ca}^{2+}$  release from cardiac sarcoplasmic reticulum (Fabiato, 1982; Nabauer et al., 1989).  $\text{Ca}^{2+}$  sensitivity of RyR1 is less critical, since RyR1 has been proposed to be coupled mechanically to L-type  $\text{Ca}^{2+}$  channels and to be activated without elevation of cytosolic  $\text{Ca}^{2+}$  (Tanabe et al., 1988). RyR3 is the least sensitive to  $\text{Ca}^{2+}$  activation and inactivation, suggesting that its threshold for  $\text{Ca}^{2+}$  mediated  $\text{Ca}^{2+}$  release is high (Takeshima et al., 1995; Chen et al., 1997b).

ATP increases the rate of  $\text{Ca}^{2+}$  release without changing  $\text{Ca}^{2+}$  dependence of any of the isoforms (Meissner et al., 1986). ATP is not hydrolyzed since ADP, AMP and non-hydrolyzeable derivatives are also activators. In the presence of ATP, the channel is open at very low  $\text{Ca}^{2+}$  concentrations, indicating that channels are activated by  $\text{Ca}^{2+}$  or adenine nucleotides. ATP may be involved in the regulation of sarcoplasmic reticulum  $\text{Ca}^{2+}$  release, since a localized increase in concentration of ATP by glycolytic enzymes restricted to the space of the triadic gap may occur (Han et al., 1992).

$Mg^{2+}$  decreases the  $Ca^{2+}$  sensitivity of  $Ca^{2+}$ -induced  $Ca^{2+}$  release and reduces the maximal rate of  $Ca^{2+}$  release at the optimum concentration of  $Ca^{2+}$  (Meissner et al., 1986). In *in vitro* studies measuring  $Ca^{2+}$  efflux from sarcoplasmic reticulum vesicles or through single channels, the effect of  $Mg^{2+}$  may be to buffer the ATP as a  $Mg^{2+}$ -ATP complex, since the addition of excess ATP can reactivate the inhibited channels. Under physiological conditions, the concentrations of  $Mg^{2+}$  and ATP are likely to be constant so that activation of the channels is not likely to occur as a result of elevations in ATP levels (Lamb and Stephenson, 1992) and in the presence of 6 mM  $Mg^{2+}$ , physiologically relevant  $Ca^{2+}$  levels cannot trigger channel activation (Meissner et al., 1986; Lamb and Stephenson, 1992). Muscle depolarization can lead to stimulation of  $Ca^{2+}$  release channel opening by DHPR either by increasing the sensitivity of the channel to activation by  $Ca^{2+}$  or by lowering its sensitivity to inhibition by  $Mg^{2+}$ . Lamb and Stephenson (Lamb and Stephenson, 1992) propose that the interaction between the voltage sensor and the  $Ca^{2+}$  release channel lowers the sensitivity of the channel to inhibition by  $Mg^{2+}$  to permit activation of RyR channel opening.  $Mg^{2+}$  inhibition of ryanodine receptor  $Ca^{2+}$  channels occurs at nanomolar  $Ca^{2+}$  concentration by competing with  $Ca^{2+}$  for the  $Ca^{2+}$  activation site, and at micromolar  $Ca^{2+}$  concentrations by binding to low affinity inhibition sites which do not discriminate between  $Ca^{2+}$  and  $Mg^{2+}$  (Laver et al., 1997).

At relatively low concentrations (2 mM), caffeine increases the  $\text{Ca}^{2+}$  sensitivity of  $\text{Ca}^{2+}$ -induced  $\text{Ca}^{2+}$  release, and increases the maximum rate of release at the optimum  $\text{Ca}^{2+}$  concentration (Meissner et al., 1986; Rousseau et al., 1988). Ryanodine at low concentrations ( $<10\ \mu\text{M}$ ) locks the channels in a partially open subconductance state (Rousseau et al., 1987; Smith et al., 1988). At high concentrations of ryanodine (10-300  $\mu\text{M}$ ), the channel is totally blocked.

Calmodulin at millimolar levels inhibits  $\text{Ca}^{2+}$  release from microsomal vesicles and decreases RyR1 channel opening in a  $\text{Ca}^{2+}$  dependent manner. It reduces single-channel open time without affecting single channel conductance (Meissner, 1986; Meissner and Henderson, 1987; Smith et al., 1989). At resting  $\text{Ca}^{2+}$  concentrations, calmodulin increases the open probability of RyR and  $\text{Ca}^{2+}$  release by several fold, whereas at activating  $\text{Ca}^{2+}$  concentrations, it has the opposite effect (Buratti et al., 1995; Tripathy et al., 1995; Ikemoto et al., 1995). These results suggest that calmodulin plays a role in modulating channel activity during contraction. Calmodulin inhibits RyRs in the absence of ATP, ruling out activation through calmodulin kinase activity and suggesting that calmodulin interacts directly with RyRs.

Ser<sup>2843</sup> in RyR1 is phosphorylated by  $\text{Ca}^{2+}$ /Calmodulin-dependent protein kinase (Suko et al., 1993), but other studies show that RyR is not phosphorylated in skeletal muscle (Strand et al., 1993; Damiani et al., 1997).

Strand *et al.* (Strand et al., 1993), however, raise the possibility that a sarcoplasmic reticulum protein which co-migrates with a degradation product of RyR on SDS-PAGE may be phosphorylated, and, through phosphorylation, might affect RyR. Various studies report conflicting effects of phosphorylation on RyR1 channel activity and remain to be fully elucidated (Coronado et al., 1994; Franzini-Armstrong and Protasi, 1997). Evidence has been presented in other studies to show that both RyR1 and RyR2 require phosphorylation to be active under physiological  $Mg^{2+}$  concentrations (Hain et al., 1995; Mayrleitner et al., 1995) and to show that RyR1 must be phosphorylated in order to be activated by ATP (Sonnleitner et al., 1997). However, phosphorylation has also been reported to inactivate RyR1 (Wang and Best, 1992). The opposing reports may have to do with the site of phosphorylation and ionic conditions of the experiments. It is not known whether phosphorylation plays a modulatory role during E-C coupling. Phosphorylation of Ser<sup>2809</sup> in RyR2 by a  $Ca^{2+}$ /calmodulin-dependent kinase has been reported to reverse the inhibitory effect of calmodulin (Witcher et al., 1991). Clearly, the role of phosphorylation in the regulation of RyR1 remains to be clarified.

Cyclic ADP ribose increases the open probability of cardiac ryanodine receptors in microsomal vesicles and of RyR2 incorporated into planar bilayers (Meszaros et al., 1993), but not in microsomal vesicles from skeletal muscles or in RyR1 incorporated into planar lipid bilayers (Meszaros et al.,

1993; Morrissette et al., 1993; Fruen et al., 1994). Other studies suggest that RyR2 may not be affected by cyclic ADP ribose (Fruen et al., 1994). In some studies (Chen et al., 1997b; Sonnleitner et al., 1998) cyclic ADP ribose did not affect RyR3 but in others an effect was observed. It is possible that activation by cyclic ADP-ribose depends on the presence of calmodulin and/or phosphorylation by  $\text{Ca}^{2+}$ /calmodulin dependent kinase, as is the case for RyRs in sea urchins eggs and rat pancreatic islets (Lee et al., 1994; Tanaka and Tashjian, 1995; Takasawa et al., 1995). In skeletal muscle E-C coupling, cyclic ADP ribose potentiates  $\text{Ca}^{2+}$  release from the sarcoplasmic reticulum induced by transverse tubule membrane depolarization, and thus, may play a role as a modulator of sarcoplasmic reticulum  $\text{Ca}^{2+}$  release (Yamaguchi and Kasai, 1997).

A number of agents that modify sulfhydryl groups also modify RyR channel activity, including heavy metals (Salama and Abramson, 1984; Abramson et al., 1983),  $\text{Cu}^{2+}$ /mercaptans (Trimm et al., 1986), reactive disulphides (Zaidi et al., 1989), phthalocyanine dyes (Abramson et al., 1988b), anthraquinones (Abramson et al., 1988a), porphyrins (Abramson et al., 1993), thimerosal (Abramson et al., 1995), nitric oxide (Xu et al., 1998), and the reactive oxygen species hydrogen peroxide (Favero et al., 1995a; Favero et al., 1995b; Oba et al., 1998). In general, agents which reduce RyR sulfhydryl groups inhibit channel opening and agents which oxidize RyR sulfhydryl groups activate channel opening without changing the  $\text{Ca}^{2+}$  dependence of

channel activation. Reduction of sulfhydryl groups by glutathione , which is abundant in eukaryotic cells, may serve to down-regulate the gating of the sarcoplasmic reticulum  $\text{Ca}^{2+}$  channel (Zable et al., 1997). Oxidative stress, induced by oxygen-derived free radicals, can directly oxidize RyR thiols (Favero et al., 1995a; Favero et al., 1995b) or oxidize reduced glutathione to glutathione disulfide. Disruptions in the redox balance of glutathione may have implications for the regulation of E-C coupling and contractile function.

FK506 binding proteins (FKBP) are cis-trans peptidyl-prolyl isomerases that bind the immunosuppressant drug FK506 (Standaert et al., 1990). FKBP co-purify with RyR with a stoichiometry of one FKBP12 per RyR monomer (Timmerman et al., 1993). FKBP12-depleted skeletal muscle sarcoplasmic reticulum terminal cisternae vesicles have a decreased threshold for caffeine-induced  $\text{Ca}^{2+}$  release, and a slower rate of  $\text{Ca}^{2+}$  uptake (Timmerman et al., 1993). Single channel studies of RyR1 show an increased open probability and extended opening events at subconductance levels, resulting in increased mean ensemble current and increased sensitivity to caffeine (Ahern et al., 1994; Brillantes et al., 1994). Reconstitution of FKBP12 in vesicles previously depleted of this protein or studies of the channel properties of RyR1 expressed in insect Sf9 cells in the presence of FKBP12, restores stable RyR1 conductance and decreases channel opening (Timmerman et al., 1993; Brillantes et al., 1994). FKBP also blocks cytoplasmic

to lumen currents, favouring the reverse current (Chen et al., 1994; Ma et al., 1995).

Lipid and polycationic metabolites have also been found to modulate RyR activity (el-Hayek et al., 1993; Sabbadini et al., 1992; Palade, 1987; Zarka and Shoshan-Barmatz, 1992). Their role in E-C coupling is not known, however, since the level of these metabolites reflects the metabolic state of the muscle these compounds may be important for regulating  $\text{Ca}^{2+}$  release activity in low or high metabolic states of muscle that require concurrent modulation of  $\text{Ca}^{2+}$  release.

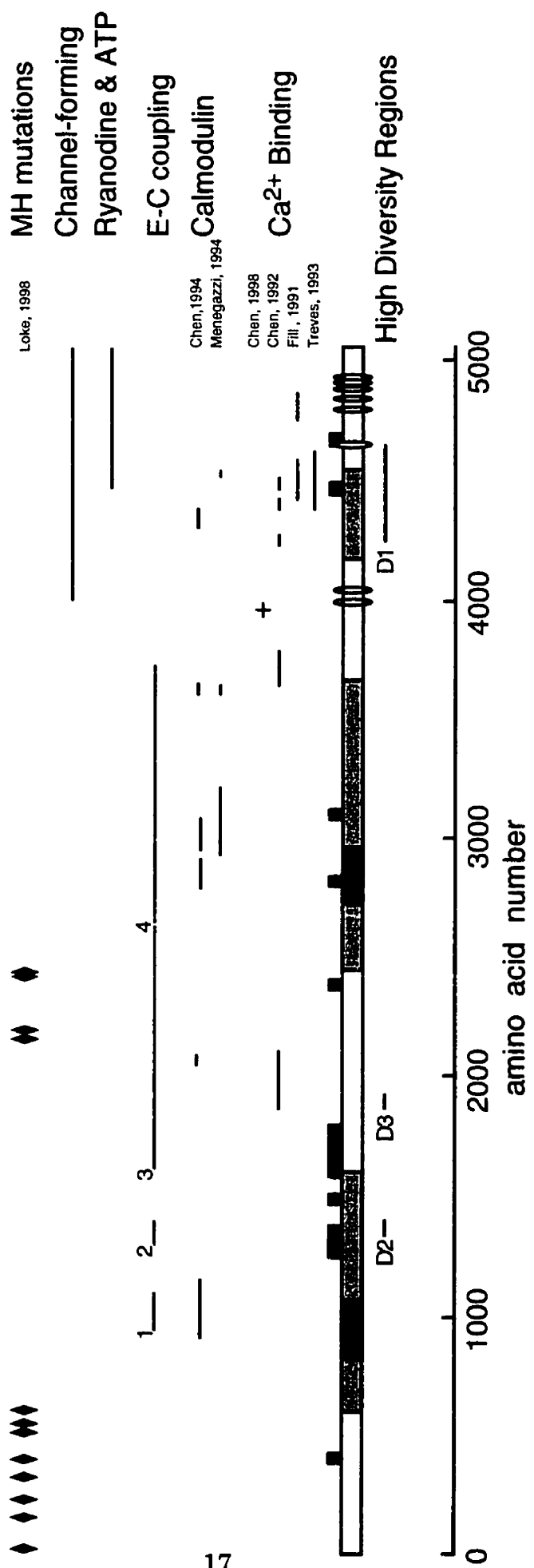
### **2.1.2 Functional Domains of Ryanodine Receptors**

Functional domains in proteins can be predicted by analysis of proteolytic fragmentation and by comparison with known structures of homologous proteins. Although proteins have numerous potential cleavage sites, many of these are exposed on the surface of proteins. Thus cleavage sites which are not buried within the hydrophobic core of structural domains are often located between domains. These accessible fragments which link domains can often interact with ligands and other proteins.

One approach for identifying proteolytic fragments is to sequence the fragments and align the sequence with the RyR1 protein sequence to deduce the cleavage site. N-terminal sequencing of RyR1 endoproteinase Lys-C and Glu-C fragments (Marks et al., 1990), RyR1 tryptic fragments (Callaway et al., 1994), and of RyR1 calpain fragments (Wu et al., 1997) were used to map



**Figure 1.2: Schematic of RyR1 illustrating functional domains and regulatory sites.** The bottom line indicates amino acid sequence numbers. Regions of high sequence diversity are indicated by lines below the bar labeled D2, D3 and D1 (Sorrentino and Volpe, 1993). The thick bar represents the full-length RyR1 sequence. Predicted transmembrane sequences are indicated by ovals (Takeshima et al., 1989; Zorzato et al., 1990); black areas represent repeat sequences (Zorzato et al., 1990); white areas represent regions of homology with IP<sub>3</sub>; grey areas represent RyR1 sequences not present in IP<sub>3</sub> (Furuichi et al., 1989); black rectangles projecting above the bar represent areas of high protease sensitivity (Chen et al., 1993a; Callaway et al., 1994) (Marks et al., 1990; Wu et al., 1997). Ca<sup>2+</sup> binding sites are indicated by three layers of short lines representing different findings (Chen et al., 1992; Fill et al., 1991; Treves et al., 1993). The E3885A mutation in RyR3 which decreases Ca<sup>2+</sup> sensitivity is indicated by (+) (Chen et al., 1998). Calmodulin binding sites are indicated by two more layers of short lines representing different findings (Chen and MacLennan, 1994; Menegazzi et al., 1994). Three layers of long lines represent large regions of RyR1 implicated in E-C coupling, 1 (Leong and MacLennan, 1998b; Leong and MacLennan, 1998a), 2 (Yamazawa et al., 1997), 3 and 4 (Nakai et al., 1998), ryanodine and ATP binding (Callaway et al., 1994; Zarka and Shoshan-Barmatz, 1992) and channel formation (Bhat et al., 1997a). Mutations linked to malignant hyperthermia are clustered in two regions and are represented as diamonds (Loke and MacLennan, 1998).



six tryptic sites to residues 426, 1508, 2401, 2840, 3119, and 4475, and an additional endoproteinases Lys-C and Glu-C and calpain sensitive site to between 4676 and 4683 (Fig. 1.2). An alternate approach is to develop a series of antibodies against different regions of RyR1 and to use these antibodies to identify by Western Blotting a series of tryptic fragments to deduce the positions in the linear sequence where proteolysis occurred (Chen et al., 1993a). The tryptic sites estimated from mobility of tryptic fragments on SDS-PAGE correspond to the protease sensitive regions identified by N-terminal sequencing of endoproteinases Lys-C and Glu-C RyR1 fragments (Marks et al., 1990) and were confirmed by N-terminal sequencing of tryptic fragments (Callaway et al., 1994), with the exception of the cleavage site at 1508 which Chen et al. (Chen et al., 1993a) report as being two cleavage sites (one between 1273 and 1363 and another between 1609 and 1790 (Fig. 1.2)).

A complementary method for predicting the boundaries of structural domains is to compare the sequences of two related proteins which have diverged to serve different functional roles. Ryanodine and IP<sub>3</sub> receptors can be compared in this way, since both proteins form intracellular Ca<sup>2+</sup> release channels, but are expressed on separate genes and are regulated by different ligands. An alignment of ryanodine and IP<sub>3</sub> receptor sequences reveals large insertions in the RyR sequence (Furuichi et al., 1989). These insertions are likely to represent functional domains unique to RyRs so that the boundaries between domains unique to RyRs and domains held in common with IP<sub>3</sub>

receptors may represent the boundaries of structural and functional domains in these receptors. The first domain unique to RyR lies between amino acids 628 and 1589, the second lies between 2258 and 3663, and the third lies between 4198 and 4535 (Fig. 1.2). These six domain boundaries predicted by sequence alignment correspond roughly to protease-sensitive sites. Evidence that these boundaries do represent functional domains comes from studies of the localization of mutations associated with malignant hyperthermia which are clustered between Cys<sup>35</sup> and Arg<sup>415</sup> and between Arg<sup>2162</sup> and Arg<sup>2458</sup>. These sequences have been proposed to represent regulatory domains common to both ryanodine and IP<sub>3</sub> receptors (Loke and MacLennan, 1998).

Potential binding sites for ligands such as calmodulin, Ca<sup>2+</sup>, and ATP, that modulate the RyR channel have been postulated on the basis of primary structure (Takeshima et al., 1989; Zorzato et al., 1990; Otsu et al., 1990; Nakai et al., 1990; Hakamata et al., 1992; Tunwell et al., 1996). Experimental data have confirmed some of the predicted binding sites and identified new ones.

Three Ca<sup>2+</sup> binding regions 4226-4267, 4382-4417, and 4478-4512 (Chen et al., 1992) were identified in studies in which RyR1 fusion proteins immobilized on nitrocellulose membranes were overlaid with <sup>45</sup>Ca (Fig. 1.2). These regions included sequences predicted on the basis of sequence analysis to be Ca<sup>2+</sup> binding sites (Takeshima et al., 1989). Antibodies against these regions immunoprecipitated native RyR1 suggesting that at least parts of

these sequences are surface exposed. When antibodies raised against amino acids 4478 to 4512 were added to solutions bathing RyR1 in planar lipid bilayers, single channels were activated suggesting that this region forms part of the  $\text{Ca}^{2+}$ -induced activation domain. The addition of other antibodies raised against amino acids 4380 to 4625, however, decreased  $\text{Ca}^{2+}$ -induced  $\text{Ca}^{2+}$  release from passively loaded terminal cisternae vesicles (Treves et al., 1993) and other antibodies against amino acids 4445 to 4586 or 4760 to 4877 decreased RyR1 channel open probability (Fill et al., 1991). These apparently contradictory results could be reconciled by further studies by Chen *et al.* (Chen et al., 1992) in which antibodies which were affinity-purified using the peptide PEPEPEPEPE, within the RyR1 4478 to 4512 sequence, were found to inhibit  $\text{Ca}^{2+}$  activated channel activities (Chen et al., 1993c). Thus, the RyR1 sequence between amino acids 4478 and 4512 is important for  $\text{Ca}^{2+}$  regulation of RyR1 and antibodies against different epitopes in this region can either increase  $\text{Ca}^{2+}$  sensitivity or decrease inhibiting  $\text{Ca}^{2+}$  sensitivity. The characterization of a recombinant RyR3 channel with a E3885A mutation reveals that a Glu<sup>3885</sup> conserved in RyR1, RyR2, and RyR3, is important for  $\text{Ca}^{2+}$  activation since mutation of this residue decreases the sensitivity of the channel to  $\text{Ca}^{2+}$  activation without altering gating by other ligands (Chen et al., 1998). Additional  $\text{Ca}^{2+}$  binding regions between amino acids 1861 and 2094 and 3657 and 3776 were identified in <sup>45</sup>Ca overlay of RyR1 fusion

proteins immobilized on nitrocellulose but the functional importance of these sites has not been characterized (Chen and MacLennan, 1994).

RyR1 fusion proteins immobilized on nitrocellulose membranes, and overlaid with [ $^{125}$ I]-calmodulin, identified six  $\text{Ca}^{2+}$ -dependent calmodulin binding regions 921 to 1173, 2063 to 2091, 2804 to 2930, 2961 to 3084, 3611 to 3642, and 4303 to 4382 (Chen and MacLennan, 1994) (Fig. 1.2). Similar calmodulin overlay studies identified a  $\text{Ca}^{2+}$ -independent calmodulin binding site between amino acids 2936 and 3225, and another  $\text{Ca}^{2+}$ -dependent binding sites between amino acids 4534 and 4552, and a third between amino acids 3610 and 3629 (Menegazzi et al., 1994). Measurement of fluorescence emission of dansyl-calmodulin upon incubation with synthetic peptides corresponding to RyR1 sequences showed that the calmodulin binding sites identified by Menegazzi et al. (Menegazzi et al., 1994) are conserved in brain and cardiac isoforms (Guerrini et al., 1995). The identification of multiple calmodulin binding sites supports data from studies of [ $^{125}$ I]-calmodulin binding to sarcoplasmic reticulum vesicles or to purified RyR1 which showed that 16 calmodulins bind with high affinity to one tetramer at low  $\text{Ca}^{2+}$  concentrations ( $<0.1 \mu\text{M}$ ), whereas 4 calmodulins bind at higher  $\text{Ca}^{2+}$  concentrations (Tripathy et al., 1995). The identification of separate calmodulin binding sites for  $\text{Ca}^{2+}$ -dependent and  $\text{Ca}^{2+}$ -independent binding support functional studies which show that calmodulin activates RyR1 at low

$\text{Ca}^{2+}$  and inhibits RyR1 at high  $\text{Ca}^{2+}$  (Meissner, 1986; Meissner and Henderson, 1987; Smith et al., 1989; Buratti et al., 1995; Tripathy et al., 1995; Ikemoto et al., 1995).

In different studies, labeling of RyR1 with photoaffinity analogs of ATP have localized ATP binding sites to 27 kDa and 13 kDa fragments within a 76 kDa C-terminal tryptic fragment (Zarka and Shoshan-Barmatz, 1993), to an 160 kDa N-terminal calpain fragment and a fragment between 230-370 kDa from the N-terminal (Brandt et al., 1992) (Fig. 1.1). The binding site on RyR1 for [ $^3\text{H}$ ]-ryanodine and a photoaffinity analog of ryanodine has been localized to the C-terminal 76 kDa tryptic fragment (Witcher et al., 1994; Callaway et al., 1994).

The transmembrane sequences of the ryanodine receptor are predicted to form the  $\text{Ca}^{2+}$  release channel. Two groups have used hydropathy plots derived from deduced amino acid sequences to predict potential transmembrane sequences. Four transmembrane sequences in the C-terminal end of the ryanodine receptor are strongly hydrophobic with hydropathy indices between 2.0 and 2.9 and are clearly transmembrane (Takeshima et al., 1989). However, 8 have hydropathy indices between 0.8 and 1.6 and could also form transmembrane helices with more polar features (Zorzato et al., 1990). These observations led to the proposal that as many as 12 transmembrane helices organized as hairpins might exist in the protein: M'/M''; M1/M2; M3/M4, M5/M6, M7/M8 and M9/M10. Subsequent cloning has

demonstrated that proposed transmembrane sequences M1/M2, M5/M6, M7/M8, and M9/M10 are highly conserved. Thus the M3/M4 hairpin is unlikely to be transmembrane, but 8 transmembrane helices are probable (Fig 1.2).

Site directed antibodies against proposed luminal sequences have showed that the N- and C-termini are cytoplasmically localized (Marty et al., 1994b). Two segments in the C-terminal region, amino acids 4581 to 4640, and 4860 to 4886 are likely to be luminal (Grunwald and Meissner, 1995). A truncated form of the ryanodine receptor from amino acid 4006 to 5035 at the C-terminus, has been expressed and shown to form a channel that is activated by  $\text{Ca}^{2+}$  (Bhat et al., 1997b). From these studies, it can be concluded that the C-terminal fifth of RyR constitutes a regulated  $\text{Ca}^{2+}$  conducting pore while the cytoplasmic domain of RyR1 is a regulated domain which appears to contact components of the T-tubule (Block et al., 1988) and senses the depolarization of the sarcolemma through its physical interaction with the dihydropyridine (DHP) receptor in the T-tubule (Marty et al., 1994a; Murray and Ohlendieck, 1997; Leong and MacLennan, 1998b), and thereby, regulates channel opening and closing.

### **2.1.3 Diseases Associated with Ryanodine Receptors**

#### **2.1.3.1 Malignant Hyperthermia**

Malignant hyperthermia (MH) is a genetic abnormality which arises from a malfunction in the regulation of sarcoplasmic  $\text{Ca}^{2+}$ -ion fluxes. In



genetically susceptible individuals, the administration of potent inhalational anesthetics and depolarizing skeletal muscle relaxants leads to high fever and skeletal muscle rigidity (Britt and Kalow, 1970). A defect in a  $\text{Ca}^{2+}$  regulatory protein in the excitation-contraction coupling pathway within skeletal muscle could account for all of the signs of MH. Chronic elevation of intracellular  $\text{Ca}^{2+}$  could result in muscle contracture. Since  $\text{Ca}^{2+}$  plays a regulatory role in glycogenolysis through its activation of phosphorylase kinase (Brostrom et al., 1971), excess  $\text{Ca}^{2+}$  would activate the first steps in the pathway leading to enhanced glycolysis. Muscle contracture and the transport of excessive amounts of cytoplasmic  $\text{Ca}^{2+}$  to the lumen of the sarcoplasmic reticulum would consume ATP. The adenosine diphosphate (ADP) formed would stimulate glycolysis, the subsequent mitochondrial oxidation of pyruvate derived from glucose and the production of excess lactic acids, which is expelled into the blood. Mitochondrial oxidation would also be stimulated by mitochondrial uptake of  $\text{Ca}^{2+}$  following elevation of cytosolic  $\text{Ca}^{2+}$  concentrations. These hypermetabolic responses would lead to depletion of ATP, glycogen, and oxygen, to the production of excess lactic acid and  $\text{CO}_2$  and, ultimately, to the disruption of intracellular and extracellular ion balances, with consequent muscle damage. These reactions, leading to high turnover of ATP would be responsible for the elevated temperatures associated with MH episodes.

The RYR1 gene on human chromosome 19q13.1 (MacKenzie et al., 1990) encoding the skeletal muscle  $\text{Ca}^{2+}$  release channel has been linked to malignant hyperthermia (MH) in humans (MacLennan et al., 1990; McCarthy et al., 1990) and pigs (Fujii et al., 1991; Otsu et al., 1991). Continued analysis of the RYR1 sequence in probands from MH families has now associated MH with at least 17 mutations (Fig. 1.2), accounting for the abnormality in roughly 40% of MH families (Loke and MacLennan, 1998). A mutation in the CACNL1A3 gene encoding the L-type voltage-dependent  $\text{Ca}^{2+}$  channel has also been linked to MH in a single family (Monnier et al., 1997). This mutation is located in the loop between domains III and IV of the  $\text{Ca}^{2+}$  channel suggesting that there is a direct functional interaction between the III-IV loop of the  $\alpha 1$ -subunit of the DHPR and the RyR which can lead to susceptibility to MH, probably through defective regulation of the  $\text{Ca}^{2+}$  release channel. The DHPR mutation does not lead to any other symptoms of ion channel disease, suggesting that it does not affect L-type  $\text{Ca}^{2+}$  channel function.

A series of RyR1 activators; including, caffeine, halothane, 4-chloro-m-cresol, and ryanodine have been used to compare the sensitivity of  $\text{Ca}^{2+}$  release from normal muscle and from muscle from individuals suspected of being susceptible to malignant hyperthermia. Mutations in RyR1 which lead to MH susceptibility have been shown to lead to an increase in the sensitivity

of the channel to activation by caffeine and halothane (Kalow et al., 1970; Ellis et al., 1972; Mickelson and Louis, 1996; Otsu et al., 1994; Treves et al., 1994; Tong et al., 1997). Dantrolene is an antidote to an MH crisis (Harrison, 1975) through its apparent ability to close  $\text{Ca}^{2+}$  release channels. Dantrolene is a direct-acting muscle relaxant that inhibits intracellular  $\text{Ca}^{2+}$  release from SR vesicles at elevated temperatures (Ellis et al., 1973; Desmedt and Hainaut, 1977; Ohta et al., 1990). Dantrolene has been shown to act directly and specifically on single  $\text{Ca}^{2+}$  release channels (Nelson et al., 1996; Fruen et al., 1997).

#### **2.1.3.2 Central Core Disease**

Central Core Disease (CCD) is an autosomal dominant, non-progressive myopathy involving predominantly proximal muscles and presenting in infancy (Dubowitz and Platts, 1965; Patterson et al., 1979). CCD is linked to RYR1 and is closely associated with susceptibility to malignant hyperthermia (Zhang et al., 1993; Quane et al., 1993; Quane et al., 1994).

CCD is diagnosed based on the lack of oxidative enzyme activity in central regions of skeletal muscle cells (Loke and MacLennan, 1998). This defect arises from the abnormal regulation of  $\text{Ca}^{2+}$  release into the muscle cell, and the failure of pumps and exchangers in the plasma membrane and organellar systems of mitochondria and sarcoplasmic reticulum to remove excess  $\text{Ca}^{2+}$  from the sarcoplasm, thereby causing  $\text{Ca}^{2+}$ -induced damage in the

cell. Plasma membrane  $\text{Ca}^{2+}$  pumps, and  $\text{Na}^+/\text{Ca}^{2+}$  exchangers might be more effective in protecting the periphery of the cell than the interior of the cell where the full burden of regulation of excess  $\text{Ca}^{2+}$  would fall on the sarcoplasmic reticulum and mitochondria. Excess  $\text{Ca}^{2+}$  in the mitochondria can lead to the loss of mitochondria which would lead to lower ATP synthesis and might be an underlying cause of the disorganization of the central core, leading to muscle weakness and muscle atrophy. Elevated  $\text{Ca}^{2+}$  in the interior of the muscle might have the same effects on the core of the muscle as MH would have on the whole cell. The differential contraction of the core of the muscle, in relation to the periphery could lead to the disorganization and streaming of both fibres and membrane systems that is observed in the central cores. The profusion of sarcoplasmic reticulum and transverse tubules might be induced at the gene level by high  $\text{Ca}^{2+}$  concentrations. Extrusion of excess  $\text{Ca}^{2+}$  from the cell might itself have deleterious effects on the skeletal muscle cell, which is believed to carry out intracellular cycling of a constant level of  $\text{Ca}^{2+}$  without uptake and expulsion of external  $\text{Ca}^{2+}$ .

#### **2.1.4 Evidence that the Ryanodine Receptor is the Sarcoplasmic Reticulum $\text{Ca}^{2+}$ Release Channel**

##### **2.1.4.1 Inhibition by Ryanodine**

An unidentified ryanodine receptor was first predicted to be involved in excitation-contraction coupling by studies which demonstrated that

ryanodine interfered with excitation-contraction coupling (Jenden and Fairhurst, 1969). Ryanodine was shown to bind with high affinity to a receptor localized to the junctional sarcoplasmic reticulum (Pessah et al., 1985; Pessah et al., 1986).

#### **2.1.4.2 Characterization of the Purified Ryanodine Receptor**

Although  $\text{Ca}^{2+}$  release from the sarcoplasmic reticulum was measurable in biochemical assays (Weber and Herz, 1968; Miyamoto and Racker, 1981; Meissner, 1983; Meissner, 1984), it was not until 1986 that the single channel properties of the  $\text{Ca}^{2+}$  release channel were identified (Smith et al., 1986a). The purification of the ryanodine receptor and its incorporation into planar lipid bilayers led to the identification of the ryanodine receptor as the  $\text{Ca}^{2+}$  release channel of the sarcoplasmic reticulum (Smith et al., 1986a; Inui et al., 1987a; Campbell et al., 1987; Lai et al., 1988; Hymel et al., 1988). Purified and reconstituted ryanodine receptors revealed intrinsic  $\text{Ca}^{2+}$  channel activity with all of the single channel properties which Smith *et al.* (Smith et al., 1986b) had described for the native  $\text{Ca}^{2+}$  release channels (Smith et al., 1988; Imagawa et al., 1987; Lai et al., 1988; Hymel et al., 1988).

#### **2.1.4.3 Conformational Changes of RyR1**

A change in conformation of RyR1 has been shown to occur after depolarization of the T-tubule, and just prior to the release of  $\text{Ca}^{2+}$  stored in the sarcoplasmic reticulum (Yano et al., 1995). RyR1 proteins in muscle triad

microsomes were labeled with a fluorescent probe, and fluorescence intensity of the probe was monitored during T-tubule depolarization induced by reducing the  $K^+$  concentration of the buffer. The increase and decrease in fluorescence intensity of the conformational probe occurred at the same time as activation of channel function by  $Ca^{2+}$  and inhibition of channel function by ryanodine (Kang et al., 1992). Depolarization was observed to produce a rapid increase in fluorescence intensity of the probe, the change occurring at a much faster rate than the release of  $Ca^{2+}$ . These observations suggested that RyR1 opening precedes the release of lumenal  $Ca^{2+}$ .  $Mg^{2+}$  and  $\mu M$  neomycin blocked  $Ca^{2+}$  release from sarcoplasmic reticulum through RyR1, but had no effect on the conformational changes resulting from depolarization induced in the T-tubule portion of triad preparations. Open and closed conformations of RyR1 have also been shown using electron cryomicroscopy in the presence and absence of  $Ca^{2+}$  and ryanodine (Orlova et al., 1996).

#### **2.1.4.4 Studies of *RYR1*-deficient Mice**

The observation that skeletal-type E-C coupling is abolished in mice with a targeted mutation in *RYR1* is definitive evidence that RyR1 is critical for E-C coupling (Takeshima et al., 1994). Electron microscopic analysis of these mutant mice showed that triad junctions lack the cytoplasmic domain of RyR (Takekura et al., 1995a). RT-PCR analysis indicated that RyR3 is expressed in cultured *RYR1*-deficient myocytes, but that neither RyR1 nor

RyR2 proteins are present. Due to the presence of RyR3, *RYR1*-deficient myocytes retained the ability to release  $\text{Ca}^{2+}$  in response to caffeine, AMP, and  $\mu\text{M}$   $\text{Ca}^{2+}$ , and non-junctional RyR cytoplasmic domains were observed. An unexpected finding in myotubes with a targeted disruption in *RYR1* was a 30 fold reduction in L-type  $\text{Ca}^{2+}$  current density that was not due to a reduction in the expression of DHPRs (Nakai et al., 1996). RyR1 enhances  $\text{Ca}^{2+}$  channel function of DHPR. Expression of transfected RyR2 can support  $\text{Ca}^{2+}$ -induced  $\text{Ca}^{2+}$  release, but neither RyR2 nor RyR3 expressed in *RYR1*-deficient myocytes could reconstitute skeletal-type E-C coupling nor transmit a retrograde signal that enhances  $\text{Ca}^{2+}$  channel activity in the skeletal DHPR (Yamazawa et al., 1996; Nakai et al., 1997).

#### **2.1.4.5 Repolarization-Induced Stop of Caffeine-Activated $\text{Ca}^{2+}$ Release**

During depolarization, a second  $\text{Ca}^{2+}$  release peak can be induced by caffeine. The caffeine-induced  $\text{Ca}^{2+}$ -release is also stopped by membrane repolarization demonstrating that repolarization-induced stop of  $\text{Ca}^{2+}$  release involves RyR1 (Suda and Penner, 1994). Free  $\text{Ca}^{2+}$  at resting concentrations of 100-200 nM is usually below the threshold for induction of contraction, but a transient contraction can be evoked in the presence of 0.5-2 mM caffeine (Endo et al., 1970). Caffeine-induced contraction is the consequence of caffeine-activated release of  $\text{Ca}^{2+}$  from the sarcoplasmic reticulum (Weber and

Herz, 1968; Endo et al., 1970). It is well established that RyR is the site of action of caffeine (Rousseau et al., 1988). Thus, when caffeine opens RyR a second time while the T-tubule is depolarized, the observed closure of caffeine-activated RyR channels upon repolarization of the T-tubular membranes suggests that a direct interaction with the voltage sensor or DHPR induces a second structural alteration in RyR, resulting in closure of the RyR channel.

## **2.2 The Dihydropyridine Receptor or L-type $\text{Ca}^{2+}$ Channel**

The skeletal muscle L-type  $\text{Ca}^{2+}$  channel is a member of a family of voltage-gated ion channels that includes  $\text{Na}^+$ ,  $\text{Ca}^{2+}$ , and  $\text{K}^+$  channels (De Waard et al., 1995; Catterall, 1996). A similar motif is found in the principal subunits of each of these four channels, and the characterization of each family member has provided a molecular template for probing the relationship between structure and function in the voltage-gated channel family.

### **2.2.1 Subunits of L-type $\text{Ca}^{2+}$ Channels**

Voltage-gated  $\text{Ca}^{2+}$  channels are a complex of five protein subunits;  $\alpha 1$ ,  $\alpha 2$ ,  $\beta$ ,  $\gamma$ , and  $\delta$ . The  $\alpha 1$ -subunit is the receptor for  $\text{Ca}^{2+}$  antagonists and can function as a voltage-gated ion channel (Lacerda et al., 1991; Mikami et al., 1989). The association of the  $\beta$ -subunit with  $\alpha 1$  increases the efficiency of



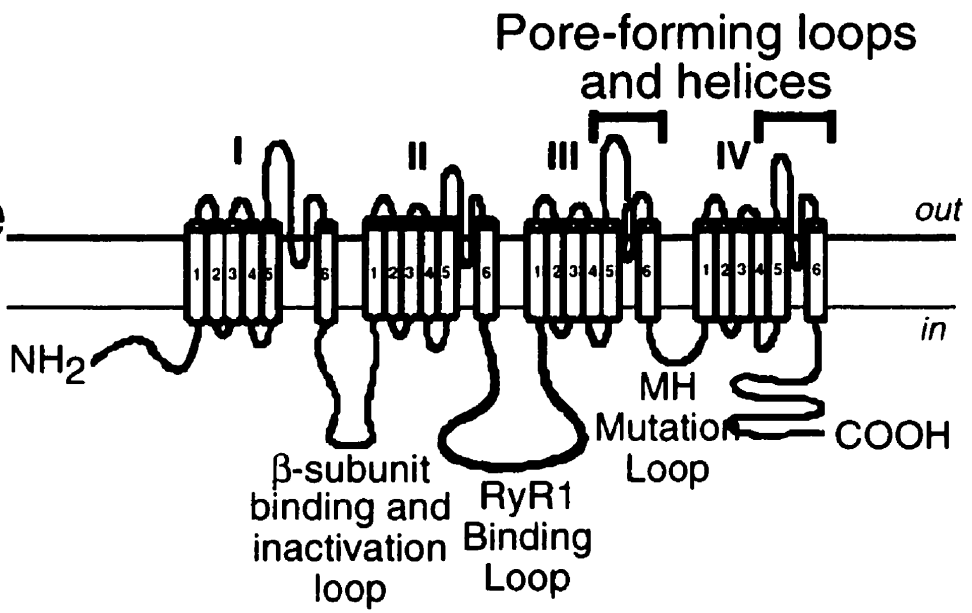
coupling between voltage sensing and pore opening (Olcese et al., 1994), and increases the current amplitude substantially (Wei et al., 1991). The association of  $\alpha 2\delta$  with  $\alpha 1\beta$  increases current amplitude and rate of inactivation (Singer et al., 1991; De Waard and Campbell, 1995). In N- and P/Q-type  $\text{Ca}^{2+}$  channels, the interaction of the loop connecting domains I and II in the  $\alpha 1$ -subunit (the I-II loop) with the  $\beta\gamma$  subunits and a heterotrimeric G-protein leads to inhibition of the channel, but this interaction does not occur with skeletal and cardiac  $\alpha 1$ -subunits (De Waard et al., 1996).

### **2.2.2 Functional Regions in the $\alpha 1$ -subunit**

The  $\alpha 1$ -subunit contains four homologous transmembrane domains, each of which contains six transmembrane  $\alpha$ -helices (Fig. 1.3). The fourth transmembrane sequence (S4) in each of the 4 domains contains positively charged (Arg or Lys) residues in every third or fourth position. This could constitute the structural correlate of a charge movement that is observed following plasma membrane depolarization and preceding  $\text{Ca}^{2+}$  release. Mutations of charged residues to neutral or negative residues caused a decrease in apparent gating charge, indicating that the channel had a reduced sensitivity to changes in membrane potential (Garcia et al., 1997). Movement of these sequences in the membrane in response to depolarization could lead to channel opening. Analysis of chimeric skeletal and cardiac  $\alpha 1$ -

**Figure 1.3:** Schematic of the  $\alpha 1$ -subunit of L-type  $\text{Ca}^{2+}$  Channels illustrating functional domains and regulatory sites.

**Dihydropyridine  
Receptor  
(DHPR)**



subunits has shown that S3 segments in domain I and the adjacent linker region connecting to S4 are determinants of the rate of activation (Nakai et al., 1994). Amino acids in S6 and the loop linking S5 and S6 from each of the four domains contribute to the  $\text{Ca}^{2+}$  channel pore and amino acids in the loop linking S5 and S6 are critical determinants of ion conductance and selectivity (De Waard et al., 1996; Catterall, 1996). In  $\text{Na}^+$  channels, the loop linking domains III and IV is the inactivation gate and the S6 segment in domain IV may be the inactivation gate receptor (McPhee et al., 1994). In  $\text{Ca}^{2+}$  channels, however, the III-IV loop has not been implicated in voltage-dependent inactivation, but S6 in domain I and the cytoplasmic loop linking domains I and II are involved in the inactivation of  $\text{Ca}^{2+}$  channels (Zhang et al., 1994). The cytoplasmic loop linking domains I and II interacts with the  $\beta$  subunit and the binding of the  $\beta$  subunit may modulate the inactivation process in the  $\alpha 1$ -subunit (Pragnell et al., 1994). The C-terminal region contains important elements for the regulation of  $\text{Ca}^{2+}$  channel activity (Wei et al., 1994). The skeletal  $\alpha 1$ -subunit loop linking domains II and III is involved in skeletal muscle E-C coupling (Tanabe et al., 1990a), and a mutation in the loop linking domain III and IV has been linked to malignant hyperthermia (Monnier et al., 1997), an abnormality of  $\text{Ca}^{2+}$  release (Loke and MacLennan, 1998).

### **2.2.3 Evidence that the Dihydropyridine Receptor is the "Voltage Sensor"**

#### **2.2.3.1 Inhibition by Dihydropyridine**

The first evidence that the L-type  $\text{Ca}^{2+}$  channel of skeletal muscle plasma membranes is the voltage sensor came from studies which demonstrated that low concentrations of dihydropyridine inhibited intramembrane charge movements and sarcoplasmic reticulum  $\text{Ca}^{2+}$  release in parallel (Rios and Brum, 1987).

The role of the DHPR as the voltage sensor for terminating  $\text{Ca}^{2+}$  release was demonstrated in studies measuring the rate of decay of  $\text{Ca}^{2+}$  concentration after repolarization in the presence of low concentrations of dihydropyridines (Suda, 1995). The sarcoplasmic reticulum  $\text{Ca}^{2+}$  ATPase (SERCA) is responsible for the decay in cytoplasmic  $\text{Ca}^{2+}$  concentrations to resting levels once  $\text{Ca}^{2+}$  release channels have closed (Lytton and MacLennan, 1992). Repolarization was observed to accelerate the decay of  $\text{Ca}^{2+}$  concentration and the decay of  $\text{Ca}^{2+}$  concentration after repolarization was slowed in the presence of low concentrations of dihydropyridines (Melzer et al., 1987; Schneider and Simon, 1988; Rios and Pizarro, 1991; Suda, 1995). Since the binding of dihydropyridines to DHPRs block intra-membrane charge movements both upon depolarization and repolarization (Rios and Brum, 1987), both depolarization and repolarization must cause structural

alterations in the DHPR which induce structural alterations in the  $\text{Ca}^{2+}$  release channel, leading to opening and closing of the  $\text{Ca}^{2+}$  release channel.

#### **2.2.3.2 Studies of Dysgenic Mice**

Mice with muscular dysgenesis have a point mutation in the  $\alpha_1$ -subunit of the L-type  $\text{Ca}^{2+}$  channel which results in undetectable levels of protein (Tanabe et al., 1988). In dysgenic fibres, the defect correlates with a decrease in dihydropyridine binding, lack of slow  $\text{Ca}^{2+}$  currents and charge movement and interruption of E-C coupling. Voltage-dependent intramembrane charge movement is restored in dysgenic skeletal muscle by injection of either skeletal or cardiac DHPR cDNA (Adams et al., 1990). This is as predicted since S4 segments, which are likely to sense voltage (Noda et al., 1984; Noda et al., 1986; Stuhmer et al., 1989; Garcia et al., 1997) are highly conserved between skeletal and cardiac muscle DHPR. Skeletal muscle-type excitation-contraction coupling can be restored in dysgenic mice by injection of skeletal muscle DHPR cDNA, but not with cardiac muscle DHPR cDNA (Tanabe et al., 1990b). There are differences in E-C coupling between skeletal and cardiac muscle, in particular, the dependence on  $\text{Ca}^{2+}$  current through the DHPR of cardiac muscle, but not skeletal muscle. In skeletal muscle  $\text{Ca}^{2+}$  transients, due to  $\text{Ca}^{2+}$  release from the sarcoplasmic reticulum, are fast and display a sigmoidal dependence on membrane voltage and is independent of the  $\text{Ca}^{2+}$  current through DHPR which is slow and of

small magnitude. The current peaks after contraction, and E-C coupling can occur normally in the absence of extracellular  $\text{Ca}^{2+}$ . In cardiac muscle, the kinetics of DHPR activation are fast,  $\text{Ca}^{2+}$  currents are of large amplitude and precede contraction,  $\text{Ca}^{2+}$  permeation through the channels is a prerequisite for contraction and  $\text{Ca}^{2+}$  transients due to  $\text{Ca}^{2+}$  release from the sarcoplasmic reticulum are slow and have a bell-shaped dependence on voltage which parallels the dependence of  $\text{Ca}^{2+}$  currents on voltage (Franzini-Armstrong and Protasi, 1997).

### **2.3 Other Proteins Involved In Excitation-Contraction Coupling**

Calsequestrin is a high capacity  $\text{Ca}^{2+}$ -binding protein located in the junctional SR lumen which buffers the  $\text{Ca}^{2+}$  that is released during muscle contraction (Yano and Zarain-Herzberg, 1994; Fliegel et al., 1987; Scott et al., 1988; Mitchell et al., 1988). Junctin (Jones et al., 1995) and triadin (Caswell et al., 1991; Knudson et al., 1993b; Knudson et al., 1993a) are single transmembrane anchoring proteins which have a short cytoplasmic sequence and long, basic luminal sequences. They interact with both RyR and calsequestrin, providing a means of linking these proteins, one designed to store high levels of  $\text{Ca}^{2+}$  (Wang et al., 1998) and the other designed to release these large amounts of stored  $\text{Ca}^{2+}$  (MacLennan and Reithmeier, 1998). Thus junctin and triadin appear to mediate the association of calsequestrin with the inner face of the junctional sarcoplasmic reticulum membrane.

Biochemical evidence suggests that calsequestrin actively participates in

muscle contraction by regulating the amount of  $\text{Ca}^{2+}$  released by RyR (Ikemoto et al., 1989; Ikemoto et al., 1991; Kawasaki and Kasai, 1994; Donoso et al., 1996). This regulatory effect may be mediated by calsequestrin –anchoring proteins such as triadin and junctin (Mitchell et al., 1988; Jones et al., 1995; Guo and Campbell, 1995; Guo et al., 1996). Junctin interacts with RyR, triadin, and RyR and thus, may act as a scaffold to localize diverse molecules to the junctional interface (Zhang et al., 1997).

An opposing view on the function of triadin arose from biochemical studies which found that triadin interacts with DHPR (Brandt et al., 1990) and with the cytoplasmic domain of RyRs (Kim et al., 1990b). This led to the proposal that triadin might mediate interactions between RyR and DHPR. In support of the hypothesis that triadin does not link RyR with DHPR are the observations that both cardiac and skeletal triadin isoforms (Guo and Campbell, 1995) interact with calsequestrin, while DHPR and RyR are not linked in both skeletal and cardiac muscle.

### **3 Role of $\text{Ca}^{2+}$ -induced $\text{Ca}^{2+}$ Release and $\text{Ca}^{2+}$ -inactivation of $\text{Ca}^{2+}$ Release in Skeletal Muscle Excitation-Contraction Coupling**

$\text{Ca}^{2+}$ -induced  $\text{Ca}^{2+}$  release in skeletal muscle was first shown to exist in studies of skinned skeletal muscle fibres (Endo et al., 1970; Ford and Podolsky, 1970). It is not clear whether  $\text{Ca}^{2+}$ -induced  $\text{Ca}^{2+}$  release plays a role



in skeletal muscle E-C coupling, but it is clear that it is critical for cardiac E-C coupling (Fabiato, 1982; Nabauer et al., 1989). Rios and Pizarro (Rios and Pizarro, 1988) presented a model in which the depolarization-induced peak in cytoplasmic  $\text{Ca}^{2+}$  concentration has components of  $\text{Ca}^{2+}$  released from sarcoplasmic reticulum induced by either depolarization, for channels coupled to voltage sensors, or  $\text{Ca}^{2+}$ , for channels which are not coupled to voltage sensors. They also proposed that the fast decay of the rate of  $\text{Ca}^{2+}$  release is induced by elevated  $\text{Ca}^{2+}$  by a  $\text{Ca}^{2+}$  inactivation of  $\text{Ca}^{2+}$  release.  $\text{Ca}^{2+}$  elevation during the depolarizing pulse is due to  $\text{Ca}^{2+}$  release through channels that are in direct contact with the voltage sensors. Repolarization-induced termination of  $\text{Ca}^{2+}$  release is also likely to be due to termination of release through channels which are directly coupled to voltage sensors.

Evidence for the importance of  $\text{Ca}^{2+}$ -induced  $\text{Ca}^{2+}$  release as a component of the depolarization-induced  $\text{Ca}^{2+}$ -concentration peak has been obtained in frog skeletal muscle fibres micro-injected with strong  $\text{Ca}^{2+}$  buffers (Jacquemond et al., 1991). The extensive buffering selectively eliminated the depolarization-induced peak component of  $\text{Ca}^{2+}$  release from sarcoplasmic reticulum, with no effect on steady-state  $\text{Ca}^{2+}$  levels normally observed during the depolarizing pulse. Other studies report that higher concentrations of  $\text{Ca}^{2+}$  buffers (5-6 mM fura-2) reduce  $\text{Ca}^{2+}$  activation of  $\text{Ca}^{2+}$  release and thus reduce both the maximal rate and amount of  $\text{Ca}^{2+}$  release (Jong et al., 1993).  $\text{Ca}^{2+}$ -inactivation of  $\text{Ca}^{2+}$  release was observed with lower concentrations of

$\text{Ca}^{2+}$  buffers ( $>3\text{mM}$  fura-2).  $\text{Ca}^{2+}$ -buffering reduced  $\text{Ca}^{2+}$ -inactivation of  $\text{Ca}^{2+}$  release, thus the peak rate of  $\text{Ca}^{2+}$  release and the steady state  $\text{Ca}^{2+}$  level was increased (Pape et al., 1993; Jong et al., 1993). The decrease in the rate and amount of  $\text{Ca}^{2+}$  release by a second depolarization within 15 ms of a prepulse or depolarization due to high levels of  $\text{Ca}^{2+}$  from the first release is further evidence for  $\text{Ca}^{2+}$  inactivation of  $\text{Ca}^{2+}$  release (Jong et al., 1995).

#### **4 Evidence that Protein-Protein Interactions Are Important for Activating $\text{Ca}^{2+}$ Channel Opening and Closing**

##### **4.1 Extracellular $\text{Ca}^{2+}$ is not Required for $\text{Ca}^{2+}$ Channel Opening**

In vertebrate skeletal muscle, muscle contraction is caused by a transient rise in intracellular  $\text{Ca}^{2+}$  concentration, resulting from the release of  $\text{Ca}^{2+}$  from an intracellular store in the sarcoplasmic reticulum. Release of  $\text{Ca}^{2+}$  from the sarcoplasmic reticulum is a consequence of depolarization of the T-tubules (Endo et al., 1970; Huxley and Taylor, 1958). E-C coupling in skeletal muscle does not depend on the entry of external  $\text{Ca}^{2+}$ , while E-C coupling in cardiac muscle requires extra-cellular  $\text{Ca}^{2+}$  (Fabiato, 1985; Nabauer et al., 1989). Thus, skeletal muscle can contract and relax 20-30 times in the absence of extracellular  $\text{Ca}^{2+}$ , while cardiac muscle can contract only once. Since extracellular  $\text{Ca}^{2+}$  is not required, another mechanism for the activation of  $\text{Ca}^{2+}$  release from sarcoplasmic aside from activation by  $\text{Ca}^{2+}$

entering the cell through surface membrane  $\text{Ca}^{2+}$  channels must be present in skeletal muscle.

#### **4.2 Elementary $\text{Ca}^{2+}$ -Release Events (sparks) Are Not Crucial**

DHPR-mediated opening of  $\text{Ca}^{2+}$  release channels and  $\text{Ca}^{2+}$ -induced  $\text{Ca}^{2+}$ -release channel opening have both been proposed to result in elementary  $\text{Ca}^{2+}$ -release events (sparks) which originate at the frog skeletal muscle triad and lead to further  $\text{Ca}^{2+}$  release (Klein et al., 1996). Tetracaine, which inhibits  $\text{Ca}^{2+}$ -induced  $\text{Ca}^{2+}$  release, eliminated all elementary  $\text{Ca}^{2+}$  release events in skeletal muscle, suggesting that  $\text{Ca}^{2+}$ -induced  $\text{Ca}^{2+}$  release, and not depolarization, is the mechanism for elementary  $\text{Ca}^{2+}$  release events. The phenylalkylamine, D600, a well-known inhibitor of the membrane voltage sensor, suppresses elementary  $\text{Ca}^{2+}$  release events from sarcoplasmic reticulum and the peak of depolarization-induced  $\text{Ca}^{2+}$  release (Shirokova and Rios, 1997); however, the elementary  $\text{Ca}^{2+}$  release events and depolarization-induced  $\text{Ca}^{2+}$  release can be restored by strong depolarizations suggesting that, in skeletal muscle, depolarization-induced  $\text{Ca}^{2+}$  release is the trigger for  $\text{Ca}^{2+}$ -induced  $\text{Ca}^{2+}$  release. Recent studies of rat muscle fibres suggest that elementary  $\text{Ca}^{2+}$  release events do not exist in mammalian muscle, so elementary events of  $\text{Ca}^{2+}$ -induced  $\text{Ca}^{2+}$  release cannot be a trigger for E-C coupling in mammalian muscle (Shirokova and Rios, 1998).

### **4.3 Depolarization and Intra-Membrane Charge Movements Lead to $\text{Ca}^{2+}$ Channel Opening**

The demonstration of intra-membrane charge movements led to the hypothesis that release of  $\text{Ca}^{2+}$  from the sarcoplasmic reticulum is controlled by a voltage sensor in the T-tubule membrane (Schneider and Chandler, 1973) and that activation of  $\text{Ca}^{2+}$  release may occur through protein-protein interactions between the voltage-sensor and the  $\text{Ca}^{2+}$  release channel of the sarcoplasmic reticulum. The initiation of  $\text{Ca}^{2+}$  release by the arrival of the action potential at the T-tubule-sarcoplasmic reticulum junction is accompanied by the outward movement of a positive gating charge across the T-tubule membrane in the direction of the sarcoplasmic reticulum. This depolarization may cause a molecular rearrangement of the voltage sensor and this molecular rearrangement may produce the characteristic intramembrane charge movement. Although many aspects of excitation-contraction coupling are now understood, it is not yet clear how the voltage sensor causes the  $\text{Ca}^{2+}$  release channel of the sarcoplasmic reticulum to open within milliseconds of fibre depolarization. One explanation is that the depolarization-induced movement of the T-tubule voltage sensor (the S4 transmembrane sequence) contributes to the mechanical coupling which activates  $\text{Ca}^{2+}$  channel opening in the sarcoplasmic reticulum membrane.

The role of the intra-membrane charge movement in activation of  $\text{Ca}^{2+}$  channel opening is supported by observations that a change in conformation

of the  $\text{Ca}^{2+}$  release channel, measured using a fluorescent conformational probe, has been shown to be stimulated by depolarization and to precede  $\text{Ca}^{2+}$  release (Yano et al., 1995). An interaction between the voltage sensor and the  $\text{Ca}^{2+}$  release channel leading to the activation of channel opening is suggested by studies with nimodipine, an antagonist of the voltage sensor (Rios and Brum, 1987) that inhibited both the conformational change and  $\text{Ca}^{2+}$  release.

#### **4.4 Repolarization Leads to Activation of $\text{Ca}^{2+}$ Channel Closing**

Early studies showed that the  $\text{Ca}^{2+}$  release that occurs following depolarization is turned off by subsequent repolarization. (Melzer et al., 1984; Melzer et al., 1987; Schneider and Simon, 1988; Rios and Pizarro, 1991). The rate of decay of the rate of  $\text{Ca}^{2+}$  release from the sarcoplasmic reticulum has two components, a fast decay component which immediately follows the peak of  $\text{Ca}^{2+}$  release and a slow decay component during a period of elevated cytoplasmic  $\text{Ca}^{2+}$  concentrations. The fast decay component is a result of the inactivation of  $\text{Ca}^{2+}$  release channels by  $\text{Ca}^{2+}$  (Jong et al., 1993; Simon et al., 1991). A second pool of  $\text{Ca}^{2+}$  release channels is not inactivated by  $\text{Ca}^{2+}$  and this is proposed to be due to coupling with an activating component of the voltage sensor. The observation that within a millisecond after fibre repolarization the slow decay component of the  $\text{Ca}^{2+}$  release flux becomes a fast decay of  $\text{Ca}^{2+}$  release, suggested that there is a direct mechanical interaction between the voltage sensor and the release channel, similar to the activation of  $\text{Ca}^{2+}$  release following depolarization (Rios and Pizarro, 1991).

Repolarization-induced termination of  $\text{Ca}^{2+}$  release was evident only when  $\text{Ca}^{2+}$  release was activated previously by depolarizing pulses of at least 0.5-1 seconds (Suda and Penner, 1994). The requirement for a minimum depolarization time suggested that the depolarization-induced conformational change of the voltage sensor has a finite time requirement before an interaction with the  $\text{Ca}^{2+}$  release channel of sarcoplasmic reticulum can induce a structural alteration in the  $\text{Ca}^{2+}$  release channel, resulting in closure of the channel. Coupling between the voltage sensor and the  $\text{Ca}^{2+}$  release channel is extremely slow compared to the intramembrane charge movement, which ceases within 10 ms (Adams et al., 1990). It is worth noting that the maximal activation of L-type  $\text{Ca}^{2+}$  channel conductance also required about 500 ms of depolarization. The correspondence between the length of time of depolarization required for maximal L-type  $\text{Ca}^{2+}$  channel activation and the time required for repolarization-induced inactivation of the  $\text{Ca}^{2+}$  release channel suggests that the conformational change in the voltage sensor required for L-type  $\text{Ca}^{2+}$  channel opening is a pre-requisite for the coupling between the voltage sensor and the  $\text{Ca}^{2+}$  release channel which later terminates  $\text{Ca}^{2+}$  release from the sarcoplasmic reticulum. Repolarization-induced termination of  $\text{Ca}^{2+}$  release was still evident 2-3 s after depolarization, suggesting that the voltage sensor and the  $\text{Ca}^{2+}$  release channel are closely coupled for several seconds. Repolarization-induced termination of  $\text{Ca}^{2+}$  release is less prominent if the voltage sensors are

inactivated by strong depolarization or long depolarization (Suda and Penner, 1994).

## **5 Spatial Relationships Between Dihydropyridine Receptors and Ryanodine Receptors Define the Mode of E-C Coupling**

The spatial relationships between DHPR and RyR differ in skeletal muscle, cardiac muscle, and neuronal cells. The differences in spatial relationships are not due to differences in the association between sarcoplasmic reticulum and the T-tubule, since sarcoplasmic reticulum/T-tubule junctions form in the absence of either DHPR (Flucher et al., 1992) or RyR1 (Takekura et al., 1995a). DHPRs and RyR1 fail to induce the formation of junctions between endoplasmic reticulum and plasma membrane when co-expressed in CHO cells (Takekura et al., 1995b), suggesting that an essential protein is missing, which is normally necessary for either the initial docking of the endoplasmic reticulum to the surface membrane or for maintaining the interaction between DHPR and RyR.

### **5.1 Skeletal Muscle**

In skeletal muscle, specialized domains called junctions exist where the sarcolemma or its invaginations forming the T-tubule membranes are closely opposed to the sarcoplasmic reticulum membrane, with a “foot” protein originating in the sarcoplasmic reticulum acting as a bridge between

the two membrane systems (Franzini-Armstrong, 1970). The first biochemical evidence for actual physical contact between the T-tubule and the terminal cisternae of the sarcoplasmic reticulum was the isolation of a fraction of intact triad junctions from a muscle homogenate (Caswell et al., 1976). The tannic acid mordant-staining technique was used to enhance the resolution of membrane structure (Saito et al., 1978) and to characterize structures protruding from the surface of isolated sarcoplasmic reticulum vesicles which were proposed to be the feet structures which span the 120 Å gap between the T-tubule and the junctional terminal cisternae of sarcoplasmic reticulum (Campbell et al., 1980; Block et al., 1988).

The foot protein was first isolated by Cadwell and Caswell (Cadwell and Caswell, 1982; Kawamoto et al., 1986). It appeared in gels as a doublet of high molecular weight protein bands, but the presence of 325 and 300 kDa bands is now known to have resulted from proteolysis of the 565 kDa RyR1 protein. Subsequent isolation of the ryanodine receptor (Campbell et al., 1987; Inui et al., 1987b) showed that the 565 kDa protein retained both ryanodine binding and the morphological identity of the “foot” structure. The ryanodine receptor was also found to retain the single channel properties of the Ca<sup>2+</sup> release channel (Lai et al., 1987; Imagawa et al., 1987; Hymel et al., 1988; Smith et al., 1988).

DHPRs are clustered in groups of four and positioned in exact correspondence with RyR1 tetramers so that each DHPR on the T-tubule



membrane is located immediately opposite to one of the RyR1 subunits (Block et al., 1988). Image analysis has determined that DHPRs are associated with alternate RyR1 tetramers (Block et al., 1988). The measured ratios of high affinity [ $^3\text{H}$ ]PN200-100 and [ $^3\text{H}$ ]ryanodine binding are smaller than 2:1. Two triad fractions exist in rabbit muscle which have different mechanical stability, one resistant to breakage of triad junctions by French press, hypertonic salt treatment, and protease digestion, and one not. The estimated DHPR to RyR ratio was 0.5 for the resistant fraction and 7 for the non-resistant fraction (Kim et al., 1990a; Franzini-Armstrong and Protasi, 1997). It is possible that the composition of the triads in rabbit muscle varies in different areas of the same muscle and or muscle fibre type.

In muscle with a targeted mutation in RyR1, the junctional gap is narrow, suggesting that RyR1 must be present to widen the gap sufficiently to accommodate its large cytoplasmic domain (Takekura et al., 1995a). Experiments in muscle derived from mice lacking RyR1 or DHPR show that RyR3 and DHPR are localized to junctions even in the absence of RyR1 or DHPR; however, DHPR do not form tetrads in muscle lacking RyR1 (Takekura et al., 1995a; Flucher and Franzini-Armstrong, 1996; Franzini-Armstrong and Protasi, 1997).

## **5.2 Cardiac Muscle**

In cardiac muscle, a proportion of RyR1 in the sarcoplasmic reticulum membrane is not present in junctions and their cytoplasmic domains face the

cytoplasm without connecting with an exterior membrane (Jorgensen et al., 1993). The DHPR of cardiac muscle are not grouped into tetrads and bear no apparent relationship to the position of the feet (Sun et al., 1995). The lack of tetrads indicates that a direct molecular interaction between DHPRs and RyRs may not be possible in cardiac muscle. However, the concentration of DHPRs in the junctional domain opposite to the RyRs is consistent with  $\text{Ca}^{2+}$ -induced- $\text{Ca}^{2+}$  release as the mechanism for cardiac-type E-C coupling under the local control of the L-type  $\text{Ca}^{2+}$  current (Franzini-Armstrong and Protasi, 1997).

### **5.3 Non-Muscle**

Junctions between domains of the endoplasmic reticulum and the plasmalemma, bridged by structures identified as feet have also been observed in the Purkinje cells of the cerebellum (Henkart et al., 1976) and the interactions between RyR and  $\text{Ca}^{2+}$  channels at these junctions may be important in excitation-secretion coupling in neurons.

### **5.4 Determinants of Spatial Relationships**

The spatial relationship between RyR and DHPR appear to be determined by the isoforms of RyR and DHPR expressed. The differences in amino acid sequence between isoforms likely dictate the interactions which are possible between DHPR and RyR and thus their coordinated spatial organization in the junctions. Functional studies demonstrate that skeletal-type E-C coupling in myocytes from mice with a targeted mutation in RYR1

can be restored by transfection with cDNA encoding RyR1, but not with RyR2 or RyR3 (Yamazawa et al., 1996; Nakai et al., 1997). Similarly, skeletal-type E-C coupling can be restored in mice lacking a functional DHPR by transfection with skeletal DHPR, but not with cardiac DHPR (Tanabe et al., 1990a).

The junctions between the sarcoplasmic reticulum and T-tubule in skeletal muscle provide a structure where RyR and DHPR are oriented in a geometry that is conducive to multiple ligand-receptor interactions (Franzini-Armstrong and Protasi, 1997). The structure of skeletal muscle triad junctions promotes the tight coupling between RyR1 and DHPR and the proper structure is likely to be critical for activation and inactivation events that occur during E-C coupling. These hypotheses are supported by the observation that skeletal type E-C coupling in RyR1 knockout mice cannot be rescued by expression of a mutant of RyR1 with amino acids 1303-1406 deleted, although replacement of the deleted RyR1 sequence with RyR2 sequence in a chimeric molecule does not disrupt E-C coupling (Yamazawa et al., 1997). Thus, deletion of RyR1, amino acids 1303-1406, may lead to the loss of E-C coupling because the interaction site between DHPR and RyR1 is missing or because the RyR1 structure is so altered that proper junctions can no longer form, even though interaction sites are intact.

## **6 Identification of Regions of Skeletal Muscle RyR1 and DHPR Involved in Activation of Sarcoplasmic Reticulum Ca<sup>2+</sup> Release.**

### **6.1 Skeletal and Cardiac DHPR Chimeras**

The identification of interaction sites between RyR and DHPR is critical to understanding the molecular interactions leading to their spatial organization in the muscle junctions and to understanding of their complex interaction during E-C coupling. The demonstration that skeletal DHPR, but not cardiac DHPR can rescue skeletal muscle-type E-C coupling suggested that chimeras between skeletal and cardiac DHPRs could be used to identify the region in skeletal DHPR which is the determinant of skeletal muscle-type E-C coupling. The main differences in primary structure between the skeletal and cardiac muscle DHPR reside in the large cytoplasmic regions at the N- and C-termini, and the DHPR I-II loop and the DHPR II-III loop sequences. To test whether the cytoplasmic regions of the skeletal DHPR could rescue skeletal-type E-C coupling, chimeric skeletal/cardiac DHPR constructs with skeletal DHPR sequences in cytoplasmic regions and cardiac DHPR sequences in the remainder of the molecule were expressed in dysgenic myotubes (Tanabe et al., 1990a). Ca<sup>2+</sup> currents through DHPR were measured by patch clamp and contraction was measured by optical recording. The substitution of any or all of the cytoplasmic regions of the cardiac DHPR with the corresponding region from skeletal DHPR did not alter the rapid rate of

inactivation that characterizes cardiac DHPR's , nor did any of these substitutions affect the selectivity of  $\text{Ca}^{2+}$  over  $\text{Ba}^{2+}$ . Only the skeletal DHPR II-III sequence was able to rescue myotube contraction in  $\text{Ca}^{2+}$ -free solutions or in solution that contained  $\text{Cd}^{2+}$ , a  $\text{Ca}^{2+}$  channel blocker. These studies identified the DHPR II-III loop as a critical sequence for skeletal muscle-type E-C coupling. Since chimeric constructs with the skeletal DHPR II-III loop, but cardiac activation kinetics, were able to rescue skeletal-type E-C coupling, it was apparent that the slow activation of the skeletal muscle DHPR channel is not critical for skeletal-type E-C coupling. It is possible that the III-IV loop also plays a role in E-C coupling, but this property cannot be demonstrated using DHPR chimeras because the DHPR III-IV loop is highly conserved between skeletal and cardiac DHPR.

## **6.2 *In Vitro* Studies**

Experiments measuring  $\text{Ca}^{2+}$  currents through RyR1 in planar lipid bilayers (Lu et al., 1994; Lu et al., 1995) and experiments measuring activation of  $\text{Ca}^{2+}$  release from muscle triad preparations (el-Hayek et al., 1995) have confirmed the importance of the DHPR II-III loops in activation of RyR. These studies provide evidence that the interaction between RyR1 and DHPR is direct. In the planar lipid bilayer studies, the DHPR II-III loop was expressed in *E. coli*., but RyR was purified from rabbit muscle by solubilization in detergent, followed by rate density gradient centrifugation. Single channel activity through RyR1 was studied in planar lipid bilayers in

the absence and presence of purified DHPR II-III loops. Contrary to what had been observed *in vivo*, skeletal and cardiac DHPR II-III loop peptides were equally effective activators of RyR1 channel opening. However, DHPR II-III loop peptides only activated RyR1, and not RyR2. Lu *et al.* (Lu et al., 1994) and others have observed non-specific activation of RyR1 channel opening by BSA and polylysine, and attributed these results to a protein-stabilizing effect. The DHPR sequence important for interaction with RyR1 has been further localized to Glu<sup>666</sup>-Glu<sup>726</sup> (Lu et al., 1995) by overlaying [<sup>32</sup>P]-Ser<sup>687</sup> phosphorylated DHPR II-III loop onto nitrocellulose on which gradient-purified RyR1 was blotted. Unlabelled DHPR peptide, Glu<sup>666</sup>-Glu<sup>726</sup>, was able to block the interaction of phosphorylated DHPR II-III with RyR1. The phosphorylated DHPR II-III loop failed to activate RyR1, suggesting that phosphorylation of the DHPR II-III loop may be a potential regulatory mechanism for E-C coupling. Ryanodine binding and calcium release assays identified a DHPR peptide, Thr<sup>671</sup>-Leu<sup>690</sup>, which activated RyR1 opening (el-Hayek et al., 1995). A nearby DHPR sequence, Glu<sup>724</sup>-Pro<sup>760</sup>, diminished the stimulatory effects of the Thr<sup>671</sup>-Leu<sup>690</sup> sequence.

A 37 amino acid sequence in RyR1, Leu<sup>1076</sup>-Asp<sup>1112</sup>, was shown to bind to the skeletal muscle DHPR II-III loop and to Na<sup>+</sup> channel II-III loops, but not to the cardiac DHPR II-III (Leong and MacLennan, 1998b). A 14 amino acid sequence within the skeletal muscle DHPR activation region is

KAKAEERKRRKMSR. The corresponding amino acid sequence in the skeletal muscle Na<sup>+</sup> channel is RGKILSPKEIILSE and in the cardiac DHPR is KEEEEEEKERKKLAR. A comparison of similarities and differences showed that net charge ranges from 0 to +6, that lysine occurs at positions 3 and 8 of the 14 amino acid sequence in the skeletal DHPR and the Na<sup>+</sup> channel (both of which bind to RyR1), and that glutamate occurs at positions 3 and 8 in the cardiac DHPR (which does not bind to RyR1). The double mutation K677E/K682E in the skeletal DHPR II-III loop decreased binding to RyR1. Thus, the presence of positive charges at positions 3 and 8 seems to be an important feature for binding of RyR1, but net charge does not. Nevertheless, phosphorylation of Ser<sup>687</sup> (found at position 13 in both the skeletal muscle DHPR and the Na<sup>+</sup> channel sequence defined above) has been shown to inhibit the activation of RyR1 by the skeletal DHPR II-III loop (Lu et al., 1995), without affecting the ability of the peptide to bind to RyR1, suggesting that charged residues at the C-terminal end of this 14 amino acid sequence in the skeletal DHPR II-III loop may play a functional role.

Lumenal sequences of triadin and junctin contain alternating positive and negatively charged residues which are especially enriched in lysine and glutamic acid. Zhang *et al.* (Zhang et al., 1997) hypothesize that the KEKE motifs shared by junctin and triadin are required for their specific interactions with each other, as well as with other junctional sarcoplasmic

reticulum proteins that contain a high density of charged residues. Recurring sequences of this type have been described as "KEKE" association motifs and are thought to be involved in the promotion of several types of protein-protein binding interactions. Realini *et al.* (Realini et al., 1994; Realini and Rechsteiner, 1995) have noted that such KEKE motifs are present in a number of Ca<sup>2+</sup> binding proteins and have proposed that such charged regions represent protein association domains. Similar protein association domains, described as "polar zippers" have been described by Perutz *et al.* (Perutz, 1994). The skeletal muscle DHPR II-III KAKAEERKRRKMSR sequence might represent a KEKE motif important for high affinity interactions with RyR1.

### **6.3 RyR1 and RyR2 Chimeras**

A comparison of sequences among RyR subtypes reveals that divergence is higher in three regions, D1, D2, and D3 (Sorrentino and Volpe, 1993). D2 (amino acids 1303-1406) and D3 (amino acids 1872-1923) have been shown to be important for E-C coupling in skeletal muscle (Yamazawa et al., 1997; Nakai et al., 1998)) by reconstituting E-C coupling in myotubes from *RYR1* knockout mice. Yamazawa *et al.* (Yamazawa et al., 1997) reported that deletion of D2 abolishes the ability of RyR1 to mediate skeletal E-C coupling, but the deletion of D2 may alter the structure of RyR and thus disrupt interactions with DHPR. E-C coupling is preserved, however, when the sequence of the D2 region is substituted with the RyR2 sequence



suggesting that the homology between RyR1 and RyR2 D2 sequences is sufficient to preserve native RyR structure. Nakai *et al.* (Nakai et al., 1998) used chimeras between RyR1 and RyR2 to show that RyR1 (1635-2636), which includes the D3 region, is sufficient for skeletal *vs.* cardiac muscle-type E-C coupling and that RyR1 (1635-2636) and RyR1 (2659-3720) are sufficient for enhancement of DHPR Ca<sup>2+</sup> channel activity. It is not clear whether these regions interact directly with DHPR or whether these sites are, in fact, regulatory sites in RyR1 which are modulated by DHPR binding to a distinct site on RyR1. The Arg<sup>1076</sup>-Asp<sup>1112</sup> sequence in RyR1 which interacts directly with the DHPR II-III loop may be important for activation of RyR1 by DHPR upon muscle depolarization (Leong and MacLennan, 1998b).

## **7 The Role of the DHPR III-IV Loop in Malignant Hyperthermia and in Channel Activation and Inactivation**

The mutation, A1086H, in the DHPR III-IV loop has been associated with susceptibility to malignant hyperthermia (MH), a malfunction in the mechanism regulating sarcoplasmic Ca<sup>2+</sup>-ion fluxes (Monnier et al., 1997). The *RYR1* gene has also been linked to MH in human and pigs (MacLennan and Phillips, 1992; Mickelson and Louis, 1996; Loke and MacLennan, 1998). Mutations in RyR1 which lead to MH susceptibility have been shown by intracellular Ca<sup>2+</sup> measurements to lead to an increase in the sensitivity of

the channel to activation by caffeine and halothane (Otsu et al., 1994; Treves et al., 1994; Tong et al., 1997).  $\text{Ca}^{2+}$  flux through wild-type DHPR is slow and of small magnitude (Tanabe et al., 1988), but fluxes through the mutant channel may be different.

A mutation in the DHPR III-IV loop is unlikely to alter  $\text{Ca}^{2+}$  conductance, since this loop does not form part of the channel pore and has not been identified as being important for either activation or inactivation of DHPR (Catterall, 1996). The DHPR mutation does not lead to other symptoms of ion channel disease, suggesting that it does not affect L-type  $\text{Ca}^{2+}$  channel function (Monnier et al., 1997). A mutation in this loop could modify the coupling between the DHP and ryanodine receptors, delaying or inhibiting closure of RyR1 upon repolarization (Suda, 1995). The physiological effect would be similar to *RYR1* mutations that are causal of MH which lead to inadequate control of  $\text{Ca}^{2+}$  release through RyR. Although the use of chimeric RyR1/RyR2 molecules in studies of reconstitution of E-C coupling in myocytes from dysgenic mice identified the II-III loop as critical for RyR1 activation, they did not rule out a role for the III-IV loop in E-C coupling (Tanabe et al., 1990a), because of the high amino acid sequence identity between skeletal and cardiac DHPR III-IV loops. Thus, it is possible that the DHPR III-IV loop interacts with RyR1 during repolarization to terminate  $\text{Ca}^{2+}$  release through RyR1. A peptide corresponding to DHPR C-terminal cytoplasmic amino acids Asn<sup>1487</sup>-Leu<sup>1506</sup>, was found to inhibit

ryanodine binding and to decrease the activity of RyR1 channels in planar lipid bilayers (Slavik et al., 1997). This peptide has the same effect on both skeletal and cardiac RyR1. Thus, the C-terminus of DHPR is also a candidate site for interaction between DHPR and RyR1 that closes the RyR1 channel following repolarization.

## **8 Thesis Objectives**

### **8.1 Evidence for RyR1 and Skeletal DHPR Interactions and Identification and Characterization of Domains of RyR1 Interacting with Domains of DHPR**

The presence of a direct interaction between RyR1 and DHPR has long been proposed, and much effort has gone into proving that this interaction exists. Elucidation of the nature of interactions between RyR1 and DHPR is interesting because these two proteins clearly play a crucial role in E-C coupling. The first biochemical evidence of direct interaction between proteins in the T-tubule membrane and the sarcoplasmic reticulum membrane was the observation that [ $^{125}\text{I}$ ]-labeled T-tubules, when mixed with sarcoplasmic reticulum, transferred  $^{125}\text{I}$  to a protein doublet of molecular weight 325 kDa and 300 kDa which are now believed to be major proteolytic fragments of RYR1 (Cadwell and Caswell, 1982). The bond between the surface membranes and sarcoplasmic reticulum must be strong

for junctions to survive the strains of muscle contraction, as well as the stringent fractionation procedures used in the isolation of triads (Caswell et al., 1976). Even after forced dissociation, junctional T-tubule and sarcoplasmic reticulum vesicles were capable of re-associating in the presence of 0.6 M potassium cacodylate (Caswell et al., 1979).

RyR1 and DHPR have been coimmunoprecipitated from triad vesicles solubilized in CHAPS by antibodies directed against DHPR, providing more direct evidence for binding between RyR1 and DHPR (Marty et al., 1994a). Immunoprecipitation with antibodies against RyR1 also co-precipitated both RyR1 and DHPR (Marty et al., 1994a). A hydrophobic cross-linker, dithio-bis-succinimidyl propionate, which is able to cross-link proteins at distances up to 1.2 nm (Lomant and Fairbanks, 1976), when added to skeletal muscle membrane fractions, resulted in the formation of a high-molecular mass complex between RyR and DHPR (Murray and Ohlendieck, 1997). Earlier studies used [ $^{125}$ I]-RyR1 overlay of subcellular organelles immobilized on nitrocellulose to show binding to an unknown 95 kDa protein, aldolase and GAPDH, but not to DHPR or calsequestrin (Kim et al., 1990a). It is possible that secondary structure is important for the association between DHPR and RyR1. The coimmunoprecipitation and cross-linking studies did not use purified proteins. Thus it is possible that other proteins may link RyR1 to DHPR. In my studies, presented in Chapter 2, I was able to demonstrate direct interaction between short amino acid sequences in RyR1 and DHPR in

experiments in which DHPR II-III loops were expressed in *E. coli*, and used as affinity columns for binding of *in vitro* translated [<sup>35</sup>S]-labeled fragments of RyR1 (Leong and MacLennan, 1998b).

During my studies of the interaction between RyR1 and the DHPR II-III loop, a paper was published showing that a mutation in the DHPR III-IV loop could be linked to malignant hyperthermia (Monnier et al., 1997). This suggested that the mutation in DHPR had a significant effect on Ca<sup>2+</sup> release from RyR1. This led to my next study designed to determine whether there is a site of interaction between the DHPR III-IV loop and RyR1. The DHPR III-IV loop was purified following its expression in *E. coli* and assayed for interactions with RyR1 fragments prepared from a cell-free *in vitro* translation system. The results of these studies are described in Chapter 3. These studies indicated that DHPR II-III and III-IV loops interact with a contiguous sequence on RyR1 (Leong and MacLennan, 1998a), offering the intriguing possibility that the interaction site on RyR1 for the DHPR II-III and III-IV loops could have the potential for dual functions, such as opening and closing the Ca<sup>2+</sup> release channel. This interaction site may be important during depolarization to open the channel and during repolarization, to terminate Ca<sup>2+</sup> release through RyR1.

## **8.2 Expression and Characterization of Recombinant RyR1**

The cloning of cDNA encoding the skeletal muscle ryanodine receptor (RyR1) in Dr. MacLennan's laboratory (Zorzato et al., 1990) led to a program

aimed at the characterization of the recombinant RyR1 channel. This program required the development of a heterologous expression system for RyR1 that would facilitate the type of structure/function analysis of the  $\text{Ca}^{2+}$  release channel that was being carried out so successfully for the  $\text{Ca}^{2+}$  pump (MacLennan et al., 1992). Early attempts to express RYR1 cDNA in COS-1 cells, led to the characterization of a recombinant channel which was modulated by  $\text{Ca}^{2+}$ , ATP,  $\text{Mg}^{2+}$ , ruthenium red, and ryanodine; but which displayed multiple, anomalous conductances (Chen et al., 1993b). The occurrence of multiple conductance states made it difficult to contemplate further studies of kinetics, conductance, and ligand gating properties of the  $\text{Ca}^{2+}$  release channel. A early goal of my project was to develop an alternative expression system in collaboration with Dr. Wayne Chen, which would facilitate studies of a fully functional RyR1. This work (Chen et al., 1997a) is described in Chapter 4.

## **Chapter 2**

### **A 37 Amino Acid Sequence in the Skeletal Muscle Ryanodine Receptor Interacts with the Cytoplasmic Loop between Domains II and III in the Skeletal Muscle Dihydropyridine Receptor**

## Chapter Summary

Interactions between the  $\text{Ca}^{2+}$  release channel of skeletal muscle sarcoplasmic reticulum (ryanodine receptor or RyR1) and the loop linking domains II and III (II-III loop) of the skeletal muscle L-type  $\text{Ca}^{2+}$  channel (dihydropyridine receptor or DHPR) have been shown to be important for excitation-contraction coupling in skeletal muscle. Protein affinity columns were made as GST- or His peptide-fusion proteins with the DHPR II-III loop. [ $^{35}\text{S}$ ]-labeled, *in vitro*-translated fragments from the N-terminal 3/4 of RyR1 were passed over the protein affinity columns to permit identification of interactions between the two proteins. RyR1 residues Leu<sup>922</sup>-Asp<sup>1112</sup> bound specifically to the DHPR II-III loop column, but the corresponding fragment from the cardiac ryanodine receptor (RyR2) did not. Through the use of chimeras between RyR1 and RyR2 the interaction site was localized to 37 amino acids, Arg<sup>1076</sup>-Asp<sup>1112</sup>, in RyR1. The RyR1 922-1112 fragment did not bind to the cardiac DHPR II-III loop, but did bind to the skeletal muscle  $\text{Na}^{+}$  channel II-III loop. The skeletal DHPR II-III loop double mutant K677E/K682E lost most of its capacity to interact with RyR1, suggesting that two positively charged residues at specific locations in DHPR are important in the interaction between RyR and DHPR.



## INTRODUCTION

The events linking electrical stimulation of skeletal muscle and the release of  $\text{Ca}^{2+}$  from the sarcoplasmic reticulum, leading to muscle contraction, are understood in broad terms, but many details are lacking. Immunolabelling and electron microscopic images of the junction between the transverse tubule and the sarcoplasmic reticulum of skeletal muscle provide structural evidence for a direct interaction between the  $\text{Ca}^{2+}$  release channel of skeletal muscle sarcoplasmic reticulum (the ryanodine receptor or RyR1) and the L-type  $\text{Ca}^{2+}$  channel of skeletal muscle (the dihydropyridine receptor or DHPR) located in the transverse tubule (Schneider and Chandler, 1973; Rios and Pizarro, 1991; Block et al., 1988; Franzini-Armstrong and Protasi, 1997). This physical interaction almost certainly plays a key role in excitation-contraction (E-C) coupling.

Extracellular  $\text{Ca}^{2+}$  is not necessary for E-C coupling in skeletal muscle, but is required in cardiac muscle, distinguishing the mechanism of E-C coupling in these muscles (Catterall, 1991). Skeletal muscle-type E-C coupling was rescued in *RYR1* knockout mice by injection with *RYR1* cDNA (Nakai et al., 1996) and in myotubes cultured from dysgenic mouse skeletal muscle, in which functional DHPR and E-C coupling are lacking, by injection with cDNA encoding the skeletal muscle isoform of the DHPR (Tanabe et al., 1988; Tanabe et al., 1990a). Tanabe *et al.* (Tanabe et al., 1990a) used

chimeras between skeletal and cardiac DHPRs to define a region linking DHPR domains II and III as critical for skeletal *vs.* cardiac muscle-type E-C coupling. The DHPR II-III loop has been shown to activate RyR1 in studies measuring  $\text{Ca}^{2+}$  currents across planar lipid bilayer carried by RyR1 (9,10).  $\text{Ca}^{2+}$  release has also been elicited from muscle triad vesicle preparations by the addition of the DHPR II-III loop peptide (el-Hayek et al., 1995).

In attempts to obtain evidence for a physical interaction between RyR1 and DHPR, Marty *et al.* (Marty et al., 1994a) co-immunoprecipitated RyR1 and DHPR from muscle triads with antibodies against one or the other of the two proteins. Cross-linking of RyR1 and the  $\alpha 1$ -subunit of the DHPR in rabbit skeletal muscle triads was demonstrated in skeletal muscle membranes using the thiol cross-linker, dithiobis-succinimidyl propionate (Murray and Ohlendieck, 1997). Physical interactions between RyR1 and DHPR have been inferred from the demonstration of functional interactions between these proteins (Lu et al., 1994; Lu et al., 1995; el-Hayek et al., 1995; Slavik et al., 1997). Since purified proteins were not always used in these studies, it is possible that other proteins in the triadic junction may have mediated the functional interactions observed between RyR1 and DHPR.

In the present study, we purified the DHPR II-III loop following its expression in *E. coli*. RyR1 fragments were prepared from a cell-free *in vitro* translation system. The purified DHPR II-III loop was bound to a gel matrix

to permit affinity chromatography and [<sup>35</sup>S]-labeled RyR1 fragments were then passed through the column to demonstrate direct interaction between specific, expressed fragments of the two proteins. This strategy allowed us to identify a 37 amino acid sequence of RyR1 which interacts specifically with the DHPR II-III loop.

## MATERIALS and METHODS

*Chemicals and reagents* - All chemicals were of molecular biology grade.

NiNTA resin was purchased from Qiagen and Glutathione Sepharose 4B from Pharmacia. Translational grade [<sup>35</sup>S]-Met was obtained from Amersham. The coupled *in vitro* transcription and translation kit (TNT Quick) was from Promega. Rabbit skeletal and cardiac muscle cDNA was purified from  $\lambda$  phage cDNA libraries (Zorzato et al., 1990; Otsu et al., 1990) using mediprep columns from Qiagen. The rSkM1 rat skeletal muscle Na<sup>+</sup> channel cDNA (17) was a generous gift from Dr. P. Backx, University of Toronto. The full-length ryanodine receptor cDNA clone, pBS SRR10, has been described previously (Chen et al., 1993b).

*cDNA Cloning and preparation of fusion proteins* - The loops linking domains II and III were amplified and cloned using the polymerase chain reaction (PCR): Nucleotides 1990 to 2381 of the cDNA fragment encoding the rabbit skeletal muscle DHPR II-III loop with the skeletal muscle cDNA library as template; Nucleotides 2374 to 2772 of the cardiac DHPR II-III loop with the cardiac muscle cDNA library as template; Nucleotides 2389 to 3059 of the rat skeletal muscle Na<sup>+</sup> channel with rSkM1, the rat skeletal muscle Na<sup>+</sup> channel cDNA (Trimmer et al., 1989) as template. Oligonucleotide primers flanking the cDNA sequence for the respective loops were designed with exterior *Bam*HI and *Eco*RI restriction endonuclease sites for in-frame cloning

into the ptrcHisC vector (Invitrogen) or the pGEX 3X vector (Pharmacia). All cloned fragments were then verified by DNA sequence analysis. The oligonucleotides attgaattccaccaccaccaccaccaccaccaccaccacaagcttgaattcata and its complementary oligonucleotide were used to add 10 His residues to the C-terminal end of glutathione-S-transferase (GST) by self-annealing of the 2 oligonucleotides, endonuclease restriction digestion at the *EcoRI* sites flanking the His<sub>10</sub> sequence, and ligation into the *EcoRI*-site of pGEX3X (Pharmacia).

*E. coli* strain DH5 $\alpha$  (Gibco/BRL) was used for the expression of all fusion proteins and proteins were purified following standard procedures (19) in the presence of 20 mM imidazole, pH 7.0, and the protease inhibitors pepstatin, aprotinin, leupeptin, benzamidine, iodoacetamide, and phenylmethylsulfonyl fluoride. His-peptide (Invitrogen) fusion proteins were purified with NiNTA resin (Qiagen) and GST fusion proteins were purified with glutathione Separose 4B (Pharmacia). After washing, the His-peptide fusion proteins were eluted with 0.5 M imidazole, pH 7.0, in phosphate buffered saline (PBS). GST fusion proteins were eluted with 10 mM reduced glutathione and dialyzed against PBS overnight. Eluted proteins were analyzed by SDS-PAGE and coomassie blue-staining. Protein yield was determined by the Bradford assay (Bio-rad).

*Constructs for in vitro transcription and translation of ryanodine receptor*

*fragments* - Fragments for *in vitro* transcription and translation were prepared from pBS SRR10 (Chen et al., 1993b). pBS SRR10 was digested with *EcoRI* (2394) and *XbaI* (MCS), blunted-ended with Klenow and self-ligated to make pBS RYR1 F1. *PstI* restriction endonuclease fragments were subcloned into pBSKS+ ATG-*PstI*. pBSSK+ ATG-*PstI* was prepared from pBSSK+ (Stratagene) by ligation of the linker ataccaccatgggcctgcaggcccatggtggtat into the *SmaI* site, digestion with *PstI*, and re-ligation to circularize the vector. The *PstI* site is downstream of a Kozak consensus start sequence (Kozak and Shatkin, 1979) and an ATG for translation initiation. The *PstI* fragments were subcloned into the *PstI* site of pBSK+ ATG-*PstI*, in-frame with the initiator Met, following restriction endonuclease digestion of pBS RYR1 with *PstI* (Fig. 2.1A). The *PstI* fragments that were subcloned and expressed were: *PstI* (1902) to *PstI* (2769) to form pBS RYR1 F2; *PstI* (2769) to *PstI* (3660) to form pBS RYR1 F3; *PstI* (3578) to *PstI* (4842) to form pBS RYR1 F4; *PstI* (4980) to *PstI*(6285) to form pBS RYR1 F6; *PstI* (6285) to *PstI* (7425) to form pBS RYR1 F7; *PstI* (7425) to *PstI* (7860) to form pBS RYR1 F8. The *PstI*(4980) to *BglII* (5583) fragment from the *PstI* and *BglII* digest of pBS SRR10 was subcloned into pBSKS+ ATG-*PstI*, which had been digested with *HindIII*, blunt ended with Klenow, then digested with *PstI* to form pBS RYR1 F5b. The *PstI* (4842) to *PstI* (4980) fragment was ligated to pBS RYR1 F5b, previously linearized with *PstI*, to form pBS RYR1 F5. pBSK+ ATG-ANS was prepared from pBSSK+

(Stratagene) by ligation of the linker

ataccacatggacgtctcatatggcatgccatagagacgtccatggtggtat into the *Sma*I site, digestion with *Sph*I and ligation to circularize the vector. *Aat*II and *Nde*I restriction endonuclease fragments of pBS RYR1, *Aat*II(7806) to *Aat*II(9468), and *Aat*II(10523) to *Nde*I(11173), were ligated into pBSK+ ATG-ANS downstream of a Kozak consensus start sequence (Kozak and Shatkin, 1979) and in-frame with an initiator Met to form pBS RYR1 F9 and F10b. The *Aat*II (9468)-*Aat*II (10523) fragment from RYR1 was cloned into the *Aat*II site of pBS RYR1 F10b to form pBS RYR F10.

pBS RYR1 F3a was made by digestion of pBS RYR1 F3 with *Aat*II(3335) and *Eco*RI (MCS), blunt-end formation with Klenow and re-ligation. The pBS RYR2 F3a fragment, from nucleotides 2797 to 3378, was amplified by PCR from *RYR2* cDNA (Otsu et al., 1990) using the oligonucleotide primers ctgcagatgtcacttgagacctgaag and atagaattcgatccggctgacaacctg, which include *Pst*I and *Eco*RI restriction sites, respectively, for cloning into pBS-ATG-*Pst*I.

Chimeras between RyR1 and RyR2 were made using pBS RYR1 F3a and pBS RYR2 F3a through the introduction of restriction endonuclease sites by PCR-based mutagenesis (QuikChange Site-Directed Mutagenesis Kit, Stratagene) (Fig. 2.2A). A *Hind*III site was introduced into *RYR1* at base pair 2860 to form pBS RYR1 F3aH. A *Bsp*EI site was introduced into *RYR1* at nucleotide 3225 to form pBS RYR1 F3aB. A *Hind*III site was introduced into

*RYR2* at nucleotide 2894 to form pBS RYR1 F3aH. A *BspEI* site was introduced into *RYR2* at nucleotide 3036 to form pBS RYR2 F3aB. The vector pBS RYR2 F3aB was digested with *NotI* (MCS) and *BspEI* (3036) to excise nucleotides 2797 to 3036 of *RYR2* and *RYR1* nucleotides 2769 *NotI* (MCS) to *BspEI* (3225) were ligated into this site to form pBS RYR1(923-1075)/RYR2(1076-1112). The vector pBS RYR1 F3aB was digested with *NotI*(MCS) and *HindIII*(2860) to excise nucleotides 2769 to 2860 of *RYR1* and nucleotides *NotI* (MCS) to *HindIII* (2894) of *RYR2* were cloned into this site to form pBS RYR2(923-1075)/RYR1(1076-1112). The vector pBS RYR2 F3aH was digested with *HindIII* to excise the *HindIII*(2894) to *HindIII* (MCS) fragment of *RYR2* and the *HindIII* (2860) to nucleotide 3335 *HindIII* (MCS) was ligated into this site to form pBS RYR2(922-953)/RYR1(954-1112). All numbering for the chimeric constructs are based on *RYR1*, not *RYR2*.

**Binding Assay** - Affinity matrices were prepared by eluting His-peptide fusion protein (Invitrogen) or GST-His<sub>10</sub> from NiNTA resin (Qiagen) and binding them to 40 µl of fresh NiNTA at a concentration of 0.5 mg of fusion protein/mL. Purified, dialyzed GST-fusion proteins were bound to fresh glutathione sepharose to achieve the desired concentration of fusion protein (mg/ml of sepharose). The amount of protein bound to affinity matrices was confirmed by eluting a sample of the protein-bound affinity matrix with SDS, separating the eluted protein by SDS-PAGE and staining with Coomassie



Blue. Each stained fusion protein band was quantitated by densitometry (Molecular Analyst, Bio-Rad). Resins to which fusion-proteins were bound were washed with 1 ml PBS, blocked with 1 mg of BSA in 200  $\mu$ l of column buffer (10 mM Tris-HCl, pH 7.5, 0.15 M KCl, 20  $\mu$ M  $\text{CaCl}_2$ , 0.25 mM  $\text{MgCl}_2$ , 20 mM imidazole, 0.1% Tween 20) and then with 0.4 mg of BSA in 400  $\mu$ l of column buffer. [ $^{35}\text{S}$ ]-methionine-labeled fragments of RyR, synthesized by coupled *in vitro* transcription and translation (TNT Quick, Promega) were diluted 10 fold into 200  $\mu$ l of column buffer and then passed 3 times through affinity columns by gravity flow. The columns were washed with 600  $\mu$ l of column buffer. Proteins retained on the affinity columns were eluted with 100  $\mu$ l of SDS-sample buffer. SDS-PAGE (15% gel) was used to analyze 1  $\mu$ l of the *in vitro* translation product (5% of the total column input), and 20  $\mu$ l of the eluate (20% of the total column eluate). The gels were fixed 3 times in 6 vol of 10% methanol-12% acetic acid for 20 min each time. The radioactive signal was enhanced with Entensify (DuPont/NEN) and the gels were dried and exposed to either autoradiogram film (BioMax AR, Kodak) or quantitated by a PhosphorImager (Bio-Rad). Specific binding was defined as total binding less non-specific binding to GST-His<sub>10</sub> columns or GST columns.

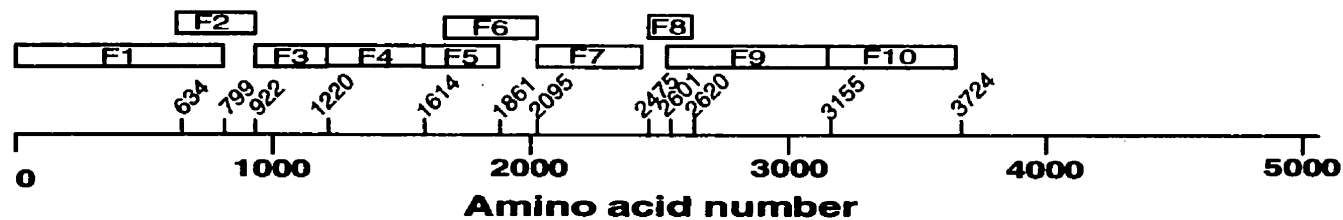
## RESULTS

*Identification of an RyR1 sequence interacting with the DHPR II-III loop* - We scanned [<sup>35</sup>S]-labeled, *in vitro* translated fragments of RyR1 for interactions with the DHPR II-III loop immobilized on a Ni<sup>+</sup> column as a His-peptide fusion protein (Fig. 2.1). We found that 20±2.7% of *in vitro* translated fragment 922-1220 was retained on the DHPR II-III loop affinity column compared to less than 5% retention for any of the other fragments of RyR1 lying between amino acids 1 and 3724. (Figs. 2.1B and C). Reduction of the RyR1 fragment to 190 amino acids, spanning residues 922-1112, increased the proportion of the *in vitro* translated fragment retained on DHPR II-III loop columns to 32±1.6% (Fig. 2.2). To test the isoform specificity of the RyR1 interaction with DHPR, we passed [<sup>35</sup>S]-labeled, *in vitro* translated fragments of RYR2 over the affinity column. We did not detect any specific binding of RyR2(933-1126) (corresponding to RYR1(922-1112)) to the skeletal DHPR II-III loop affinity column (Fig. 2.2).

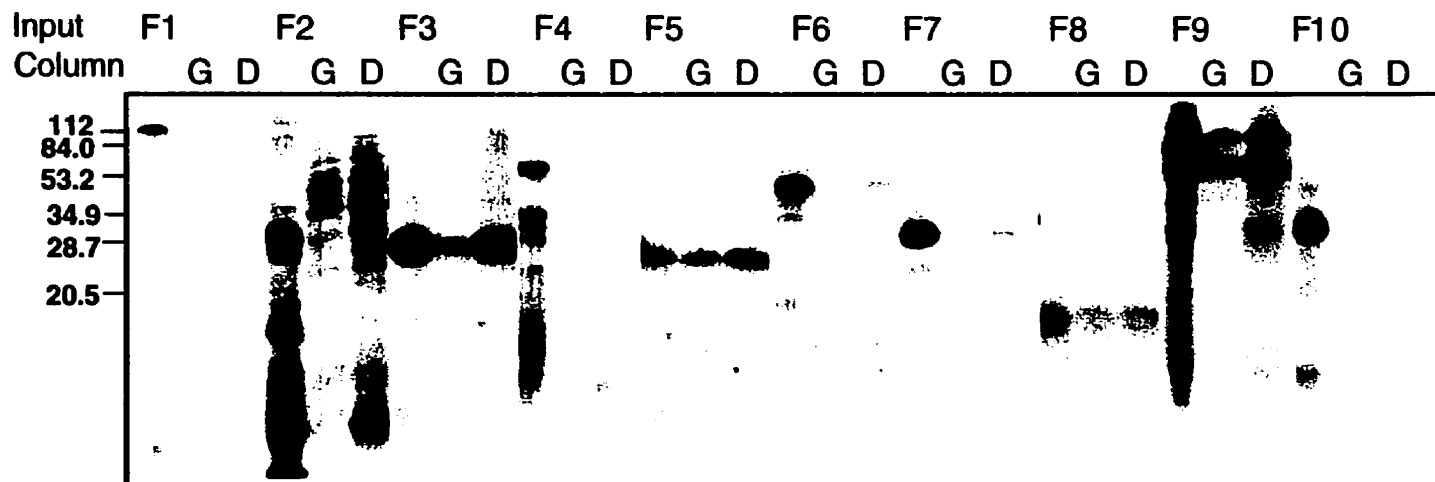
Because further reduction of the size of the RyR1 fragment led to loss of synthesis of the *in vitro* translated product, we attempted to reduce the size of the RyR1 sequence that binds to the DHPR II-III loop by making chimeras between RyR1 and RyR2, as illustrated in Fig. 2.2A. The RyR1(922-1075)/RyR2(1076-1112) (C1) chimera did not bind to the II-III loop, but 24±2.7% of the RyR2(922-953)/RyR1(954-1112) (C3) chimera and 28±2.6% of the RyR2(922-1075)/RyR1(1076-1112) (C2) chimera were retained on a

**Figure 2.1 Affinity of RyR1 fragments for the skeletal DHPR II-III loop.** *In vitro* translated fragments of RyR1 were passed through 0.5 mg/ml DHPR II-III His-peptide fusion protein columns, as described under *Materials and Methods*. **A**, schematic of RyR1 fragments cloned in-frame with a Kozak consensus start sequence (Kozak and Shatkin, 1979) and an initiator ATG codon for *in vitro* translation. **B**, autoradiogram of *in vitro* translated RyR1 fragments (F1-F10) representing 5% of input and 20% of fragments eluted from GST-His<sub>10</sub> (G) and skeletal DHPR (D) affinity columns. **C**, % specific binding of *in vitro* translated RyR1 fragments to the skeletal DHPR affinity columns, quantitated by densitometry and expressed as the mean  $\pm$  SE from at least 4 separate experiments. Specific binding was defined as total binding to DHPR II-III His-peptide fusion protein columns, less non-specific binding to GST-His<sub>10</sub>.

**A: *In vitro* translated fragments**



**B: autoradiogram**



**C: percentage binding**

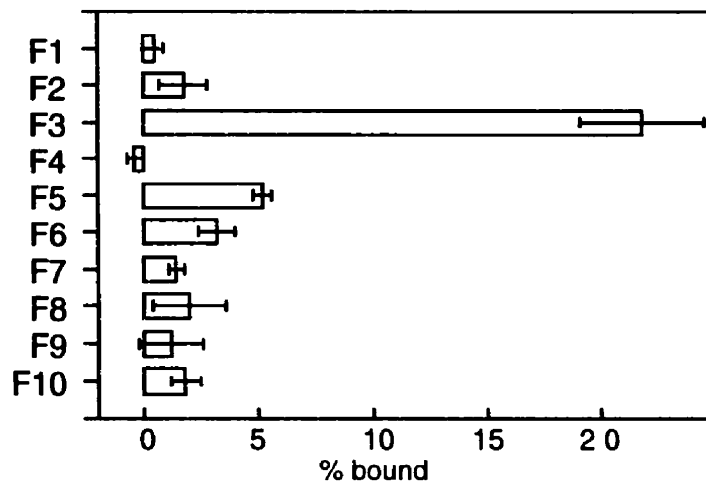
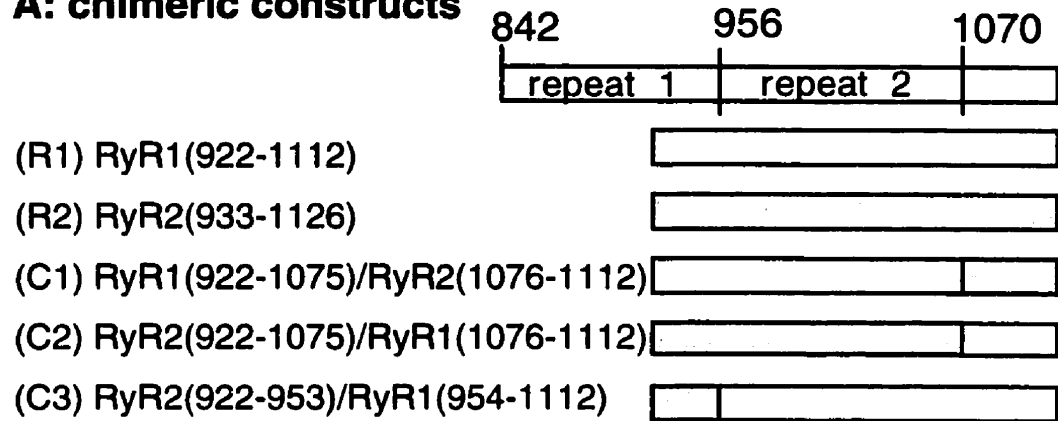
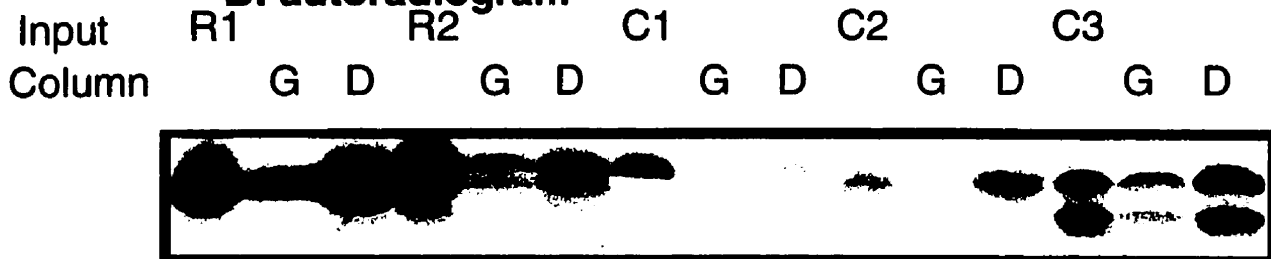


**Fig. 2.2. Affinity of chimeric RyR1/RyR2 constructs for the skeletal DHPR II-III loop.** **A**, chimeric RyR1/RyR2 constructs prepared as described under *Materials and Methods*. The first line represents a region in RyR1 containing 2 repeat sequences and defines their respective boundaries. Amino acid numbering refers to RyR1 residues in the chimeric constructs. **B**, autoradiogram of *in vitro* translated RyR1/RyR2 chimeric fragments representing 5% of input and 20% of fragments eluted from 0.5 mg/ml GST-His<sub>10</sub> (G) and skeletal DHPR II-III (D) affinity columns. **C**, % specific binding of *in vitro* translated RyR1/RyR2 chimeric fragments to the skeletal DHPR affinity columns, quantitated by densitometry and expressed as the mean  $\pm$  SE from at least 4 separate experiments. Specific binding was defined as total binding to DHPR II-III His-peptide fusion protein columns, less non-specific binding to GST-His<sub>10</sub>.

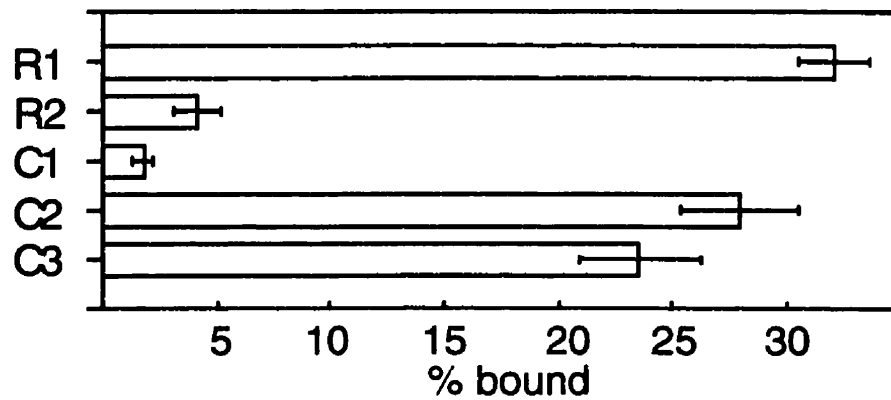
### A: chimeric constructs



### B: autoradiogram



### C: percentage binding



0.5 mg/ml DHPR II-III loop affinity column (Figs. 2.2). Accordingly, we can deduce that the 37 amino acid sequence between Arg<sup>1076</sup> and Asp<sup>1112</sup> of RyR1 is important for binding the DHPR II-III loop.

*DHPR specificity in the RyR1/DHPR interaction* - The chimeric construct, (C3), which binds to the skeletal muscle DHPR II-III loop His-peptide fusion protein, did not bind above background to either GST columns, or to a GST fusion protein constructed from the II-III loop of the cardiac DHPR receptor (cdDHPR in Figs. 2.3A and B). A GST fusion protein affinity column with the II-III loop of the skeletal muscle DHPR II-III (skDHPR) retained 12±0.4% of the input of the *in vitro* translated C3 chimera (Figs. 2.3A and B).


Surprisingly, 14±0.4% of the input of *in vitro* translated C3 chimera bound to a GST fusion protein affinity column containing the loop between domains II and III of the homologous skeletal muscle voltage-gated Na<sup>+</sup> channel (skNa in Figs. 2.3A and B).

The region of the skeletal muscle DHPR II-III loop important for activation of RyR1 has been localized to the amino acid sequence between 671 and 690 (el-Hayek et al., 1995). A 14 amino acid sequence within the skeletal muscle DHPR activation region is KAKAEERKRRKMSR (see Fig. 2.3C). The corresponding amino acid sequence in the skeletal muscle Na<sup>+</sup> channel is RGKILSPKEIILSE and in the cardiac DHPR is KEEEEEEKERKKLAR. The skeletal muscle DHPR and the Na<sup>+</sup> channel II/III loop sequences contain

**Figure 2.3. Affinity of chimeric RyR1/RyR2 constructs for skeletal and cardiac Ca<sup>2+</sup> and Na<sup>+</sup> channel II-III loop-GST fusion proteins.** **A**, autoradiogram of *in vitro* translated RYR2(922-953)/RYR1(954-1112) chimeric fragment (C3) representing 5% of input and 20% of fragments eluted from different 0.1 mg/ml GST fusion protein affinity columns: GST(G); skeletal DHPR II-III loop (skDHPR); skeletal DHPR II-III loop double mutant K677E/K682E (skDHPR(KE)); cardiac DHPR II-III loop (cdDHPR); skeletal Na<sup>+</sup> channel II-III loop (skNa). **B**, % specific binding of *in vitro* translated chimeric fragment (C3) to the II-III loop affinity columns, quantitated by densitometry and expressed as the mean  $\pm$  SE from at least 4 separate experiments. Specific binding was defined as total binding to GST fusion protein columns, less non-specific binding to GST. **C**, sequence alignment of segments of skeletal and cardiac muscle Ca<sup>2+</sup> and Na<sup>+</sup> channel II-III loops.



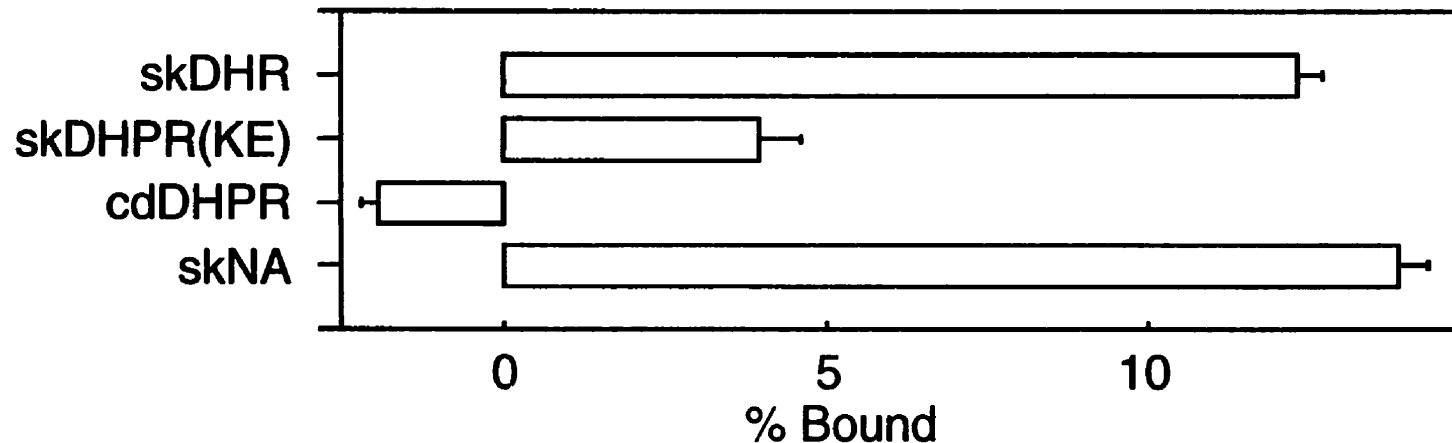
## A: autoradiogram

Input (C3) RyR2(922-953)/RyR1(954-1112) 

Column GST skDHPR skDHPR(KE) cdDHPR skNA



## B: percentage binding



## C: sequence alignment

skDHPR	(671) TSAQKAKAEERKRRKMSRGL(690)
skDHPR KE	(671) TSAQKAEAEERERRKMSRGL(690)
cdDHPR	(793) TSAQKEEEEEKERKKLARTA(812)
skNA	(840) ---LRGKILSPKEIILSEPG(856)

positive charges at positions 1, 3 and 8 of the shared sequences, a small amino acid (Ala or Gly) at position 2, and Ser at position 13. By contrast, the cardiac DHPR sequence has negative charges at positions 2, 3 and 8 and an Ala at position 13. We made the double mutations K677E/K682 E in the skeletal muscle DHPR II-III loop so that the mutated skeletal muscle DHPR sequence, KAEAEERERRKMSR, would more closely resemble the cardiac sequence in this region. This double mutation resulted in a  $66 \pm 7.1\%$  decrease in binding of the C3 chimera, from  $12 \pm 0.4\%$  binding to  $4 \pm 0.7\%$  binding.

## DISCUSSION

In this study, we localized the binding site for the skeletal DHPR II-III loop to 190 amino acids between 922 and 1112 in *in vitro* transcribed and translated products of RyR1. Decreasing the size of the fragment resulted in loss of *in vitro* translation and GST-fusion proteins of fragments shorter than 190 amino acids were unstable, suggesting that this sequence might form a stable structural domain. The 922-1112 fragment of RyR1 contains part of repeat 1 and all of repeat 2 in a series of 4 repeats in RyR1, RyR2 and RyR3 (Zorzato et al., 1990; Otsu et al., 1990; Hakamata et al., 1992). We made use of these repeat domain boundaries to create 3 RyR1/RyR2 chimeras (Fig. 2.2A). The 37 amino acid sequence between Arg<sup>1076</sup> and Asp<sup>1112</sup> in RyR1, which was retained in chimera C2 (and in C3, but not in C1) was necessary for the binding of about 25% of the input *in vitro* translation product to the DHPR II-III loop column. This sequence begins virtually at the end of repeat 2. Since the binding site lies outside of the repeat sequences, the repeats are not likely to play a role in the RyR1/DHPR interaction, but may form part of a structural domain which includes the DHPR binding site. Only 10 residues between Arg<sup>1076</sup> and Asp<sup>1112</sup> differ in RyR1 and RyR2 and several of these residues are likely to form part of the interaction site between the two proteins.

The newly-identified RyR1/DHPR interaction site is distinct from the D2 region (amino acids 1303-1406) which was shown to be important for E-C

coupling in skeletal muscle (Yamazawa et al., 1997) by reconstituting E-C coupling in myotubes from *RYR1* knockout mice. Takekura *et al.* (Takekura et al., 1995a) have reported that a functional ryanodine receptor must be provided for the formation of normal junctions between the transverse tubule and the sarcoplasmic reticulum in *RYR1* knock-out mice. Thus, deletions in RyR1 may lead to the loss of E-C coupling because the interaction site between DHPR and RyR1 is missing or because the structure of RyR1 is so altered that proper junctions can no longer form, even though interaction sites are intact. The second possibility could explain the apparent discrepancy between Yamazawa's finding (Yamazawa et al., 1997) and our own.

*In vivo* studies have shown that RyR1, but not RyR2, is capable of restoring skeletal muscle-type E-C coupling (Yamazawa et al., 1996) and peptides from II-III loops of the skeletal muscle DHPR which activate  $\text{Ca}^{2+}$  currents in RyR1 reconstituted into lipid bilayers cannot activate RYR2 (Lu et al., 1994). We have confirmed that the interaction between RyR1 and the skeletal DHPR is specific, since the corresponding RyR2 sequence did not bind to the DHPR II-III loop (Fig. 2.2). In contrast to previous *in vitro* studies in which peptides from either the skeletal or cardiac II-III loops were equally capable of activating RyR1  $\text{Ca}^{2+}$  release channel function (Lu et al., 1994; Lu et al., 1995), we have found that binding of the RyR1 954-1112 fragment is specific to the skeletal DHPR II-III loop (Fig. 2.3). Our results are also in

agreement with *in vivo* studies which showed that skeletal-type E-C coupling in dysgenic mice lacking DHPR could only be rescued with the skeletal muscle isoform of DHPR (Tanabe et al., 1988; Tanabe et al., 1990a).

An unexpected observation was that Chimera C3 was bound to a GST fusion protein affinity column made up from the loop between domains II and III of the homologous skeletal muscle voltage-gated Na<sup>+</sup> channel (skNa in Figs. 2.3A and B). These observations might suggest that loops between domains II and III of homologous Na<sup>+</sup> and Ca<sup>2+</sup> channels have homologous structures and may even share specific residues involved in protein-protein interactions.

We extended the observation that RyR1 binds to the II-III loops of the skeletal muscle Na<sup>+</sup> channel by aligning sequences which include 14 highly charged amino acids in the II-III loop of skeletal and cardiac DHPRs, shown to be important for activation of RyR1 (el-Hayek et al., 1995), with the corresponding sequence in the skeletal Na<sup>+</sup> channel sequences (Fig. 2.3C). A comparison of similarities and differences shows that net charge ranges from 0 to +6, that lysine occurs at positions 3 and 8 of the 14 amino acid sequence in the skeletal DHPR and the Na<sup>+</sup> channel (both of which bind to RyR1), and that glutamate occurs at positions 3 and 8 in the cardiac DHPR (which does not bind to RyR1). We postulated that the lysines at positions 3 and 8 may be important for the binding of the skeletal DHPR II-III loop and the Na<sup>+</sup>

channel II-III loop to RyR1. The double mutation K677E/K682E in the skeletal DHPR II-III loop decreased chimera C3 binding by 2/3 (from 13% to 4% ). The presence of positive charges at positions 3 and 8 seems to be an important feature for binding of RyR1, but net charge does not. Nevertheless, phosphorylation of Ser<sup>687</sup> (found at position 13 in both the skeletal muscle DHPR and the Na<sup>+</sup> channel) has been shown to inhibit the activation of RyR1 by the skeletal DHPR II-III loop (Lu et al., 1995), without affecting the ability of the peptide to bind to RyR1, suggesting that charged residues at the C-terminal end of this 14 amino acid sequence in the skeletal DHPR II-III loop may play a functional role.

Although this study does not deal directly with the functional interaction between the RyR1 and DHPR, numerous studies have implicated the II-III loop of the DHPR in E-C coupling (Meissner and Lu, 1995; Franzini-Armstrong and Protasi, 1997). The loss of interaction that we observed when two residues were mutated in a region of the DHPR II-III loop, previously implicated in the triggering of Ca<sup>2+</sup> release, supports our hypothesis that the interaction we have characterized is important for the activation of RyR1 during E-C coupling in skeletal muscle.

Monnier *et al.* (Monnier et al., 1997) have demonstrated that an Arg to His mutation in the loop linking DHPR domains III and IV in the  $\alpha$ -subunit of the skeletal muscle DHPR can cause susceptibility to malignant

hyperthermia (MH). The physiological basis of MH is an abnormality in the regulation of sarcoplasmic  $\text{Ca}^{2+}$  concentration and the *RYR1* gene has been linked to MH in human and pigs (MacLennan and Phillips, 1992). The involvement of both RyR1 and DHPR in MH suggests that the pathology of MH is due to aberrant E-C coupling. These observations, together with the observations that a C-terminal peptide of the DHPR can inhibit the  $\text{Ca}^{2+}$  release function of RyR1 (Slavik et al., 1997) and that there is a retrograde signal by which RyR1 enhances slow  $\text{Ca}^{2+}$  channel function (Nakai et al., 1996; Chavis et al., 1996), suggest that interactions between the RyR1 and DHPR may be complex, involving many sites in the two proteins. The protein affinity chromatography approach which we have used should be applicable to the study of interactions of other DHPR loops with RyR1 and should yield new insights into the nature of these structural and functional interactions.

## **CHAPTER 3**

**The Cytoplasmic Loops between Domains II and III and  
Domains III and IV in the Skeletal Muscle Dihydropyridine  
Receptor Bind to a Contiguous Site in the Skeletal Muscle  
Ryanodine Receptor**



## Summary

Excitation-contraction coupling in skeletal muscle is a result of the interaction between the  $\text{Ca}^{2+}$  release channel of skeletal muscle sarcoplasmic reticulum (ryanodine receptor or RyR1) and the skeletal muscle L-type  $\text{Ca}^{2+}$  channel (dihydropyridine receptor or DHPR). Interactions between RyR1 and DHPR are critical for the depolarization-induced activation of  $\text{Ca}^{2+}$  release from the sarcoplasmic reticulum, enhancement of DHPR  $\text{Ca}^{2+}$  channel activity, and repolarization-induced inactivation of RyR1. The DHPR III-IV loop was fused to glutathione S-transferase- or His-peptide and used as protein affinity columns for [ $^{35}\text{S}$ ]-labeled *in vitro*-translated fragments from the N-terminal three-fourths of RyR1. RyR1 residues Leu<sup>922</sup>-Asp<sup>1112</sup> bound specifically to the DHPR III-IV loop column, but the corresponding fragment from the cardiac ryanodine receptor (RyR2) did not. Construction of chimeras between RyR1 and RyR2 showed that amino acids Lys<sup>954</sup>-Asp<sup>1112</sup> retained full binding activity, while Leu<sup>922</sup>-Phe<sup>1075</sup> had no binding activity. The RyR1 sequence, Arg<sup>1076</sup>-Asp<sup>1112</sup>, previously shown to interact with the DHPR II-III loop (Leong, P., and MacLennan, D., H. (1998) *J. Biol. Chem.* **273**, 7791-7794), bound to DHPR III-IV columns, but with only half the efficiency of binding of the longer RyR1 sequence, Lys<sup>954</sup>-Asp<sup>1112</sup>. These data suggest that the site of DHPR III-IV interaction contains elements from both the Lys<sup>954</sup>-Phe<sup>1075</sup> fragment and the Arg<sup>1076</sup>-Asp<sup>1112</sup> fragment. The presence of  $4\pm 0.4\ \mu\text{M}$

GST DHPR II-III or  $5 \pm 0.1 \mu\text{M}$  His-peptide DHPR III-IV loop was required for half maximal co-purification of [ $^{35}\text{S}$ ]-labeled RyR1 Leu<sup>922</sup>-Asp<sup>1112</sup> on glutathione Sepharose or on NiNTA. Dose dependent inhibition of [ $^{35}\text{S}$ ]-labeled RyR1 Leu<sup>922</sup>-Asp<sup>1112</sup> binding to GST DHPR II-III by His<sub>10</sub> DHPR II-III and by His-peptide DHPR III-IV and dose dependent inhibition of [ $^{35}\text{S}$ ]-labeled RyR1 Leu<sup>922</sup>-Asp<sup>1112</sup> binding to GST DHPR III-IV by His<sub>10</sub> DHPR II-III and by His-peptide DHPR III-IV were observed. These studies indicate that the DHPR II-III and DHPR III-IV loops bind to contiguous and possibly overlapping sites on RyR1 between Lys<sup>954</sup>-Asp<sup>1112</sup>.

## INTRODUCTION

Excitation-contraction (E-C) coupling describes the events leading from electrical stimulation of muscle to the release of  $\text{Ca}^{2+}$  from the sarcoplasmic reticulum. Closure of the  $\text{Ca}^{2+}$  release channel and activation of the  $\text{Ca}^{2+}$  pump (SERCA) returns intracellular  $\text{Ca}^{2+}$  to resting levels (Lytton and MacLennan, 1992). Extracellular  $\text{Ca}^{2+}$  is not necessary for E-C coupling in skeletal muscle, but is required in cardiac muscle, distinguishing the mechanism of E-C coupling in these muscles (Catterall, 1991). E-C coupling in *RYR1* knockout mice can be restored in primary cultures of myotubes isolated from these mice by injection with *RYR1* cDNA (Nakai et al., 1996). During E-C coupling,  $\text{Ca}^{2+}$  release from the  $\text{Ca}^{2+}$  release channel of skeletal muscle sarcoplasmic reticulum (the ryanodine receptor or RyR1) is activated by the L-type  $\text{Ca}^{2+}$  channel of skeletal muscle (the dihydropyridine receptor or DHPR) (Rios and Brum, 1987). A retrograde signal from RyR1, but not RyR2 enhances the DHPR  $\text{Ca}^{2+}$  channel activity (Nakai et al., 1996; Nakai et al., 1997). In addition, the skeletal DHPR is critical for terminating  $\text{Ca}^{2+}$  release through RyR1 upon membrane repolarization (Suda and Penner, 1994; Suda, 1995; Suda and Heinemann, 1996). Regions of RyR1 important for interactions with DHPR leading to activation of  $\text{Ca}^{2+}$  release during E-C coupling and for retrograde enhancement of DHPR  $\text{Ca}^{2+}$  channel activity by

RyR1 have been identified through the study of RyR1-RyR2 chimeras in RyR1 knockout mice (Nakai et al., 1998). The complex physiology involving the multiple interactions between RyR1 and DHPR suggests that the structural interaction between RyR1 and DHPR may involve more than one site in the two proteins.

The importance of the DHPR II-III loop in E-C coupling has been demonstrated by Tanabe *et al.* (Tanabe et al., 1988; Tanabe et al., 1990a) through the study of dysgenic myotubes lacking DHPR. Skeletal-type E-C coupling can be reconstituted in these myotubes by injecting cDNA encoding chimeras between skeletal and cardiac DHPRs with only the II-III loop retaining the skeletal sequence. The DHPR II-III loop has been shown to activate the skeletal muscle ryanodine receptor in studies measuring  $\text{Ca}^{2+}$  currents across planar lipid bilayer carried by RyR1 (Lu et al., 1994; Lu et al., 1995).  $\text{Ca}^{2+}$  release has also been elicited from muscle triad vesicle preparations by the addition of the DHPR II-III loop peptide (el-Hayek et al., 1995). A protein affinity chromatography approach was used to identify an interaction site on RyR1 for the DHPR II-III loop (Leong and MacLennan, 1998b).

Malignant hyperthermia (MH) is an abnormality of  $\text{Ca}^{2+}$  regulation which is linked to *RYR1* on human chromosome 19 in at least 50% of cases (MacLennan and Phillips, 1992). A mutation in the DHPR III-IV loop has also been linked to susceptibility to MH (Monnier et al., 1997). Thus, the

DHPR III-IV loop may play a role in E-C coupling and a mutation in this loop could modify the interaction between the DHP and ryanodine receptors, mimicking the effects of mutations of RyR1 previously found to be causal for MH susceptibility. The studies in dysgenic mice (Tanabe et al., 1990a) which identify the DHPR II-III loop as being critical for RyR1 activation neither rule out nor implicate the III-IV loop in E-C coupling. In the present study we used protein affinity chromatography to demonstrate that the DHPR III-IV loop can interact with RyR1.

## MATERIALS and METHODS

*Chemicals and reagents* - All chemicals were of molecular biology grade.

NiNTA resin was purchased from Qiagen and Glutathione Sepharose 4B from Pharmacia. Translational grade [<sup>35</sup>S]-Met was obtained from Amersham. The coupled *in vitro* transcription and translation kit (TNT Quick) was from Promega. Rabbit skeletal and cardiac muscle cDNA was purified from  $\lambda$  phage cDNA libraries (Zorzato et al., 1990; Otsu et al., 1990) using mediprep columns from Qiagen. The rat N-type Ca<sup>2+</sup> channel  $\alpha 1B$  subunit III-IV loop in pTrcHis-C (Invitrogen) was a gift from W.A. Catterall, University of Washington. The full-length ryanodine receptor cDNA clone, pBS SRR10, has been described previously (Chen et al., 1993b).

*cDNA cloning and preparation of fusion proteins* - Nucleotides 1990 to 2381, encoding the rabbit skeletal muscle DHPR II-III loop were amplified and cloned using the polymerase chain reaction (PCR) as described previously (Leong and MacLennan, 1998b). Nucleotides 3198-3351, encoding Val<sup>1066</sup>-Ser<sup>1117</sup> of the DHPR III-IV loop were amplified using PCR, with the skeletal muscle cDNA library as template, and cloned; nucleotides 3492-3861 of the cardiac DHPR III-IV loop, Pro<sup>1164</sup>-Leu<sup>1287</sup>, were amplified, with the cardiac cDNA library as template, and cloned. Oligonucleotide primers flanking the cDNA sequence for the respective loops were designed with exterior *Bam*HI and *Eco*RI restriction endonuclease sites for in-frame cloning into the

ptrcHisC vector (InVitrogen) or the pGEX 3X vector (Pharmacia). Flanking *Bam*HI and *Eco*RI restriction endonuclease sites for in-frame cloning of the *RyR1* sequence encoding amino acid residues 922-1112 into the ptrcHisC vector (InVitrogen) were added to oligonucleotide primers used in PCR amplification of RyR1 nucleotides 2766-3335. All cloned fragments were verified by DNA sequence analysis. The modified pGEX vector (Pharmacia), which encodes glutathione-S-transferase (GST) with 10 His residues added to the C-terminal end of GST has been described (Leong and MacLennan, 1998b). The oligonucleotide attgaattccaccaccaccaccaccaccaccaccaccacaagcttgaattcata and its complementary oligonucleotide were used to add 10 His residues to the C-terminal end of DHPR II-III in the GST-DHPR II-III fusion protein by self-annealing of the 2 oligonucleotides, endonuclease restriction digestion at the *Eco*RI sites flanking the His<sub>10</sub> sequence, and ligation into the *Eco*RI-site of pGEX3X-DHPR II-III.

*E. coli* strain DH5 $\alpha$  (Gibco/BRL) was used for the expression of all fusion proteins. His-peptide (Invitrogen) fusion proteins, in 20 mM imidazole, pH 7.0, and protease inhibitors, were purified with NiNTA resin (Qiagen) and GST fusion proteins were purified with glutathione Separose 4B (Pharmacia) following standard procedures (Ausubel et al., 1997). After washing, the His-peptide fusion proteins were eluted with 0.5 M imidazole, pH 7.0, in

phosphate buffered saline (PBS). GST fusion proteins were eluted with 10 mM reduced glutathione and dialyzed against PBS overnight. Eluted proteins were analyzed by SDS-PAGE and coomassie blue-staining, and by dynamic light scattering (DynaPro-807, ProteinSolutions, Inc). Data analysis was performed with Dynamics (ProteinSolutions, Inc.). Protein yield was determined by the Bradford assay (Bio-rad).

GST-DHPR II-III-His<sub>10</sub> was purified by binding to 200 µl NiNTA resin. GST was cleaved from GST-DHPR II-III-His<sub>10</sub> by overnight incubation in the presence of 10 µg of Factor Xa (Sigma). The DHPR II-III His<sub>10</sub> was then eluted from NiNTA by 0.5 M Imidazole in PBS. DHPR II-III His<sub>10</sub> which had not been cleaved from GST were then removed by incubation with glutathione-sepharose.

*Preparation of ryanodine receptor fragments for in vitro*

*transcription/translation* – Fragments F1-F10 (Fig. 3.1A) for *in vitro* transcription and translation were prepared from pBS SRR10 (Chen et al., 1993b) downstream of a Kozak consensus start sequence (Kozak and Shatkin, 1979) and an ATG for translation initiation (Leong and MacLennan, 1998b). pBS RYR1 F3a, containing RyR1 nucleotides 2766-3335, and pBS RYR2 F3a, containing RyR1 nucleotides 2797 to 3378, were amplified by PCR from RYR cDNA. Chimeras between RyR1 and RyR2 were made using pBS RYR1 F3a and pBS RYR2 F3a through the introduction of restriction endonuclease



sites by PCR-based mutagenesis (QuikChange Kit, Stratagene) (Fig. 3.2A) as described previously (Leong and MacLennan, 1998b). The chimeric constructs are as follows with all numbering based on *RYR1*, not *RYR2*: pBS RYR1(923-1075)/RYR2(1076-1112), pBS RYR2(923-1075)/RYR1(1076-1112) and pBS RYR2(922-953)/RYR1(954-1112).

[<sup>35</sup>S]-Methionine –labeled RyR1 fragments were synthesized by coupled *in vitro* transcription and translation (TNT Quick, Promega), and quantified by TCA precipitation and scintillation counting (Ausubel et al., 1997).

*Column Binding Assay* – The binding assay was unchanged from Leong & MacLennan (Leong and MacLennan, 1998b). Briefly, purified His-peptide fusion protein (Invitrogen), GST fusion protein or GST-His<sub>10</sub> were bound to 40 µl fresh NiNTA or glutathione sepharose to achieve the desired concentration of fusion protein (mg/ml of sepharose). The amount of protein bound to affinity matrices was confirmed by eluting a sample of the protein-bound affinity matrix with SDS, separating the eluted protein by SDS-PAGE and staining with Coomassie Blue. Each stained fusion protein band was quantified by densitometry (Molecular Analyst, Bio-Rad). Resins to which fusion-proteins were bound were washed with 1 ml PBS, blocked with 1 mg of BSA in 200 µl of column buffer (10 mM Tris-HCl, pH 7.5, 0.15 M KCl, 20 µM CaCl<sub>2</sub>, 0.25 mM MgCl<sub>2</sub>, 20 mM imidazole, 0.1% Tween 20) and then with 0.4 mg of BSA in 400 µl of column buffer. [<sup>35</sup>S]-methionine-labeled fragments of

RyR, synthesized by coupled *in vitro* transcription and translation (TNT Quick, Promega) were diluted 10 fold into 200 µl of column buffer and then passed 3 times through affinity columns by gravity flow. The columns were washed with 600 µl of column buffer. Proteins retained on the affinity columns were eluted with 100 µl of SDS-sample buffer. SDS-PAGE (15% gel) was used to analyze 1 µl of the *in vitro* translation product (5% of the total column input), and 20 µl of the eluate (20% of the total column eluate). The gels were fixed 3 times in 6 vol of 10% methanol-12% acetic acid for 20 min each time. The radioactive signal was enhanced with Entensify (NEN Life Science Products) and the gels were dried and exposed to autoradiogram film (BioMax AR, Kodak). Radioactive signal of bands corresponding to the expected molecular mass of the RyR1 fragments were quantified by a Molecular Imager (Bio-Rad). Specific binding was defined as total binding less non-specific binding to GST-His<sub>10</sub> columns or GST columns.

*Co-purification of RyR1 fragments with DHPR loops*- Glutathione sepharose or NiNTA resin (40 µl) was blocked with 1 mg of BSA in 200 µl of column buffer and then with 0.4 mg of BSA in 400 µl of column buffer. Purified GST-DHPR II-III loop or His-peptide DHPR III-IV loop fragments at a concentration of 0.05-20µM in 200 µl column buffer were mixed for one hour with 20 µl coupled *in vitro* transcribed and translated, [<sup>35</sup>S]-methionine-

labeled RyR1 fragments and then passed once through the 40  $\mu$ l blocked glutathione sepharose or NiNTA columns. The columns were washed with 600  $\mu$ l of column buffer. RyR1 fragment-DHPR loop complexes retained on the resin were eluted with 100  $\mu$ l of SDS-sample buffer and analyzed by SDS-PAGE, and the [ $^{35}$ S]-labeled RyR1 fragments were quantified using a molecular imager as described above. The concentration of DHPR loop fusion protein required for half maximal saturation of co-purification of RyR1 fragment was estimated using curve-fitting software (CA Cricket GraphIII).

*Competition Binding Assay* – GST DHPR II-III and GST DHPR III-IV loop affinity columns were prepared as described in the column binding assay and blocked with 1 mg of BSA in 200  $\mu$ l of column buffer and then with 0.4 mg of BSA in 400  $\mu$ l of column buffer. [ $^{35}$ S]-methionine-labeled RyR1 F3a fragment (20  $\mu$ l) was mixed for one hour with 0.05-10  $\mu$ M purified His<sub>10</sub>-DHPR II-III loop or 0.05-25  $\mu$ M His-peptide DHPR III-IV loop in 200  $\mu$ l column buffer and then passed 3 times through 40  $\mu$ l GST DHPR II-III and GST DHPR III-IV affinity columns. The columns were washed with 600  $\mu$ l of column buffer. [ $^{35}$ S]-labeled RyR1 F3a-DHPR loop retained on the resin were eluted with 100  $\mu$ l of SDS-sample buffer and analyzed by SDS-PAGE, and the [ $^{35}$ S]-labeled RyR1 F3a fragment was quantified using a molecular imager as described under *column binding assay*. The concentration of DHPR loop required for

half maximal inhibition of RyR1 fragment binding was estimated using curve fitting software (CA Cricket GraphIII).

## RESULTS

### *Identification of an RyR1 sequence interacting with the DHPR III-IV loop -*

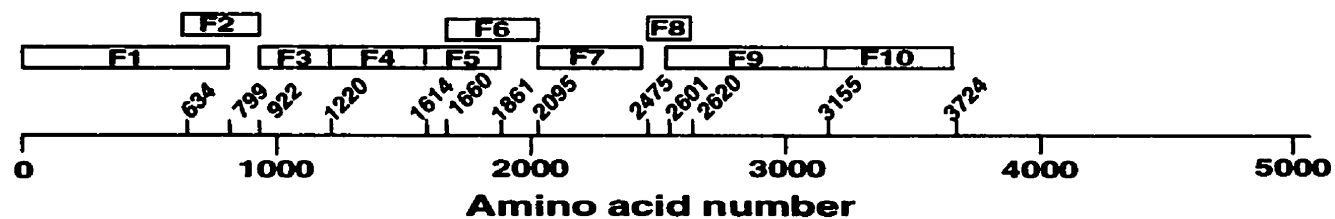
We scanned [<sup>35</sup>S]-labeled, *in vitro* translated RyR1 fragments for interactions with the DHPR III-IV loop immobilized on a Ni<sup>+</sup> column as a His-peptide fusion protein (Fig. 3.1). We found that 18±4.3% of *in vitro* translated fragment F3 (amino acids 922-1220) was retained on the DHPR III-IV loop affinity column (Figs. 3.1B and 3.1C). When the RyR1 fragment was reduced in size to 191 amino acids, spanning residues 922-1112, the proportion of the *in vitro* translated fragment retained on DHPR III-IV loop columns remained high at 13±1.3% (Figure 3.2).

We observed that the non-specific binding to GST-His<sub>10</sub> of [<sup>35</sup>S]-labeled RyR1 F5, [<sup>35</sup>S]-labeled RyR1 F8, and [<sup>35</sup>S]-labeled RyR1 F9 was over 15% of column input compared with less than 5% for the other RyR1 fragments (Fig. 3.1B).

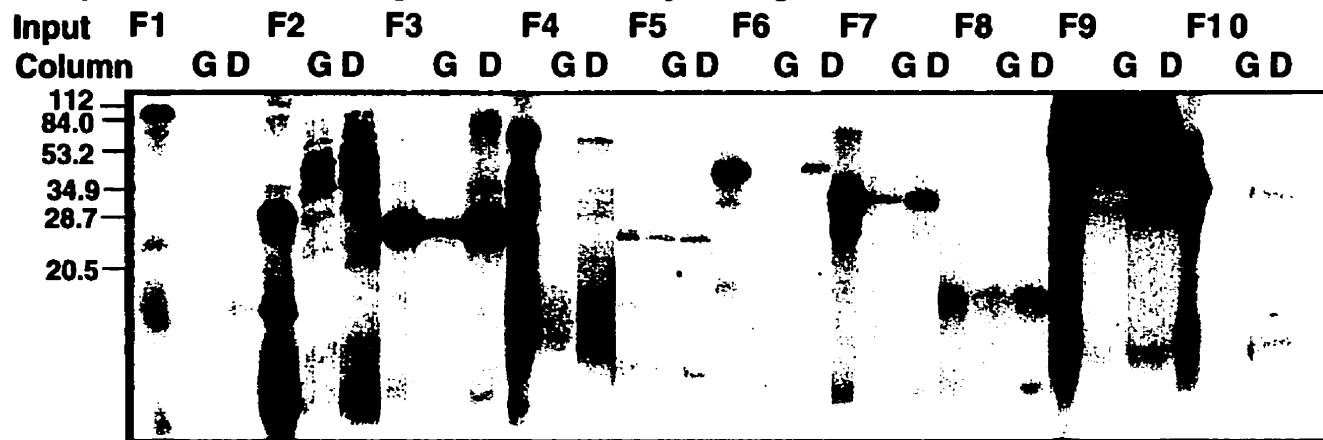
This raised the possibility that some *in vitro* transcribed/translated fragments may form non-specific aggregates with the affinity matrix and/or other proteins. In order to determine whether DHPR II-III, DHPR III-IV, or RyR1 (922-1112) fusion proteins form aggregates, we analyzed their dynamic light scattering characteristics. Assuming the proteins to be globular in nature, software-based conversion of hydrodynamic radii measurements to molecular mass (Dynamics, Protein-Solutions, Inc.) showed that 99% of the fusion proteins did not form high molecular weight aggregates. GST-DHPR II-III was estimated to be 94.8 kDa, which corresponds to the predicted

**Figure. 3.1 Binding of RyR1 fragments to the skeletal DHPR III-IV loop.** *In vitro* translated fragments of RyR1 were passed through 0.5 mg/ml His-peptide DHPR III-IV fusion protein columns, as described under *Materials and Methods*. **A**, schematic of RyR1 fragments cloned in-frame with a Kozak consensus start sequence (Kozak and Shatkin, 1979) and an initiator ATG codon for *in vitro* translation (Leong and MacLennan, 1998b). **B**, autoradiogram of *in vitro* translated RyR1 fragments (F1-F10) representing 5% of input and 20% of fragments eluted from GST-His<sub>10</sub> (G) and skeletal DHPR (D) affinity columns. Input lanes and fragments eluted from GST-His<sub>10</sub> (G) are identical to the autoradiogram in Fig. 2.1 B because experiments were done in parallel with either DHPR II-III or DHPR III-IV fusion protein columns. **C**, % specific binding of *in vitro* translated RyR1 fragments to the skeletal DHPR affinity columns, quantified by densitometry and expressed as the mean  $\pm$  SE from at least 4 separate experiments. Specific binding was defined as total binding to DHPR III-IV His-peptide fusion protein columns, less non-specific binding to GST-His<sub>10</sub>.

**A: *In vitro* translated fragments**



**B: autoradiogram of direct binding of  $^{35}\text{S}$ -labeled RyR1 fragments to DHPR III-IV**



**C: percentage binding**

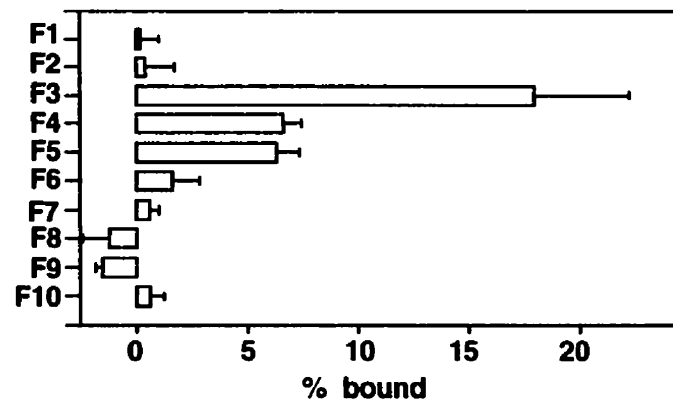
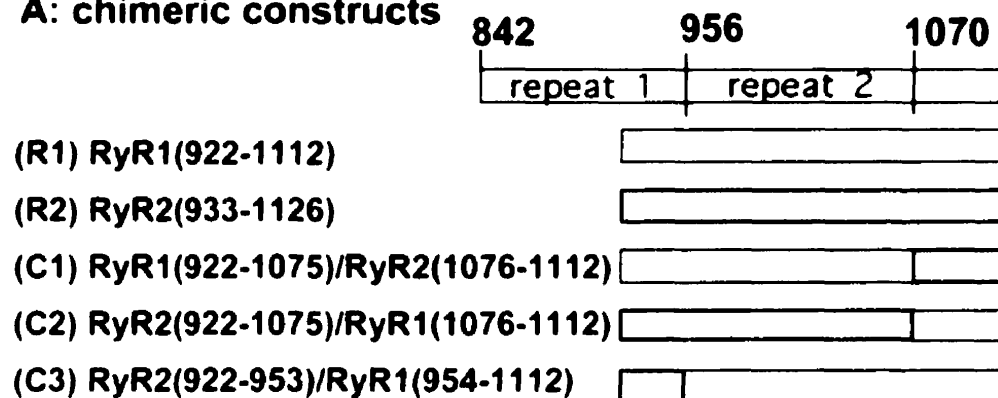


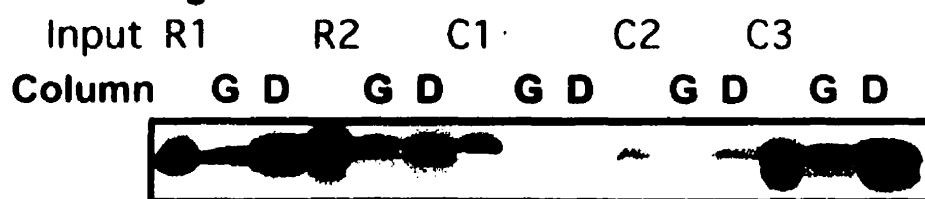
**Figure. 3.2 Binding of chimeric RyR1/RyR2 constructs to the skeletal DHPR III-IV loop.** **A**, chimeric RyR1/RyR2 constructs prepared as previously described (Leong and MacLennan, 1998b). The first line represents a region in RyR1 containing 2 repeat sequences and defines their respective boundaries. Amino acid numbering refers to RyR1 residues in the chimeric constructs. **B**, autoradiogram of *in vitro* translated RyR1/RyR2 chimeric fragments representing 5% of input and 20% of fragments eluted from 0.5 mg/ml GST-His<sub>10</sub> (G) and skeletal DHPR III-IV (D) affinity columns. Input lanes and fragments eluted from GST-His<sub>10</sub> (G) are identical to the autoradiogram in Fig. 2.2 B because experiments were done in parallel with either DHPR II-III or DHPR III-IV fusion protein columns. **C**, % specific binding of *in vitro* translated RyR1/RyR2 chimeric fragments to the skeletal DHPR affinity columns, quantified by densitometry and expressed as the mean  $\pm$  SE from at least 4 separate experiments. Specific binding was defined as total binding to DHPR III-IV His-peptide fusion protein columns, less non-specific binding to GST-His<sub>10</sub>.



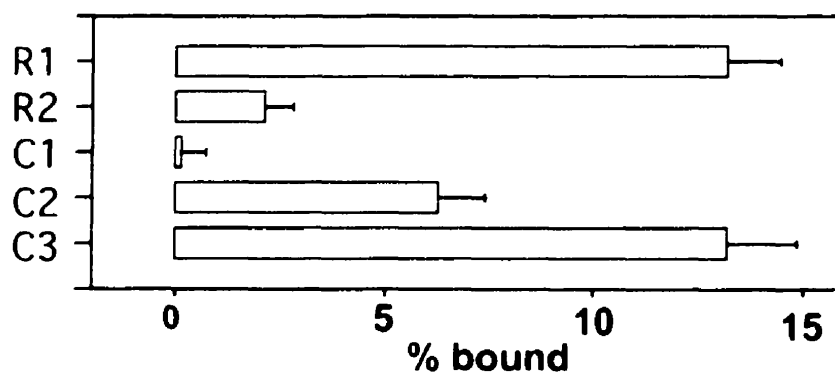
### A: chimeric constructs



### B: autoradiogram



### C: percentage binding



molecular mass of a dimer of two 49.5 kDa GST DHPR II-III fusion proteins and similarly, GST DHPR III-IV was estimated to be 65.2 kDa, which corresponds to the predicted molecular mass of a dimer of two 33.1 kDa GST DHPR III-IV fusion proteins. GST fusion proteins are known to dimerize in solution (Walker et al., 1993). Therefore, dimerization of the DHPR II-III and DHPR III-IV loop fusion proteins was expected. His-peptide RyR1 (922-1112) was estimated to be 26.9 kDa, which corresponds to its predicted molecular mass of 24.5 kDa. In addition, no high molecular weight aggregates were observed when GST-DHPR II-III and His-peptide RyR1 (922-1112) or GST-DHPR III-IV and His-peptide RyR1 (922-1112) were mixed together in a 1:1 ratio.

To test the isoform specificity of the RyR1 interaction with DHPR, we passed [<sup>35</sup>S]-labeled, *in vitro* translated fragments of RYR2 over the affinity column. We did not detect specific binding of RyR2(933-1126) (corresponding to RYR1(922-1112)) to the skeletal DHPR III-IV loop affinity column (Figure 3.2).

Because further reduction in the size of the RyR1 fragment resulted in loss of synthesis of the *in vitro* translated product, we reduced the size of the RyR1 sequence that binds to the DHPR III-IV loop by making chimeras between RyR1 and RyR2, as illustrated in Fig. 3.2A. The RyR1(922-1075)/RyR2(1076-1112) (C1) chimera did not bind to the III-IV loop, but 13±1.7% of the RyR2(922-953)/RyR1(954-1112) (C3) chimera and 6±1.1% of

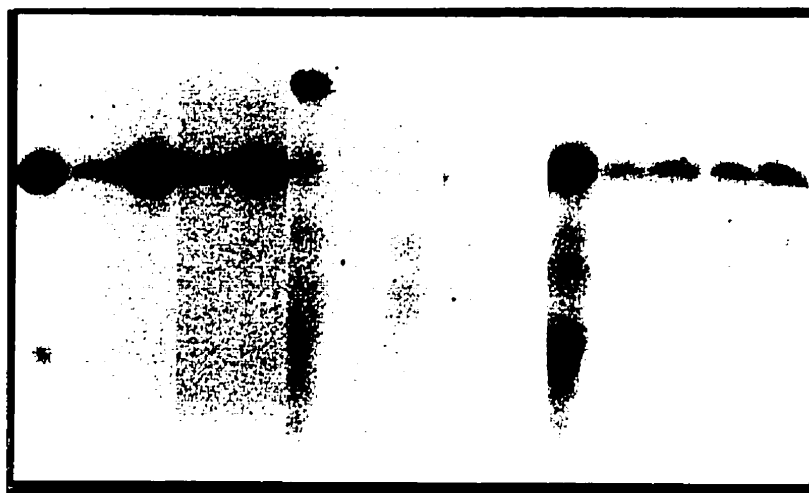
the RyR2(922-1075)/RyR1(1076-1112) (C2) chimera were retained on a 0.5 mg/ml DHPR III-IV loop affinity column (Figs. 3.2B and 3.2C). These results indicate that the 37 RyR1 amino acids, Arg<sup>1076</sup> to Asp<sup>1112</sup>, previously shown to interact with the DHPR II-III loop (15), do not by themselves form the binding site for both the DHPR II-III and DHPR III-IV loops, but do not rule out the possibility that they might contribute to the binding site for the DHPR III-IV loop. Clearly, RyR1 residues between Lys<sup>954</sup> and Val<sup>1075</sup> contribute to the binding site for DHPR III-IV.

*Co-purification of RyR1 (922-1112) with DHPR loops* – Greater than 6% of two adjacent RyR1 fragments, 1220-1614 (F4) and 1614-1861 (F5), were also retained on the His-peptide DHPR III-IV column compared to less than 2% for any of the other fragments of RyR1 lying between amino acids 1 and 3724 (Fig. 3.1). A complementary test of protein-protein interactions is to mix two potentially interacting proteins in solution and then purify complexes containing the two proteins. We found that 16±2.6% of [<sup>35</sup>S]-labeled RyR1 (922-1112) co-purified with His-peptide DHPR III-IV loops on NiNTA, while less than 2% of [<sup>35</sup>S]-labeled RyR1 F4 and less than 5% of [<sup>35</sup>S]-labeled RyR1 F5 were co-purified under similar conditions (Fig. 3.3). We also observed that 54±1.0% of [<sup>35</sup>S]-labeled RyR1 (922-1112) co-purified with GST DHPR II-III His<sub>10</sub> on NiNTA, but less than 5% of [<sup>35</sup>S]-labeled RyR1 F4 and [<sup>35</sup>S]-labeled RyR1 F5 co-purified with GST DHPR II-III His<sub>10</sub>.

**Fig 3.3 Co-purification of RyR1 fragments with DHPR loops.** *In vitro* translated fragments of RyR1 were passed through Glutathione Sepharose and NiNTA with (+) and without (-) prior incubation with DHPR loop fusion proteins, as described under *Materials and Methods*. **A**, autoradiogram of [<sup>35</sup>S]-labeled RyR1 fragments co-purified with GST DHPR II-III (2/3) on glutathione Sepharose and [<sup>35</sup>S]-labeled RyR1 fragments co-purified with His-peptide DHPR III-IV (3/4) on NiNTA representing 5% of input and 20% of fragments co-purified with DHPR II-III and DHPR III-IV loops. **B**, % specific co-purification of *in vitro* translated RyR1 fragments with DHPR loops, quantified by densitometry and expressed as the mean  $\pm$  SE from at least 4 separate experiments. Specific binding was defined as total binding to glutathione Sepharose and NiNTA columns, less non-specific binding in the absence of DHPR loop fusion proteins.

# **A: autoradiogram**

Input R1(922-1112) R1(1220-1614) R1(1614-1861)  
 20  $\mu$ M DHPR loop -2/3+2/3-3/4+3/4 -2/3+2/3-3/4+3/4 -2/3+2/3-3/4+3/4



# **B: percentage co-purification**

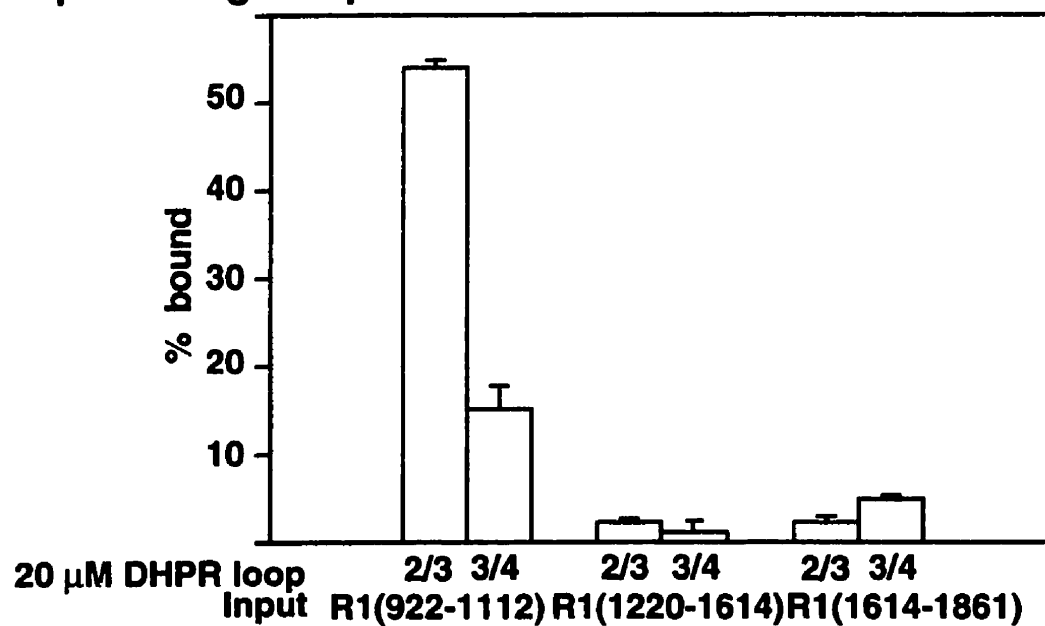
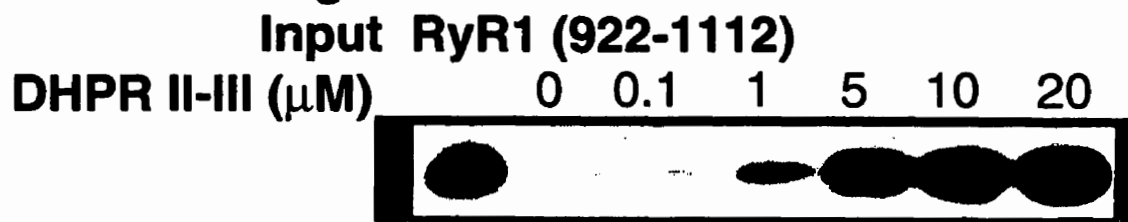
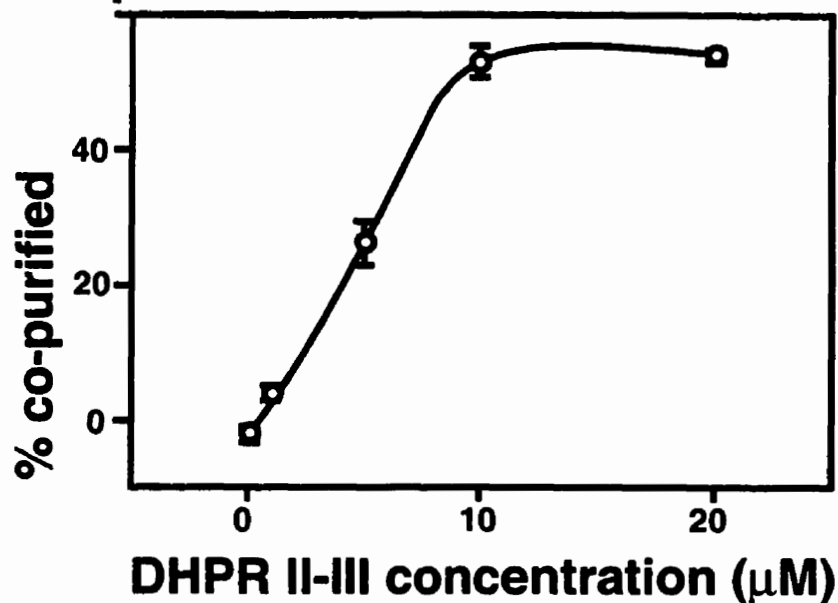


**Fig. 3.4 Saturation co-purification of RyR1 (922-1112) by DHPR II-III loop GST fusion protein and of RyR1 (922-1112) by DHPR III-IV loop His-peptide fusion proteins. A and C, autoradiogram of *in vitro* translated RyR1 (922-1112) fragment representing 5% of input and 20% of fragments co-purified with GST DHPR II-III on glutathione Sepharose or with His-peptide DHPR III-IV on NiNTA, as described under *Materials and Methods*. B and D, % specific co-purification of *in vitro* translated RyR1 fragments with DHPR II-III and DHPR III-IV, quantified by densitometry and expressed as the mean  $\pm$  SE from at least 4 separate experiments. Specific binding was defined as total binding to glutathione Sepharose or NiNTA columns, less non-specific binding in the absence of DHPR loop fusion proteins.**

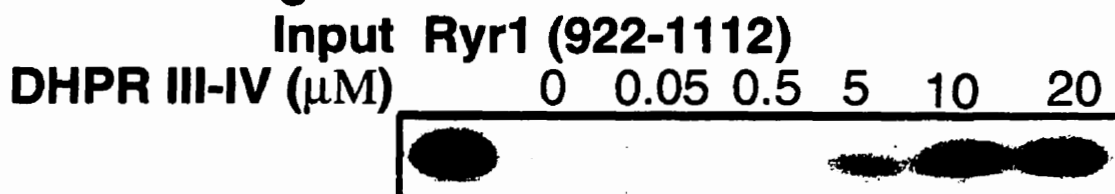
**A: autoradiogram**



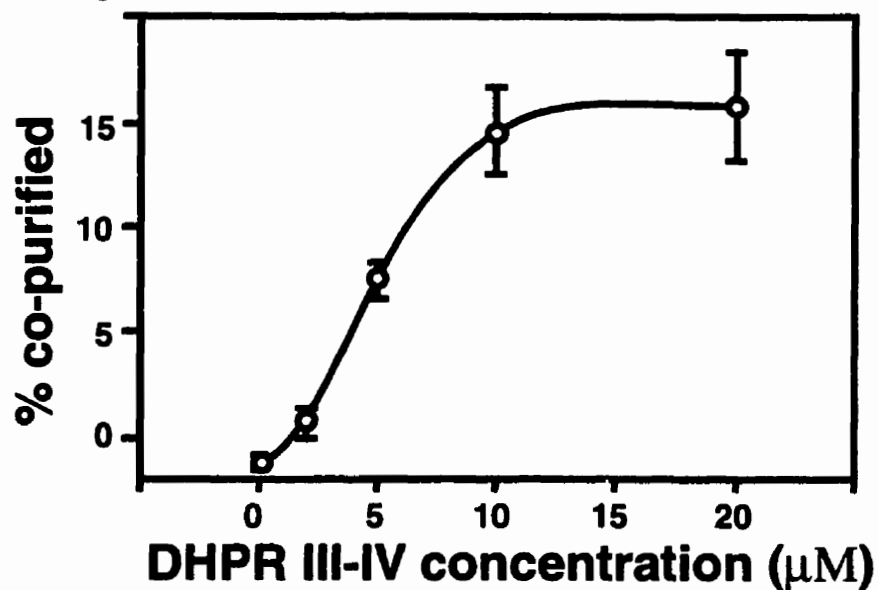
**B: saturation co-purification**



**C: autoradiogram**



**D: saturation co-purification**



We mixed [<sup>35</sup>S]-labeled RyR1 (922-1112) with DHPR II-III and DHPR III-IV to determine the concentration of DHPR loops in solution required for half-maximal co-purification of picomolar concentration of *in vitro* transcribed/translated [<sup>35</sup>S]-labeled RyR1 (922-1112) (Figure 3.4). Half maximal purification of RyR1 (922-1112) - GST DHPR II-III complexes on glutathione Sepharose was at 4±0.4 μM GST DHPR II-III fusion protein. Half maximal purification of RyR1 (922-1112) – His-peptide DHPR III-IV complexes on NiNTA was at 5±0.1 μM His-peptide DHPR III-IV fusion protein. [<sup>35</sup>S]-labeled RyR1 (922-1112) which did not associate with DHPR loops was found in the flow through (data not shown). Given the low affinity, it was not possible to use dynamic light scattering to detect complexes forming between His-peptide RyR1 (922-1112) and GST DHPR loop fusion proteins in a 1:1 mixture of the two proteins.


*Competitive Inhibition of RyR1 (922-1112) to DHPR loops* - Binding of picomolar concentrations of [<sup>35</sup>S]-labeled RyR1 to a GST-DHPR II-III affinity column was inhibited in a dose dependent manner by both His<sub>10</sub>-DHPR II-III and His-peptide DHPR III-IV at a concentration of 0.05-25 μM (Fig. 3.5A). Similarly, binding of [<sup>35</sup>S]-labeled RyR1 to GST-DHPR III-IV affinity column was inhibited in a dose dependent manner by 0.05-25 μM His<sub>10</sub>-DHPR II-III or His-peptide DHPR III-IV (Fig. 3.5B). The concentration of His<sub>10</sub>-DHPR II-III required to inhibit binding of RyR1 (922-1112) fragment to GST-DHPR II-



**Fig. 3.5. Competitive Inhibition of RyR1 (922-1112) binding to DHPR loops.** Autoradiogram of *in vitro* translated RyR1 (922-1112) mixed with the indicated concentrations of DHPR II-III and DHPR III-IV loops and passed through, **A**, GST DHPR II-III columns and, **B**, GST DHPR III-IV columns as described under *material and methods*. **C**, Inhibition of RyR1 (922-1112) binding by DHPR II-III to GST DHPR II-III columns (squares) or GST DHPR III-IV columns (diamonds) quantified by densitometry and expressed as the mean $\pm$ SE of at least 3 separate experiments. **D**, Inhibition of RyR1 (922-1112) binding by DHPR III-IV to GST DHPR II-III columns (squares) or GST DHPR III-IV columns (diamonds) quantified by densitometry and expressed as the mean $\pm$ SE of at least 3 separate experiments.


### A: Binding to GST DHPR II-III Column

Input	Ryr1 (922-1112)						
Column	G	DHPR II-III					
Competitor ( $\mu\text{M}$ )		0	DHPR II-III			DHPR III-IV	
			0.05	0.5	7.5	0.05	1.0 20

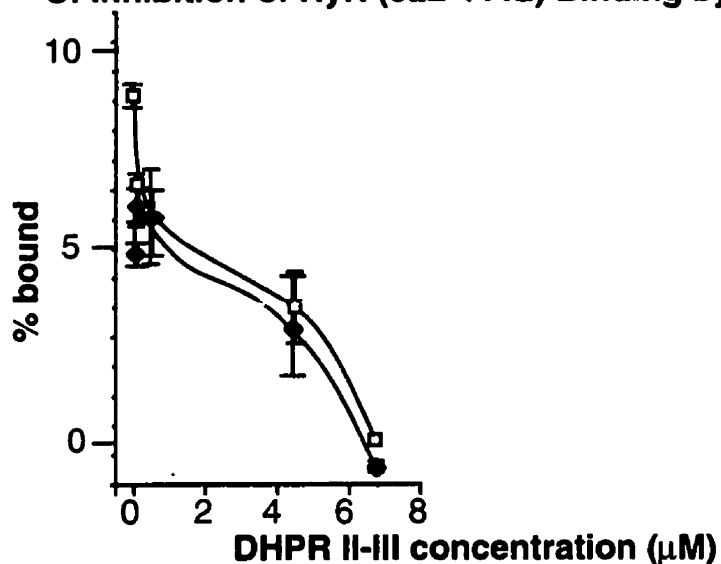


### B: Binding to GST DHPR III-IV Column

Input	RyR1 (922-1112)						
Column	G	DHPR III-IV					
Competitor ( $\mu\text{M}$ )		0	DHPR II-III			DHPR III-IV	
			0.05	0.5	7.5	0.05	1.0 20



### C: Inhibition of RyR (922-1112) Binding by DHPR II-III



### D: Inhibition of RyR (922-1112) Binding by DHPR III-IV

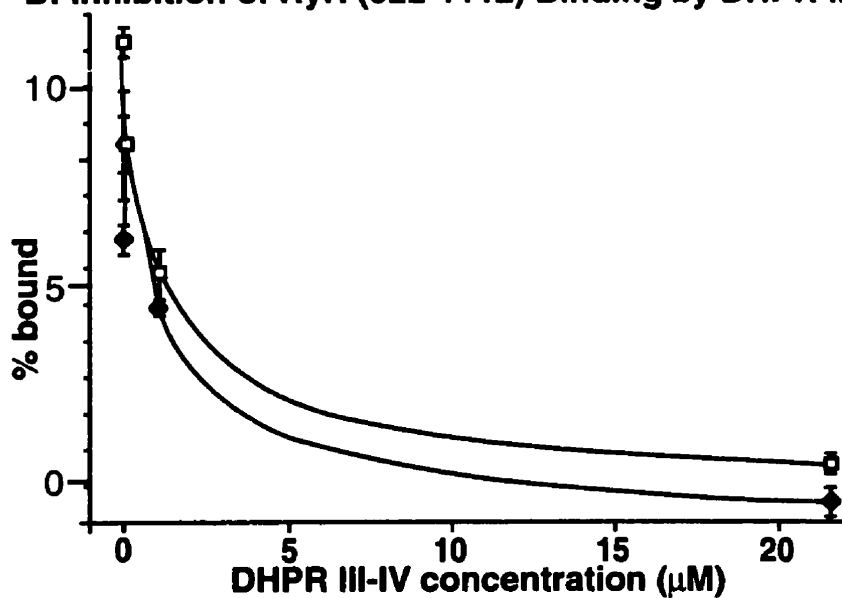
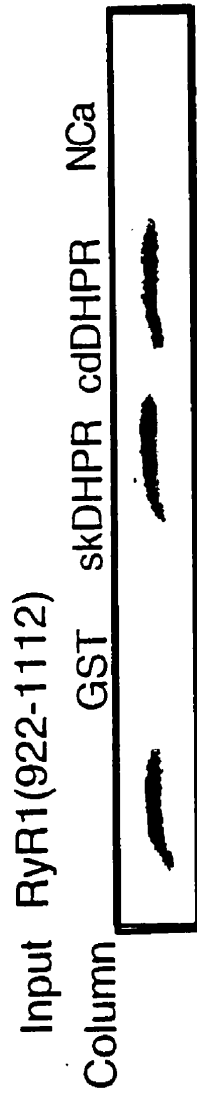
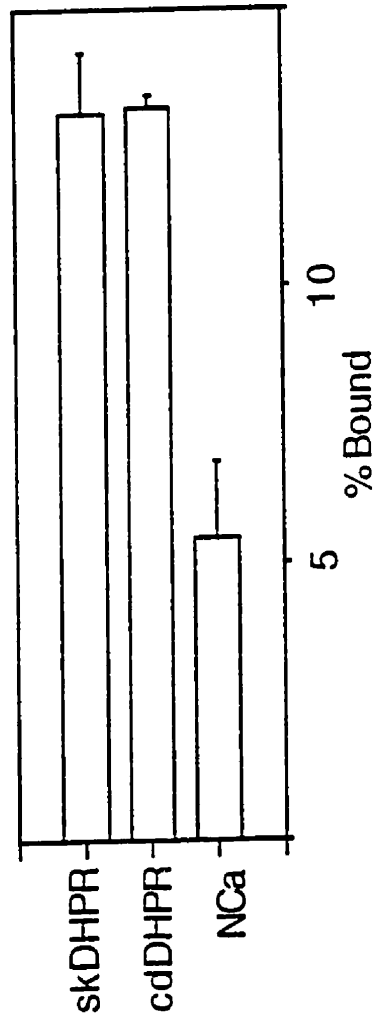


**Fig. 3.6 Binding of RyR1 (922-1112) constructs to skeletal and cardiac  $\text{Ca}^{2+}$  and N-type  $\text{Ca}^{2+}$  channel III-IV loop-GST fusion proteins.** **A,** autoradiogram of *in vitro* translated RyR1(922-1112) fragment representing 5% of input and 20% of fragments eluted from different 0.1 mg/ml GST fusion protein affinity columns: GST(G); skeletal DHPR III-IV loop (skDHPR); cardiac DHPR III-IV loop (cdDHPR); N-type  $\text{Ca}^{2+}$  channel III-IV loop (NCa). **B,** % specific binding of *in vitro* translated fragment to the III-IV loop affinity columns, quantified by densitometry and expressed as the mean  $\pm$  SE from at least 4 separate experiments. Specific binding was defined as total binding to GST fusion protein columns, less non-specific binding to GST. **C,** sequence alignment of segments of skeletal and cardiac muscle  $\text{Ca}^{2+}$  and N-type  $\text{Ca}^{2+}$  channel III-IV loops with residues different from skDHPR underlined and proportion of residues identical to skDHPR shown on the right.

### A: autoradiogram



### B: percentage binding



### C: sequence alignment

	Identity
III-IV loop	54/54
skDHPR	46/54
cdDHPR	25/54
NCa	

V	P	F	Q	E	Q	G	E	T	E	Y	K	N	C	E	L	D	K	N	Q	R	Q	C	V	Q	V	A	L	K	A	R	P	L	R	C	Y	I	P	K	N	--	P	Y	Q	Y	Q	V	W	V	V	T	S	S	Y				
V	P	F	Q	E	Q	G	E	T	E	Y	K	N	C	E	L	D	K	N	Q	R	Q	C	V	Q	V	E	Y	A	I	.	K	A	R	P	L	R	R	Y	I	P	K	N	--	Q	H	Q	Y	K	V	W	V	V	N	S	T	Y	
T	P	F	Q	E	Q	G	D	K	V	M	S	E	C	S	I	.	E	K	N	E	R	A	C	I	D	F	A	I	.	S	A	K	P	L	T	R	Y	M	P	Q	N	K	Q	S	F	Q	Y	K	T	W	T	.	V	V	S	P	P

III and GST-DHPR III-IV was comparable (Fig. 3.5C). The concentration of His-peptide DHPR III-IV required to inhibit binding to GST-DHPR II-III and GST-DHPR III-IV was comparable (Fig. 3.5D).

*DHPR specificity in the RyR1/DHPR interaction* – A GST fusion protein affinity column of skeletal muscle DHPR III-IV loop (skDHPR) retained  $13 \pm 1.1\%$  of the input of the *in vitro* translated RyR1 fragment; the corresponding cardiac muscle DHPR III-IV loop (cdDHPR) retained  $13 \pm 0.2\%$ ; and the N-type  $\text{Ca}^{2+}$  channel III-IV loop (NCa) retained  $5 \pm 1.4\%$  (Figs. 3.6A and 3.6B). Skeletal and cardiac muscle DHPR III-IV loops are identical in 46 of 54 amino acids. The fact that only 24 of 54 amino acids are identical between the N-type  $\text{Ca}^{2+}$  channel III-IV loop and the skeletal DHPR III-IV loop is consistent with the reduced binding of RyR1 (922-1112) to the GST N-type  $\text{Ca}^{2+}$  channel III–IV loop.

## DISCUSSION

In this study, we localized a binding site for the skeletal muscle DHPR III-IV loop to F3(922-1112), a 191 amino acid sequence between Leu<sup>922</sup> and Asp<sup>1112</sup>, in *in vitro* transcribed and translated fragments of RyR1 (Fig. 3.1 and 3.2). About 13% of this fragment applied to a DHPR III-IV affinity column was bound specifically. We also noted binding of about 6-7% of fragments F4 and F5 to the same column. If complexes between DHPR II-III or III-IV loops and radioactive fragments F3(922-1112), F4 or F5 were made in solution and then passed over columns that would bind the DHPR loops, copurification of F3 was observed for both the II-III and III-IV loops (Fig. 3.3), but very little copurification of F4 or F5 was observed under comparable conditions. Thus RyR1 F4 and RyR1 F5 may have been retained on His-peptide DHPR III-IV columns due to non-specific interactions with high matrix concentrations of His-peptide DHPR III-IV(Fig. 3.3). RyR1 F5 was observed to interact with proteins unrelated to DHPR, including GST, supporting the view that RyR1 F5 can interact non-specifically with proteins. The interaction between F3 (922-1112) and DHPR loops is not due to the formation of large aggregates, since analysis of dynamic light scattering determined that high molecular weight aggregates made up less than 1% by mass of His-peptide RyR1 (922-1112), GST-DHPR II-III and GST-DHPR III-

IV fusion protein preparations, either alone or in combination with each other.

Decreasing the size of the RyR1 (922-1112) fragment resulted in loss of *in vitro* translation and His-peptide fusion proteins of RyR1 fragments shorter than 191 amino acids were unstable, suggesting that the complete sequence might form a stable structural domain. We made use of repeat domain boundaries in RyR (Zorzato et al., 1990; Otsu et al., 1990; Hakamata et al., 1992) to create 3 RyR1/RyR2 chimeras (Fig. 3.2A). The chimera C2, which retained partial binding to the DHPR III-IV loop column, and chimera C3, which retained full binding, both contained the 37 amino acid sequence, Arg<sup>1076</sup> to Asp<sup>1112</sup>, previously identified as being important for interaction with the DHPR II-III loop (Leong and MacLennan, 1998b). However, the sequence, Arg<sup>1076</sup> to Asp<sup>1112</sup>, was absent from chimera C1, which did not bind the DHPR III-IV loop. The RyR1 repeat sequence 2, which is included in chimera C3, contributes to the DHPR III-IV interaction site and may form part of a structural domain and be important for proper folding.

An estimate of the affinity for RyR1 (922-1112) of DHPR II-III and DHPR III-IV can be derived from the concentration of DHPR loops required for half maximal co-purification of picomolar [<sup>35</sup>S]-labeled RyR1 (922-1112) with GST DHPR II-III on Glutathione Sepharose and with His-peptide DHPR III-IV on NiNTA (Fig. 3.4). The concentration of DHPR II-III required was  $4 \pm 0.4 \mu\text{M}$  and the concentration of DHPR III-IV was  $5 \pm 0.1 \mu\text{M}$ .

Unfortunately, the affinity was not high enough to permit resolution of RyR1-DHPR complexes using dynamic light scattering.

We attempted to verify that the RyR1 region which we identified as interacting with DHPR II-III also constituted part of the interaction site of DHPR III-IV (Fig. 3.2) through the use of a competition binding assay (Fig. 3.5). As expected, the complex between DHPR II-III and RyR1 (922-1112) was inhibited from binding to a DHPR II-III affinity column, and the complex between DHPR III-IV and RyR1 (922-1112) was inhibited from binding to the DHPR III-IV affinity column. We also observed the inhibition of binding of the complex between soluble His-peptide DHPR III-IV and RyR1 (922-1112) to a GST DHPR II-III affinity column, and the inhibition of binding of the complex between His<sub>10</sub> DHPR II-III and RyR1 (922-1112) to a DHPR III-IV column. These results can be interpreted in two ways. One possibility is that DHPR II-III binds to a site on RyR1 (922-1112) which overlaps with the binding site for DHPR III-IV. Alternatively, the accessibility of a GST DHPR loop on protein affinity columns to its binding site on RyR1 bound to a DHPR loop in solution may be restricted by the size of the fusion proteins already bound to RyR1 (922-1112). This is particularly relevant considering that the GST portion of the fusion contains about 250 amino acids. The close relationship between the concentration of DHPR II-III required for half maximal inhibition of RyR1 (922-1112) binding to GST-DHPR II-III or to GST DHPR III-IV (Fig 3.5C) suggests that soluble complexes form in solution



between DHPR II-III and RyR1(922-1112). These concentrations are equivalent to the 4  $\mu$ M DHPR II-III required for half-maximal saturation of binding to RyR1 in the RyR1 (922-1112) co-purification studies (Figs. 3.4A and 3.4B). The concentration of DHPR III-IV required for half maximal inhibition of RyR1 (922-1112) binding to GST DHPR II-III and GST III-IV affinity columns was also similar (Fig 3.5D). These concentrations are also equivalent to the 5  $\mu$ M DHPR III-IV required for half maximal saturation of formation of soluble complexes between DHPR III-IV and RyR1 (922-1112) (Figs. 3.4C and 3.4D).

Since skeletal and cardiac DHPR III-IV loop are highly conserved, it was not surprising that RyR1 (922-1112) bound to GST fusion protein affinity columns made up from both the skeletal and cardiac DHPR III-IV loops (Fig 3.6). The decrease in binding to a GST fusion protein of the loop linking domains III and IV of the rat N-type  $\text{Ca}^{2+}$  channel corresponds to the decrease in amino acid identity with DHPR III-IV.

Yamazawa *et al.* (Yamazawa et al., 1997) reported that deletion of RyR1 (1303-1406) abolishes the ability of RyR1 to mediate skeletal E-C coupling, although E-C coupling is preserved when the RyR1 (1303-1406) sequence is converted to the RyR2 sequence. The deletion of RyR1 (1303-1406) may alter the structure of RyR and thus disrupt interactions with DHPR. This is consistent with the finding that the conversion of the

RyR1(1303-1406) sequence to the corresponding RyR2 sequence does not disrupt E-C coupling, since the homology between RyR1 and RyR2 is likely sufficient to preserve native RyR structure (Yamazawa et al., 1997). Nakai *et al.* (Nakai et al., 1998) used chimeras between RyR1 and RyR2 to show that RyR1 (1635-2636) is sufficient for skeletal *vs.* cardiac muscle-type E-C coupling and that RyR1 (1635-2636) and RyR1 (2659-3720) are sufficient for enhancement of DHPR Ca<sup>2+</sup> channel activity. It is possible that the sites defined in these studies of RyR1-RyR2 chimeras may reflect an interaction resulting from the folding of RyR that brings together amino acids which are very distant in the linear sequence. Thus, the comparatively short sequences which we use to test for interactions may not contain all of the amino acids required for a high affinity interaction site. The high levels of non-specific binding of some RyR1 fragments to GST-His<sub>10</sub>, including RyR1 F4 and RyR1 F5 may mask weaker binding interactions to DHPR loops. The possibility that some RyR1 fragments may aggregate, thereby preventing their interaction with DHPR, may also mask weaker binding interactions.

Monnier *et al.* (Monnier et al., 1997) have demonstrated that an A1086H mutation in the loop linking DHPR domains III and IV in the  $\alpha$ 1-subunit of the skeletal muscle DHPR can be linked to susceptibility to malignant hyperthermia (MH). A mutation in DHPR which disrupts the termination of Ca<sup>2+</sup> release through RyR1 upon repolarization (Melzer et al., 1987; Schneider and Simon, 1988; Rios and Pizarro, 1991; Suda, 1995) might

display the same clinical phenotype as a mutation in RyR1 which alters the regulation of  $\text{Ca}^{2+}$  release (Mickelson and Louis, 1996; Otsu et al., 1994; Treves et al., 1994; Tong et al., 1997). The  $\text{Ca}^{2+}$  flux through wild-type DHPR is slow and of small magnitude (Tanabe et al., 1988), and the mutant is unlikely to be different. A mutation in the DHPR III-IV loop is unlikely to alter  $\text{Ca}^{2+}$  conductance since this loop does not form part of the channel pore and has not been identified as being important for either regulation or inactivation of DHPR (Catterall, 1996). The DHPR mutation does not lead to other symptoms of ion channel disease, suggesting that it does not affect L-type  $\text{Ca}^{2+}$  channel function (Monnier et al., 1997). The chimera studies in dysgenic mice (Tanabe et al., 1990a) identifying the II-III loop as being critical to EC coupling were not used either to rule out or to implicate the III-IV loop in E-C coupling. Thus, we propose that a possible function arising from the interaction between RyR1 (954-1112) and the DHPR III-IV loop is to terminate  $\text{Ca}^{2+}$  release through RyR1 during repolarization. A C-terminal peptide from amino acids 1487-1506 of the skeletal DHPR has been shown to inhibit the  $\text{Ca}^{2+}$  release function of RyR1 (Slavik et al., 1997), but the RyR1 interaction site is not known. It is possible that amino acids 1487-1506 in the C-terminal end of skeletal DHPR act in conjunction with amino acids in the DHPR III-IV loop.

The region we have identified may be important in the DHPR interaction with RyR1 at the junction between T-tubules and the terminal

cisternae of sarcoplasmic reticulum. In skeletal muscle, but not cardiac muscle, DHPRs are clustered in groups of four and positioned in exact correspondence with RyR1 tetramers so that each DHPR is located immediately opposite to one of the RyR1 subunits (Block et al., 1988; Franzini-Armstrong and Protasi, 1997). Structural studies of mice with a targeted disruption of the skeletal muscle *RYR1* gene have shown that the arrangement of DHPRs into groups of four is dependent on the presence of RyR1 (Takekura et al., 1994). Thus another possible function for the interaction between RyR1 (954-1112) and the DHPR III-IV loop that we have identified might be clustering of DHPR into groups of four in skeletal muscle. The absence of interaction with DHPR that we observe with the RyR2 sequence corresponding to RyR1 (922-1112) would be in line with this proposal (Figure 3.2).

Alignment of inositol triphosphate (IP<sub>3</sub>) and ryanodine receptor sequences reveals that the Ca<sup>2+</sup> channel forming domain and the domains which are important for regulation of channel opening are conserved between IP<sub>3</sub> Receptors and RyR. The region that we have identified as an interaction site between RyR1 and both DHPR II-III and DHPR III-IV is not present on IP<sub>3</sub> receptors (Furuichi et al., 1989; Loke and MacLennan, 1998) and is, therefore, a domain unique to RyR which might be important for E-C coupling.

Site directed mutagenesis of residues between Leu<sup>954</sup> and Asp<sup>1112</sup> which differ between RyR1 and RyR2 are likely to yield information on the amino acids which constitute the interaction site between the two proteins. Generation of antibodies against these sequences or high resolution structural studies of RyR1-DHPR complexes should yield detailed information concerning these interactions. The introduction of RyR1/RyR2 chimeras into myoblasts lacking RyR1 will define the functional importance of the interaction of DHPR II-III with RyR1 (1076-1112) and DHPR III-IV with RyR1 (954-1112). The introduction of RyR/IP<sub>3</sub> receptor chimeras into myoblasts lacking RYR1 will allow characterization of a domain unique to RyR.

## **CHAPTER 4**

### **Single Channel Properties of the Recombinant Skeletal Muscle $\text{Ca}^{2+}$ Release Channel (Ryanodine Receptor)**

## Chapter Summary

We report transient expression of a full length cDNA encoding the  $\text{Ca}^{2+}$  release channel of rabbit skeletal muscle sarcoplasmic reticulum (ryanodine receptor) in HEK-293 cells. The single channel properties of the CHAPS-solubilized and sucrose gradient-purified recombinant  $\text{Ca}^{2+}$  release channels were investigated using single channel recordings in planar lipid bilayers. The recombinant  $\text{Ca}^{2+}$  release channel exhibited a  $\text{K}^+$  conductance of 780 pS when symmetrical 250 mM KCl was used as the conducting ion and a  $\text{Ca}^{2+}$  conductance of 116 pS in 50 mM luminal  $\text{Ca}^{2+}$ . Opening events of the recombinant channels were brief, with an open time constant of about 0.22 ms. The recombinant  $\text{Ca}^{2+}$  release channel was more permeable to  $\text{Ca}^{2+}$  than to  $\text{K}^+$ , with a  $\text{pCa}^{2+}/\text{pK}^+$  ratio of 6.8. The response of the recombinant  $\text{Ca}^{2+}$  release channel to various concentrations of  $\text{Ca}^{2+}$  was biphasic, with the channel being activated by micromolar  $\text{Ca}^{2+}$  and inhibited by millimolar  $\text{Ca}^{2+}$ . The recombinant channels were activated by ATP and caffeine, inhibited by  $\text{Mg}^{2+}$  and ruthenium red, and modified by ryanodine. Most recombinant channels were asymmetrically blocked, conducting current unidirectionally from the luminal to the cytoplasmic side of the channel. These data demonstrate that the properties of recombinant  $\text{Ca}^{2+}$  release channel expressed in HEK-293 cells are very similar, if not identical, to the native channel.

## INTRODUCTION

The  $\text{Ca}^{2+}$  release channel of skeletal muscle sarcoplasmic reticulum (the ryanodine receptor) is located in the junctional terminal cisternae, in close apposition to the transverse tubular membrane (Inui et al., 1987a). It plays a key role in the release of  $\text{Ca}^{2+}$  from the sarcoplasmic reticulum, following depolarization of the transverse tubular membrane. The single channel properties of ryanodine receptors have been characterized extensively following their incorporation into planar lipid bilayers (Coronado et al., 1994). They form a high conductance,  $\text{Ca}^{2+}$  selective channel which is activated by micromolar  $\text{Ca}^{2+}$  and millimolar ATP, and inhibited by millimolar  $\text{Ca}^{2+}$  and  $\text{Mg}^{2+}$  and micromolar ruthenium red. Ryanodine, a plant alkaloid, decreases the maximal conductance of the channel and shifts the channel into states with long-lived openings and brief closings.

Skeletal muscle ryanodine receptor cDNAs have been cloned and sequenced (Takeshima et al., 1989; Zorzato et al., 1990). They encode a protein of up to 5,038 amino acids, depending on alternative splicing, with a mass of about 563,584 Da (Phillips et al., 1996). The ryanodine receptor protein has been expressed from its cDNA in several expression systems. Penner *et al.* (Penner et al., 1989) reported its expression in CHO cells and demonstrated that transfected CHO cells, but not nontransfected cells, release  $\text{Ca}^{2+}$  from intracellular organelles following the addition of caffeine or



ryanodine. Similar observations have been made in measurements of whole cell  $\text{Ca}^{2+}$  transients of C2C12 mouse myoblast cells (Otsu et al., 1994) and COS-7 cells (Treves et al., 1994) transfected with skeletal muscle ryanodine receptor cDNA, or by measuring the  $\text{Ca}^{2+}$ -activated  $\text{Cl}^-$  current in *Xenopus* oocytes injected with ryanodine receptor RNA (Nakai et al., 1990). These studies indicate that recombinant ryanodine receptors form functional  $\text{Ca}^{2+}$  release channels in whole cells, but single channel properties of these recombinant channels have not been reported.

We have expressed rabbit skeletal muscle ryanodine receptor cDNA in COS-1 cells and demonstrated that single recombinant channels responded to modulators such as  $\text{Ca}^{2+}$ , ATP,  $\text{Mg}^{2+}$ , ruthenium red and ryanodine. However, the channels expressed in COS-1 cells displayed multiple, anomalous conductances (Chen et al., 1993b). Multiple subconductance states were also detected in single  $\text{Ca}^{2+}$  release channels expressed in Sf9 cells (Brillantes et al., 1994). The conductance and stability of the recombinant channels expressed in Sf9 cells were improved by coexpressing FK506 binding protein 12 (FKBP12). The occurrence of multiple conductance states made it difficult to contemplate further studies of kinetics, conductance and ligand gating properties of the  $\text{Ca}^{2+}$  release channel. Therefore, the development of an alternative expression system for the functional ryanodine receptor was required.

In this report, we describe the expression of the ryanodine receptor cDNA in HEK-293 cells and the detailed characterization of the single channel properties of the expressed protein. The recombinant channels expressed in HEK-293 cells have the identical conductance, kinetics of opening, current-voltage relationship,  $\text{Ca}^{2+}$  permeability, and modulation by physiological and pharmacological ligands as the native rabbit skeletal muscle  $\text{Ca}^{2+}$  release channel. The establishment of the HEK-293 cell expression system is a significant advance in the studies of structure-function relationships of the ryanodine receptor, opening the potential for understanding the molecular mechanism of the channel.

## MATERIALS AND METHODS

*Materials* - Ryanodine was obtained from AgriSysems International (Wind Gap, PA). Brain phosphatidylethanolamine, and brain phosphatidylserine were obtained from Avanti Polar Lipids. The affinity-purified anti-13c2 antibody against the rabbit skeletal muscle ryanodine receptor was generated as described previously (*Chen et al., 1992*). The construct for the expression of SERCA1 from cDNA was obtained from Toyofuku et al. (*Toyofuku et al., 1994*) and has been characterized previously. Horseradish peroxidase-conjugated goat anti-rabbit IgG was obtained from Promega Biotech. CHAPS and other chemicals were purchased from Sigma. The rabbit ryanodine receptor cDNA has been described previously (*Zorzato et al., 1990; Chen et al., 1993b*).

*Cell culture and DNA transfection* - HEK-293 cells were maintained in Dulbecco's modified Eagle's medium (DMEM) supplemented with 0.1 mM minimum Eagle's Medium nonessential amino acids, 4 mM L-glutamine, 100 units of penicillin/ml, 100 mg of streptomycin/ml, 4.5 g of glucose/Liter and 10 % fetal calf serum, at 37°C under 5% CO<sub>2</sub>. DNA transfection was carried out using calcium phosphate (Ausubel et al., 1997). Cells were plated in 100 mm-tissue culture dishes 18-22 hours before transfection and were transfected with 12 µg of skeletal muscle ryanodine receptor cDNA and/or 5 µg of SERCAI cDNA per dish. Control cells were treated in the same way

with no DNA or with expression vector DNA alone. Microsomal membranes were isolated from cells harvested 19-21 hr after transfection.

*Immunocytochemical Staining* - A glass coverslip was placed in a 10 cm tissue culture dish. Cell culture and DNA transfection were then carried out as described above. The coverslip was washed 3 times with PBS, fixed with 4% formaldehyde in PBS for 15 min., and washed with PBS and PBS containing 0.1 % saponin for 5 min. each time. The slide was blocked with blocking solution (2% skim milk powder and 0.1% saponin in PBS) for 30 min. before being washed and incubated with anti-13c2 antibody raised against a short amino acid sequence of rabbit RyR1 (Chen et al., 1992) for 2 h. The coverslip was washed with blocking buffer and incubated with horseradish peroxidase-conjugated anti-rabbit IgG in blocking buffer for 1 h. The sample was then washed, and the bound antibodies were detected by their reaction in blocking buffer with 0.2 mg/ml 3,3'-diaminobenzidine tetrahydrochloride dihydrate, 0.03% H<sub>2</sub>O<sub>2</sub>, and 0.01% cobalt chloride.

*Partial purification of the recombinant ryanodine receptor* - Microsomal membranes were prepared from transfected and non-transfected HEK-293 cells as described previously (Chen et al., 1993b). Cells were washed twice with PBS and then incubated in PBS/5 mM EDTA to detach them from plates. The cells were collected by centrifugation at 4 K for 3 min, SS-34 rotor, and the cell pellet was suspended in 5 ml ice-cold PBS. The cells were again pelleted by centrifugation and resuspended in 2 ml LIS (10 mM

Tris.HCl, pH 7.5, 0.5 mM MgCl<sub>2</sub>) and allowed to swell for 10 min. on ice. Cells were homogenized in a Teflon-glass Dounce homogenizer in the presence of protease inhibitors with 20 strokes of the B (loose) pestle. An equal volume of Solution A (0.5 M sucrose, 0.3 M KCl, 10 mM Tris.HCl, pH 7.5, 40 μM CaCl<sub>2</sub>, 6 mM 2-mercaptoethanol) was added to the homogenates, and homogenized for an additional 20 strokes. Nuclei and mitochondria were removed from the homogenate through low-speed centrifugation (30 min., 8 K, SS-34 rotor). The concentration of KCl was increased to 0.6 M, and microsomal membranes were pelleted by ultracentrifugation at 180 000 g for 60 min. at 4°C. The microsomes were then resuspended in solution B (0.25 M sucrose, 0.15 M KCl, 10 mM Tris.HCl, pH 7.5, 20 μM CaCl<sub>2</sub>, 3 mM 2-mercaptoethanol). They were stored frozen in small aliquots and thawed only once before use. Heavy sarcoplasmic reticulum was isolated from rabbit fast-twitch skeletal muscle as described by Campbell and MacLennan (Campbell and MacLennan, 1981).

Solubilization and purification of ryanodine receptors from heavy sarcoplasmic reticulum and from microsomal membranes of the transfected and non-transfected HEK-293 cells were carried out as described previously (Chen et al., 1993b). Membrane preparations (2.5 mg/ml) were solubilized in a solution containing 50 mM Tris-HEPES, pH 7.4, 0.5% CHAPS, 1 M NaCl, and protease inhibitors for 90 min. at 0°C. The suspension was spun at 35000 rpm in a Beckman Ti60 rotor for 1 h at 4°C, and 2 ml of the supernatant was

layered on top of a 10 ml (10-30% w/v) linear sucrose gradient containing 50 mM Tris-HEPES, pH 7.4, 0.3 M NaCl, 0.1 mM CaCl<sub>2</sub>, 2 mM DTT, 3% CHAPS, and 0.15% L-phosphatidylcholine and protease inhibitors. The tubes were centrifuged at 30 000 rpm in a Bechman SW-40 rotor for 17 h at 4°C. Fractions of 0.5 ml each were collected and monitored for protein content and immunoreactivity by immunoblotting and ELISA.

*Polyacrylamide Gel Electrophoresis and Immunoblotting* - Membrane proteins (5-50 µg) were denatured in Laemmli sample buffer at 100°C for 2 min and separated on 5% SDS-PAGE. A constant voltage of 50 V was applied for the first 90 min., and then 150 V was applied. The resolved proteins were electroblotted onto nitrocellulose at 50 V for 4 h at 4°C. The membranes were blocked for 1 h with a solution of 10 mM Tris-HCl, pH 8.0, 150 mM NaCl, 0.1% Tween-20, and 5% skim milk powder, incubated overnight with polyclonal antibody 13c2 in the same solution, and washed 3 times with the same solution. Bound antibodies were then visualized by the alkaline phosphatase reaction using alkaline phosphatase-conjugated anti-rabbit IgG with nitroblue tetrazolium and 5-bromo-4-chloro-3-indolyl phosphate as substrate.

*Enzyme-linked Immunoabsorbent Assay* - Aliquots of 10-50 µl of the sucrose density gradient fractions were added to microtiter wells containing 150 µl of 50 mM sodium carbonate buffer, pH 9.6. The microtiter plate was incubated

at 4°C for 18 h and then blocked with 5% skim milk powder in 50 mM sodium carbonate buffer, pH 9.6 for 1 h at room temperature. The plate was washed 3 times with PBS containing 5% skim milk powder and 0.1% Tween-20, incubated with monoclonal antibody 13c2 in the same buffer for 2 h, washed again, and allowed to react with alkaline phosphatase–conjugated anti-rabbit IgG for 1 h. The samples were again washed, and bound antibodies were quantitated by the alkaline phosphatase reaction in diethanolamine buffer containing 10% diethanolamine, pH 9.8, 5 mM MgCl<sub>2</sub>, and one phosphatase substrate tablet (Sigma) per 5 ml of buffer.

*Single channel recordings in planar lipid bilayers-* Single channel recordings were obtained after incorporation into an artificial lipid bilayer of sucrose density gradient-purified ryanodine receptors from either rabbit skeletal muscle heavy sarcoplasmic reticulum or from transfected HEK-293 cells, as described previously (Chen et al., 1993b). Brain phosphatidylserine and brain phosphatidylethanolamine, dissolved in chloroform, were combined in a 3:5 ratio (w/w), dried under nitrogen gas and suspended in 30 µl of n-decane at a concentration of 35 mg of lipid /ml. Bilayers were formed across a 250-µm hole in a Delrin partition separating two chambers. The trans chamber (400 µl) was connected to the head stage input of a model EPC-7 amplifier (List-Electronics, Darmstadt, FRG). The cis chamber (1 ml) was held at virtual ground. Unless indicated otherwise, the luminal (trans) potentials

were varied and reported. A symmetrical solution containing 250 mM KCl and 25 mM Hepes, pH 7.4, was used for recordings. A 0.5 -1.0  $\mu$ l aliquot of sucrose density gradient-purified native ryanodine receptor or a 2-4  $\mu$ l aliquot of sucrose density gradient-purified recombinant ryanodine receptor was added to the cis chamber. Spontaneous channel activities were each tested for sensitivity to EGTA and/or  $\text{Ca}^{2+}$ , thereby providing information about  $\text{Ca}^{2+}$  sensitivity, orientation in the bilayer and stability of the incorporated channel. Unless indicated otherwise, all further additions were made to that chamber in which the addition of EGTA inhibited the activity of the incorporated channel. This chamber presumably corresponds to the cytoplasmic side of the  $\text{Ca}^{2+}$  release channel. In the experiments in which the trans chamber required perfusion, the configuration of electrodes was reversed so that the cis chamber was connected to the input of the amplifier and the trans chamber was grounded to avoid a current surge. In this case, the cytoplasmic (cis) potentials were varied and reported. Recordings were filtered at 10,000 HZ digitized at 44.1 KHZ (PCM-2 A/D VCR Adapter, Medical Systems Corp., Greenvale, N.Y.) and recorded on VHS videotapes. Upon playback, the data were filtered at 1,000 HZ and acquired at 5KHZ and analyzed using pClamp 5.5 software (Axon Instruments Inc.). A 50% threshold was applied to detect open events.

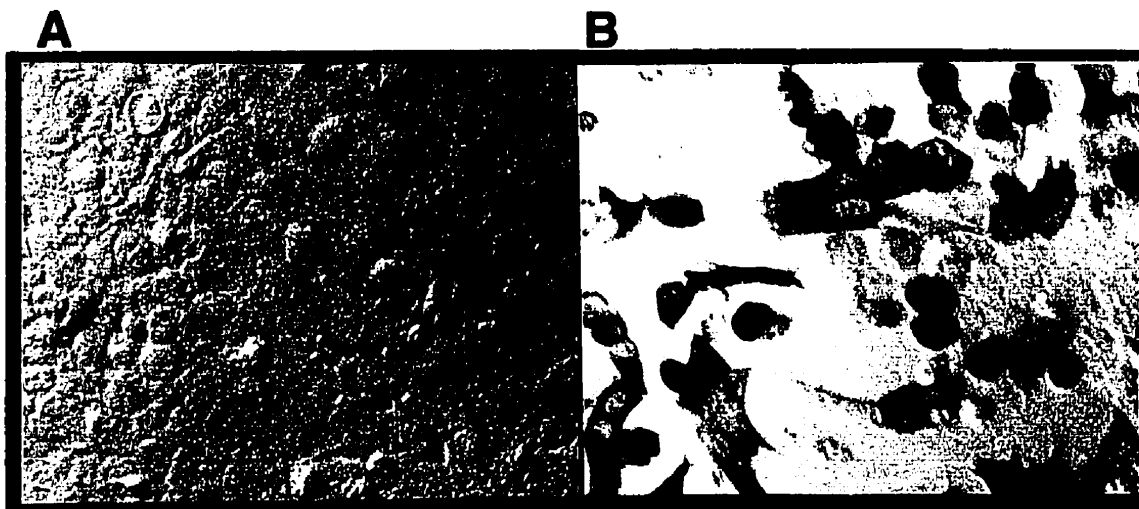


## RESULTS

*Expression in HEK-293 cells:* In a previous paper (Chen et al., 1993b), we reported the expression of rabbit skeletal muscle ryanodine receptor cDNA in COS-1 cells (Chen et al., 1993). We found that the transfection efficiency of the COS-1 cell expression system was less than 1%. In searching for a better expression system, we examined the transfection efficiency of several other cell lines including COS-7, Rat-2, NIH-3T3, and HEK-293 cells. Of these cell lines, transfection of HEK-293 cells using a  $\text{Ca}^{2+}$  phosphate-mediated transient transfection method gave the highest transfection efficiency. Fig. 4.1 shows the immunocytochemical staining with anti-13C2 antibody raised against a short amino acid sequence of the rabbit skeletal muscle ryanodine receptor (Chen et al., 1992) of HEK-293 cells transfected with or without the full length cDNA encoding the rabbit skeletal muscle ryanodine receptor. Expression of ryanodine receptor proteins could be detected in more than 25 % of the transfected HEK-293 cells, while no specific staining was observed in non-transfected cells. Thus, the ryanodine receptor cDNA can be transiently expressed in HEK-293 cells with a transfection efficiency 25-fold higher than that of the COS-1 cell system.

HEK-293 cells express virtually no excitable membrane currents and are readily transfected (Ukomadu et al., 1992). Endoplasmic reticulum isolated from HEK-293 cells is not leaky to  $\text{Ca}^{2+}$  under conditions ( $\mu\text{M}$  free

**Figure 4.1. Immunocytochemical staining of control and transfected HEK-293 cells.** HEK-293 cells were transfected without (A) or with (B) the full length rabbit skeletal muscle ryanodine receptor cDNA using a  $\text{Ca}^{2+}$  phosphate-mediated transfection method. Cells were fixed and permeabilized 19-21 h after transfection. Expressed ryanodine receptor proteins were detected by immunocytochemical staining using an anti-ryanodine receptor antibody, anti-13C2 (Chen *et al.*, 1992), with horseradish-conjugated anti-rabbit IgG as a secondary antibody.



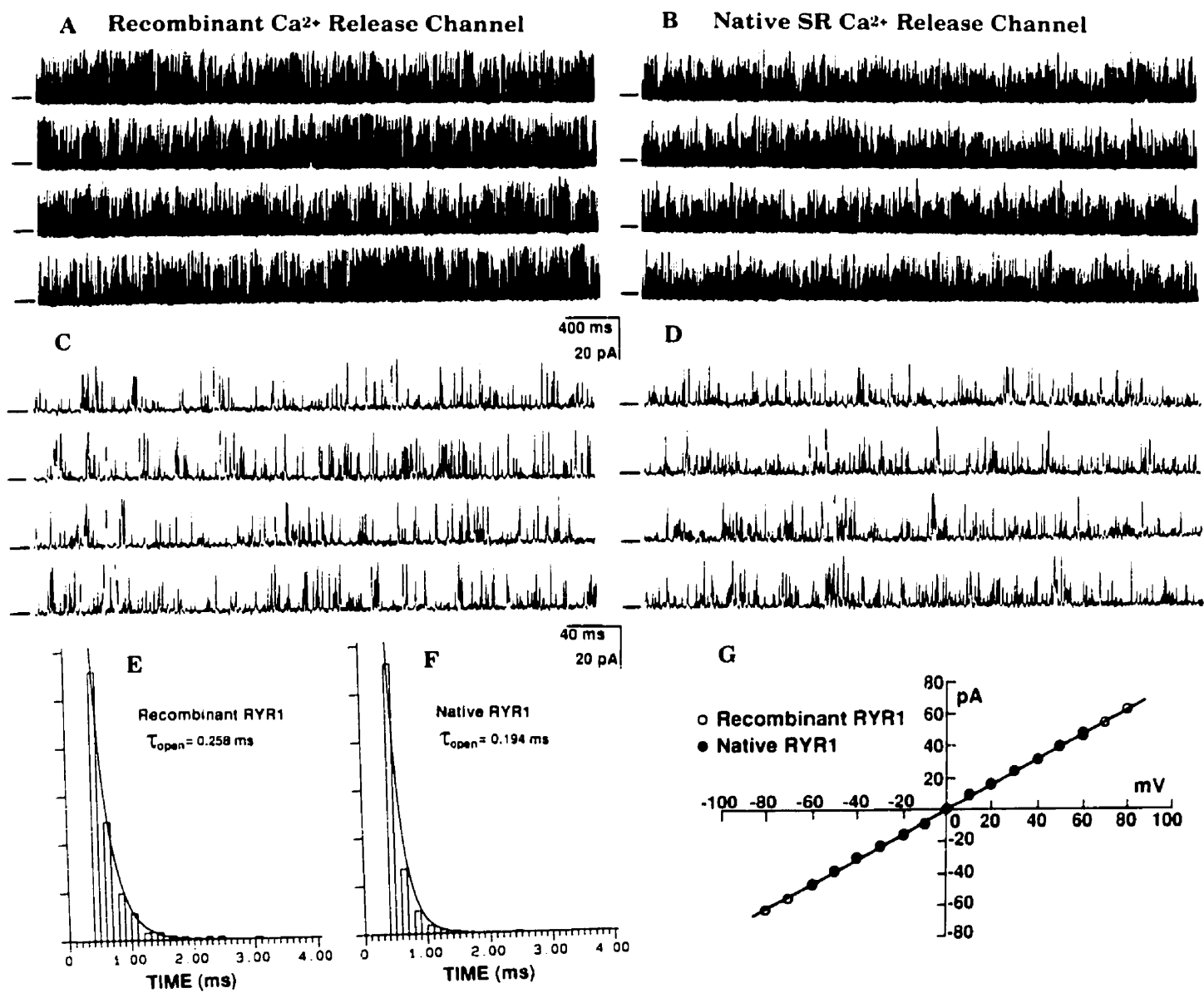
$\text{Ca}^{2+}$  and mM ATP) which activate  $\text{Ca}^{2+}$  release channels (Toyofuku et al., 1994). Using immunoblotting and enzyme-linked immunosorbent assay (ELISA), we were unable to detect any ryanodine receptor like-immunoreactivity in microsomal membranes of untransfected HEK-293 cells (unpublished observations). These findings, along with our inability to observe either ryanodine- or caffeine-sensitive  $\text{Ca}^{2+}$  release from internal stores of untransfected HEK-293 cells or the formation of ryanodine- or caffeine-sensitive  $\text{Ca}^{2+}$ -release channels in hundreds of bilayers exposed to extracts from untransfected HEK-293 cells, over a period of several years, suggests that this cell line contains, at most, trace levels of intrinsic ryanodine- or caffeine-sensitive  $\text{Ca}^{2+}$  release channels. Thus, the HEK-293 cell line is an excellent mammalian expression system in which to study the structural and functional properties of  $\text{Ca}^{2+}$  release channels.

*Comparison of conductance and open time constants:* Ryanodine receptors from rabbit skeletal muscle heavy sarcoplasmic reticulum membranes and from microsomal membranes of transfected HEK-293 cells were solubilized in CHAPS and partially purified by sucrose density gradient centrifugation. ELISA was used to localize ryanodine receptors in sucrose gradients.

Gradient fractions containing the peak of immunoreactivity were pooled and used for single channel recordings in planar lipid bilayers.

Single channel currents of both native and recombinant ryanodine receptor channels were recorded in a solution containing symmetrical 250 mM KCl and 25 mM HEPES, pH 7.4 and in the presence of 2.5  $\mu$ M free  $\text{Ca}^{2+}$  added to the *cis* (cytoplasmic) chamber (Fig. 4.2). Maximal single current amplitudes were about 23 pA at a holding potential of +30 mV (luminal) (Figs. 4.2A and B). A large number of open events with submaximal single current amplitudes were found in the current records of both native and recombinant channels (Figs. 4.2C and 4.2D). They are most likely events that are too brief to be completely resolved by our bilayer system. On the other hand, long-lived open events with submaximal current amplitudes were seldom observed, indicating that well resolved and long-lived subconductance states were rare in these channels. Open dwell-time histograms of recombinant and native channels are shown in Figs. 4.2E and 4.2F. Both recombinant and native  $\text{Ca}^{2+}$  release channels exhibited very fast kinetics. Fittings of open dwell-time histograms yielded an open time constant of  $0.224 \pm 0.027$  ms ( $n=4$ ) for the recombinant channels and  $0.220 \pm 0.022$  ms (mean  $\pm$  S.D.) ( $n=4$ ) for the native channels. The mean closed times of recombinant and native channels under these conditions are  $7.30 \pm 1.45$  and  $8.09 \pm$ , respectively. Some incompletely resolved open events may have been missed

**Fig. 4.2. Comparison of single channel properties of recombinant and native single  $\text{Ca}^{2+}$  release channels.** Sucrose density gradient-purified ryanodine receptors from rabbit skeletal muscle heavy sarcoplasmic reticulum vesicles and microsomal membranes of HEK-293 cells transfected with skeletal muscle ryanodine receptor cDNA were incorporated into lipid bilayers as described under Materials and Methods. The *trans* chamber was connected to the head-stage input of an amplifier. The *cis* chamber was held at virtual ground. In this experiment, the luminal (*trans*) potentials were varied and reported. A symmetrical recording solution containing 250 mM KCl and 25 mM Hepes, pH 7.4, was used for all recordings. Recordings were filtered at 1 kHz and digitized at 5 kHz. Both native and recombinant single  $\text{Ca}^{2+}$  channels were first inhibited by 0.1 mM EGTA (*cis*) and then reactivated by 0.1 mM  $\text{CaCl}_2$  (*cis*), indicating that the cytoplasmic face of the channel was located in the *cis* chamber. Single channel current fluctuations of the recombinant and native channels in the presence of 2.5  $\mu\text{M}$  free  $\text{Ca}^{2+}$  (0.1 mM EGTA plus 0.1 mM  $\text{CaCl}_2$ ) at +30 mV are shown in panels A and B, respectively. Current traces illustrated in panels C and D are taken from panels A and B and shown in a 10 fold shorter time scale. Base lines are indicated by lines to the left of each current trace. Continuous recordings are shown in each panel. Dwell-time histograms of open events of recombinant and native channels are illustrated in E and F, respectively. The average open time constant is  $0.224 \pm 0.027$  ms (mean  $\pm$  SD) (n=4) for the recombinant channel and  $0.220 \pm 0.022$  ms (mean  $\pm$  S.D.) (n=4) for the native channel. Panel G shows the current-voltage (I-V) relationship of the recombinant channel (open circles) and native (closed circles) channels. Both display a linear relationship with slope conductances of  $780 \pm 12.8$  pS (mean  $\pm$  SD) (n=3) for the recombinant channel and  $778 \pm 5.66$  (mean  $\pm$  SD) (n=2) for the native channel.



in our data analysis using a 50% discriminator for detecting openings. Thus, the open time constants of both recombinant and native channels may have been overestimated, but comparisons between recombinant and native channels are believed to be valid. The current-voltage relationships of native and recombinant channels were very similar. They displayed a linear relationship with slope conductances of  $780 \pm 12.8$  pS (mean  $\pm$  S.D.) ( $n = 3$ ) for the recombinant channels and  $778 \pm 5.66$  pS ( $n = 2$ ) for the native channels (Fig. 4.2G). We reported earlier that the slope of the inward current conductance (luminal to cytoplasmic current) of the native skeletal muscle ryanodine receptor channel differed from the slope of the outward current conductance (cytoplasmic to luminal current) in a recording solution containing 250 mM NaCl, 50 mM Tris and 100 mM HEPES, pH 7.4 (Chen et al., 1994). We found that the difference between the inward and outward current conductance resulted from an asymmetrical blockade of the channel by Tris (data not shown). In the absence of Tris, however, outward and inward current conductances were identical, as shown in Fig. 4.2G. Therefore, the  $\text{Ca}^{2+}$  release channel expressed in HEK-293 cells exhibited single channel conductance and channel kinetics very similar to those of the native channel.

**$\text{Ca}^{2+}$  permeability of the recombinant single  $\text{Ca}^{2+}$  release channel.** The  $\text{Ca}^{2+}$  permeability of the recombinant  $\text{Ca}^{2+}$  release channels was investigated

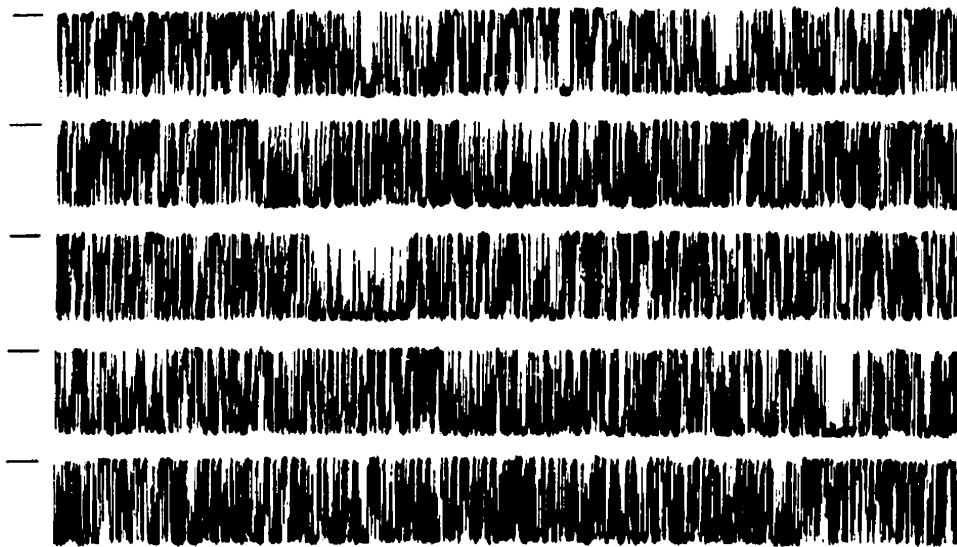


by examining the effect of luminal addition of  $\text{CaCl}_2$  on the  $\text{K}^+$  conductance of the recombinant  $\text{Ca}^{2+}$  release channels. In this series of experiments, the cytoplasmic (*cis*) potentials were varied and reported. A single recombinant channel current was recorded in symmetrical 250 mM KCl. The addition of 2.5 mM  $\text{CaCl}_2$  to the luminal side of the channel decreased inward  $\text{K}^+$  current conductance (luminal to cytoplasmic current) from 780 pS to  $450 \pm 44.8$  pS ( $n = 3$ ) as estimated from the current-voltage relationship between -20 and -60 mV (cytoplasmic), with no significant change of outward current conductance (cytoplasmic to luminal current) (Fig. 4.3). The outward current conductance (cytoplasmic to luminal current) in the presence of 2.5 mM  $\text{CaCl}_2$  was  $761 \pm 54.6$  ( $n = 3$ ), as estimated from the current-voltage relationship between +20 and +60 mV (cytoplasmic). The zero current potential, with symmetrical 250 mM KCl and 2.5 mM luminal  $\text{CaCl}_2$  was  $2.57 \pm 0.45$  mV (mean  $\pm$  S.D.) ( $n = 3$ ) (Fig. 4.4C). The shift in the zero current potential from 0 to 2.57 mV indicated that the recombinant  $\text{Ca}^{2+}$  release channel was capable of conducting  $\text{Ca}^{2+}$ .

To determine the  $\text{Ca}^{2+}/\text{K}^+$  permeability ratio of the recombinant  $\text{Ca}^{2+}$  release channel, single channel currents were recorded initially under symmetrical 250 mM KCl. The *trans* chamber (luminal) was then perfused with 50 mM  $\text{Ca}(\text{OH})_2$ , adjusted to pH 7.4 with HCl. Under these bi-ionic conditions, the reversal potential was approximately 16 mV and the

**Figure 4.3.  $\text{Ca}^{2+}$  permeability and  $\text{Ca}^{2+}$  conductance of recombinant single  $\text{Ca}^{2+}$  release channels.** To facilitate perfusion of the *trans* chamber, the electrode configuration was reversed in this experiment. The *trans* chamber was held at virtual ground, while the *cis* chamber was connected to the head-stage input of the amplifier. The cytoplasmic (*cis*) potentials were varied and reported in this experiment. (A) Control single channel currents, shown as downward deflections, were recorded at -30 mV (cytoplasmic) in symmetrical 250 mM KCl and 25 mM Hepes, pH 7.4, and in the presence of 0.1 mM  $\text{CaCl}_2$  (*cis*), 0.1 mM EGTA (*cis*), and 2.5 mM ATP (*cis*). The channel was incorporated into the lipid bilayer with its cytoplasmic side facing the *cis* chamber and its luminal side facing the *trans* chamber, since its activity was inhibited by the *cis* addition of EGTA and reactivated by the *cis* addition of  $\text{CaCl}_2$  (not shown) and further activated by the *cis* addition of ATP. Panel B shows single channel currents after subsequent addition of 2.5 mM  $\text{CaCl}_2$  to the *trans* chamber (the luminal side) of the control channel. Note that the single channel current amplitude was reduced. Base lines are indicated by a line to the left of each current trace. Recordings (20 s) shown in panels A and B are continuous recordings from the same channel. The effects of luminal  $\text{Ca}^{2+}$  on I-V relationships of the recombinant  $\text{Ca}^{2+}$  release channel are illustrated in panel C. The I-V relationship in symmetrical 250 mM KCl (open circles) is the same as that shown in Fig. 2. In the presence of 2.5 mM luminal  $\text{CaCl}_2$  and symmetrical 250 mM KCl (open triangles), the unitary conductance was  $450 \pm 44.8$  pS between -60 mV and -10 mV and  $761 \pm 54.6$  pS (mean  $\pm$  SD) ( $n = 3$ ) between +10 mV and +60 mV. The reversal potential was  $2.5 \pm 0.45$  mV (mean  $\pm$  SD) ( $n = 3$ ). The unitary conductance in the presence of luminal 50 mM  $\text{Ca(OH)}_2$  and cytoplasmic 250 mM KCl (solid circles) was  $116 \pm 7.64$  pS (mean  $\pm$  SD) ( $n=3$ ) between -10 mV and -80 mV. The reversal potential under this condition was about 16 mV.

**A control (-30 mv)**



400 ms  
20 pA

**B + 2.5 mM CaCl<sub>2</sub> (lumen) (-30 mv)**

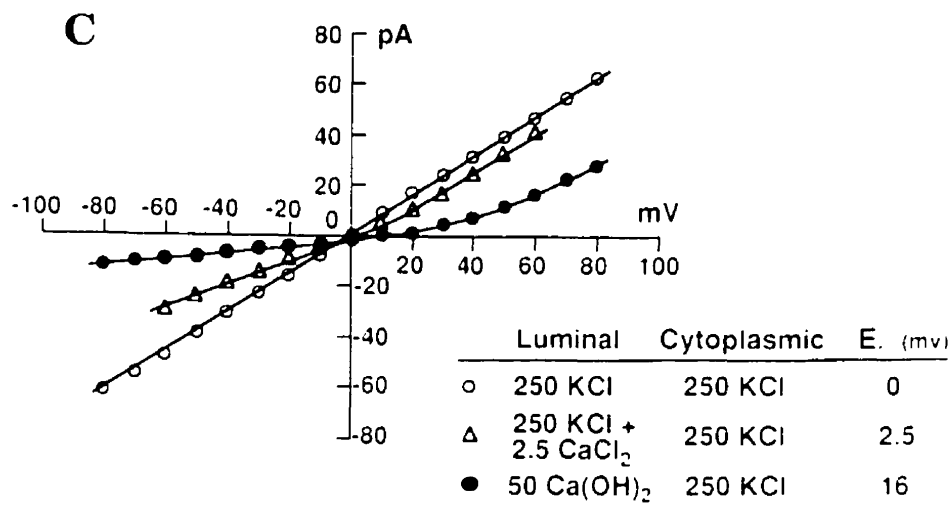
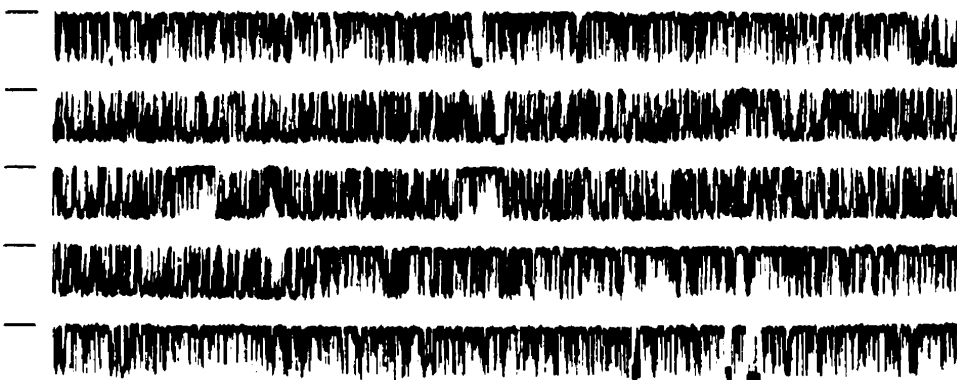
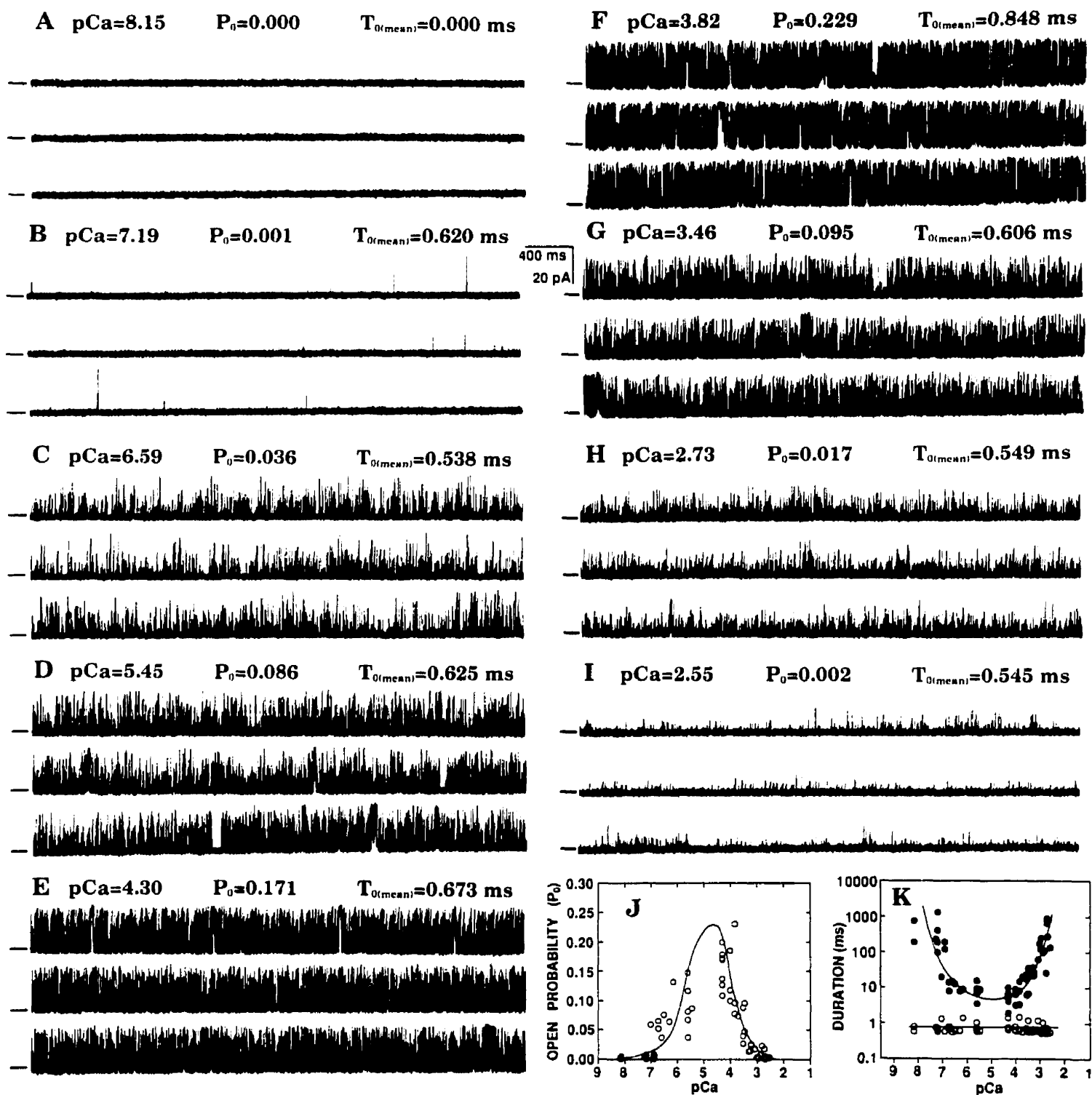


**Figure 4.4. The response to cytoplasmic  $\text{Ca}^{2+}$  of recombinant single  $\text{Ca}^{2+}$  release channels.** Single channel currents were recorded at +30 mV (luminal) in symmetrical 250 mM KCl, as described in Fig. 2. (A) A spontaneous single channel was first blocked by 0.1 mM EGTA (*cis*), indicating that the cytoplasmic side of the channel was facing the *cis* chamber. The  $\text{Ca}^{2+}$  concentration of the *cis* chamber (cytoplasmic  $\text{Ca}^{2+}$  level) was then increased gradually from pCa 8.15 to pCa 2.55 by the sequential addition of an aliquot of 10 mM or 100 mM  $\text{CaCl}_2$  solution. The pCa value, open probability ( $P_o$ ) and arithmetic mean open time ( $T_o$ ) at each free cytoplasmic  $\text{Ca}^{2+}$  concentration are indicated on the top of each panel. A continuous channel recording (12 s) is shown in each of panels (A- I). Openings are upward and base lines are indicated by a line to the left of each current trace. All recordings are from the same channel. The relationship between the open probability and the  $\text{Ca}^{2+}$  concentration is shown in panel J. Each point represents the average open probability of an average recording time of 128 s at a  $\text{Ca}^{2+}$  concentration varying from pCa 8.15 to pCa 2.55. A total of 64 points were obtained from seven separate experiments conducted like that shown in panels A-I. The relationship between the dwell time and the  $\text{Ca}^{2+}$  concentration is illustrated in panel K. The open circles denote the arithmetic mean open times and the solid circles indicate the arithmetic mean closed times at different  $\text{Ca}^{2+}$  concentrations. Arithmetic mean open and closed times were obtained from single channel recordings from which panel J was derived. Note that the arithmetic mean open times remained relatively unchanged when the  $\text{Ca}^{2+}$  concentration was varied. The average arithmetic mean open time was 0.702 ms.



permeation ratio of  $p\text{Ca}^{2+}/p\text{K}^{+}$  was estimated to be 6.8 (Fatt and Ginsborg, 1958). The  $\text{Ca}^{2+}$  conductance of the recombinant channel, estimated from the current-voltage relationship between -20 and -80 mV (cytoplasmic), was  $116 \pm 7.64$  pS under these bi-ionic conditions ( $n = 3$ ) (Fig. 4.3C). We also determined the  $\text{Ca}^{2+}$  conductance under conditions in which the luminal chamber was perfused with 50 mM  $\text{Ca}(\text{OH})_2$  and the cytoplasmic chamber was subsequently perfused with 125 mM Tris. This measurement yielded a similar  $\text{Ca}^{2+}$  conductance of 128 pS. These  $\text{Ca}^{2+}$  permeation and conductance values are very similar to those reported previously for the native  $\text{Ca}^{2+}$  release channel (Smith et al., 1988).

**Activation and inactivation of the recombinant single  $\text{Ca}^{2+}$  release channel by cytoplasmic  $\text{Ca}^{2+}$ .** The first sign of integration of  $\text{Ca}^{2+}$  release channels into the bilayer was spontaneous single channel activity stimulated by the presence of contaminating  $\text{Ca}^{2+}$  in the recording solution (not shown). The concentration of  $\text{Ca}^{2+}$  in the bath was then lowered to about pCa 8.15 by the *cis* addition of 0.1 mM EGTA. Under these conditions, the channel was inactivated (Fig. 4.4A), indicating that it was incorporated into the planar lipid bilayer with its cytoplasmic side facing the *cis* chamber. All further additions were then made to the *cis* (cytoplasmic) chamber. To determine the effect of cytoplasmic  $\text{Ca}^{2+}$  on channel activity,  $\text{Ca}^{2+}$  concentrations in the cytoplasmic chamber were increased stepwise by sequential additions of an

aliquot of  $\text{CaCl}_2$  solution. A few open events were detected when the  $\text{Ca}^{2+}$  concentration was raised to pCa 7.19. The channel was further activated by increasing the  $\text{Ca}^{2+}$  concentration. The open probability ( $P_o$ ) increased from 0.001 to 0.036, 0.086, 0.171 and 0.229 when the  $\text{Ca}^{2+}$  concentration was raised to pCa 7.19 to 6.59, 5.45, 4.39, and 3.82, respectively. At  $\text{Ca}^{2+}$  concentrations above 100  $\mu\text{M}$  (pCa about 4), however,  $\text{Ca}^{2+}$  became inhibitory.  $P_o$  decreased from 0.229 to 0.095, 0.017 and 0.002 when  $\text{Ca}^{2+}$  concentrations were raised to pCa 3.82 to 3.46, 2.73 and 2.55, respectively.

A curve depicting the effect of  $\text{Ca}^{2+}$  concentration on  $P_o$  was bell-shaped (Fig.4.4J increasing  $\text{Ca}^{2+}$  concentration in the range between 0.1  $\mu\text{M}$  and 100  $\mu\text{M}$ , peaked at about 100  $\mu\text{M}$  and decreased with increasing  $\text{Ca}^{2+}$  concentration in the range between 100  $\mu\text{M}$  and 2 mM. Further kinetic analysis of the effect of cytoplasmic  $\text{Ca}^{2+}$  on  $P_o$  revealed that changes in  $P_o$  were due mainly to changes in the duration of the mean closed time (Fig. 4.4K). The duration of the mean open time varied about 2 fold, from 0.567 ms to 1.18 ms, while the duration of the mean closed time changed more than 100-fold when  $\text{Ca}^{2+}$  concentrations were changed from pCa 8.15 to 2.55. Similarly, the mean open time varied about 2 fold and the mean closed time varied about 100 fold for the native  $\text{Ca}^{2+}$  release channel of rabbit skeletal muscle sarcoplasmic reticulum were also observed when pCa was varied from

8.15 to 3.0 (not shown).  $\text{Ca}^{2+}$ , therefore, activates and inactivates the channel primarily through modulating the duration of the closed state of the channel.

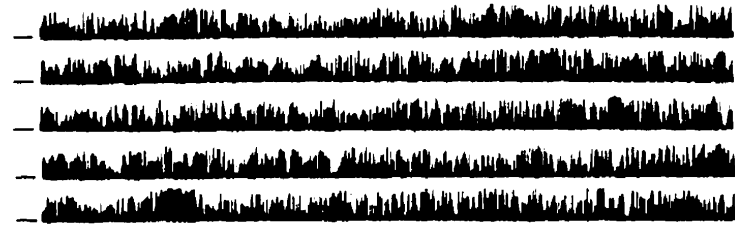
#### **Effects of modulators on recombinant single channel activity.**

Besides  $\text{Ca}^{2+}$ , the recombinant channel was also modulated by ATP,  $\text{Mg}^{2+}$ , caffeine, ryanodine and ruthenium red (Fig. 4.5). A spontaneous channel was first inhibited by the *cis* (cytoplasmic) addition of 0.1 mM EGTA (not shown) and reactivated by the *cis* addition of 0.1 mM  $\text{CaCl}_2$  (Fig. 4.5A). Subsequent addition of 2 mM ATP increased the  $P_o$  and mean open time, and decreased the mean closed time (Fig. 4.5B). In a total of nine similar experiments, the increase in  $P_o$  and mean open time, and the decrease in mean closed time after addition of ATP are statistically significant (paired t-test). After the addition of ATP, the average  $P_o$  was increased  $5.63 \pm 3.0$  fold ( $P < 0.0001$ ), the average mean open time was increased  $2.02 \pm 0.4$  fold ( $P < 0.005$ ) and the average mean closed time was decreased to  $23 \pm 13\%$  ( $P < 0.002$ ) compared with values before the addition of ATP. Subsequent addition of 2.2 mM  $\text{MgCl}_2$  decreased both  $P_o$  and mean open time, and increased mean closed time (Fig. 4.5C). After the addition of  $\text{MgCl}_2$ , the average  $P_o$  was decreased to  $13 \pm 10\%$  ( $P < 0.0005$ ), the average mean open time was decreased to  $47 \pm 15\%$  ( $P < 0.02$ ) and the average mean closed time was increased  $9.33 \pm 6.1$  fold ( $P < 0.03$ ) ( $n=7$ ) compared with those before the addition of  $\text{MgCl}_2$ . The  $\text{Mg}^{2+}$ -inhibited channel could be reactivated by the addition of 3 mM caffeine

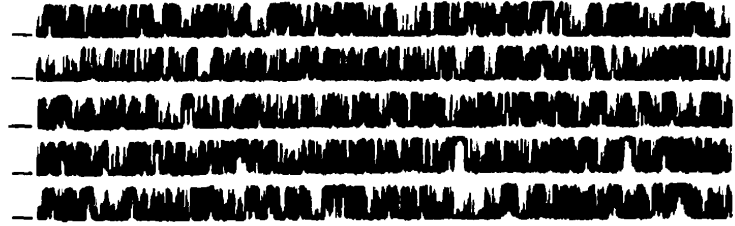


**Figure 4.5. Ligand gating properties of recombinant single  $\text{Ca}^{2+}$  release channels.** Single channel recordings were carried out as described in the legend to Fig. 4.2. A spontaneous single channel activity was first inhibited by the addition of 0.1 mM EGTA (*cis*) (not shown) and reactivated by the addition of 0.1 mM  $\text{CaCl}_2$  (*cis*), as shown in the control recording (panel A), suggesting that the channel was incorporated into the bilayer with its cytoplasmic side facing the *cis* chamber. Single channel currents before (control) and after sequential additions (*cis*) of 2.0 mM ATP (B), 2.2 mM  $\text{MgCl}_2$  (C), 3.0 mM caffeine (D), 10  $\mu\text{M}$  ryanodine (E) and 30  $\mu\text{M}$  ruthenium red (F) were recorded in symmetrical 250 mM KCl at +30 mV (luminal). The average open probability ( $P_o$ ) of 4-5 min continuous recordings and arithmetic mean open time ( $T_o$ ) for each condition are indicated on the top of each panel (A-D). Amplitude histograms of 4-5 min of continuous recording of control (G), after sequential additions of 2.0 mM ATP (H), 2.2 mM  $\text{MgCl}_2$  (I), 3.0 mM caffeine (J), and 10  $\mu\text{M}$  ryanodine (K) are displayed in panels G-K. All current recordings were from the same channel. A diary plot of open probability is shown in panel L. Each point represents the average open probability of a 20 second recording. The average open probability for each condition is indicated by a horizontal line.

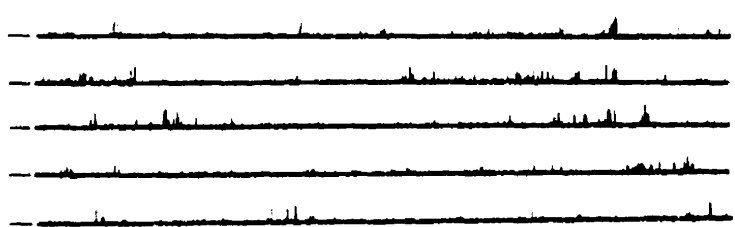
**A** Control (2.5  $\mu$ M  $\text{CaCl}_2$ )  $P_0=0.072$   $T_{0(\text{mean})}=0.596\text{ms}$



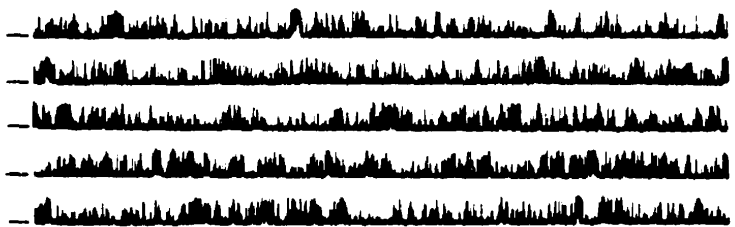
**B** +2.0 mM ATP  $P_0=0.396$   $T_{0(\text{mean})}=1.170$  ms



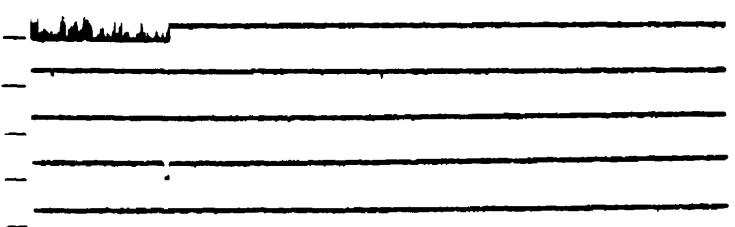
**C** +2.2 mM  $\text{MgCl}_2$   $P_0=0.005$   $T_{0(\text{mean})}=0.592$  ms



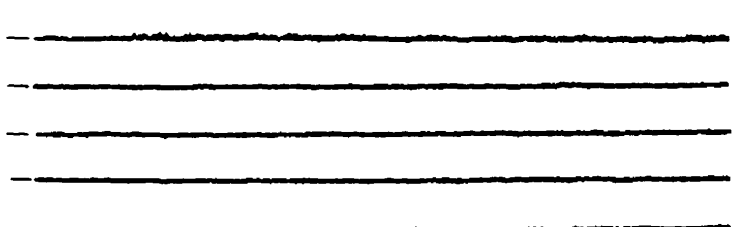
**D** +3.0 mM caffeine  $P_0=0.066$   $T_{0(\text{mean})}=0.713$  ms



**E** +10  $\mu$ M ryanodine



**F** +30  $\mu$ M ruthenium red



400 ms  
20 pA

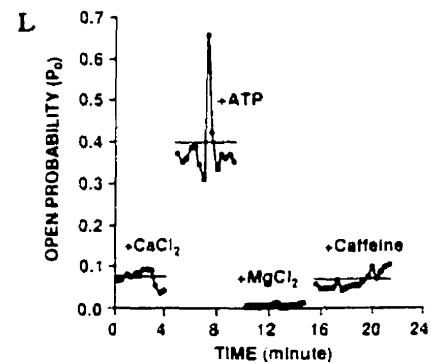
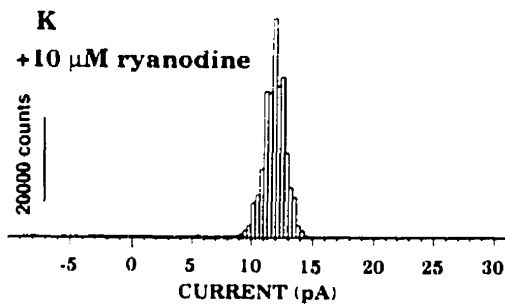
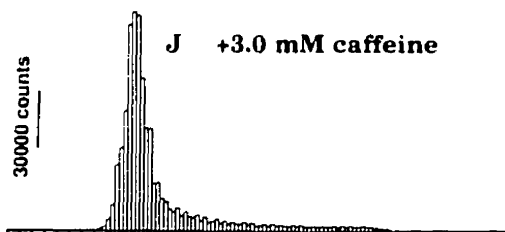
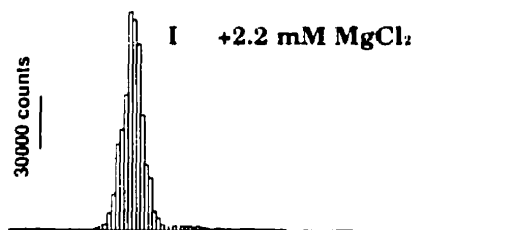
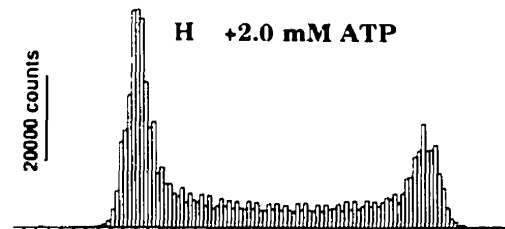
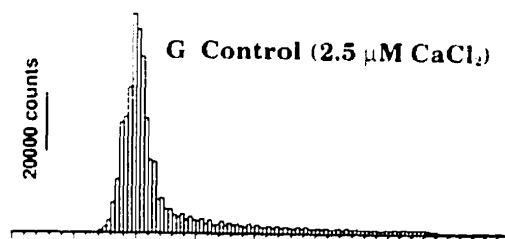
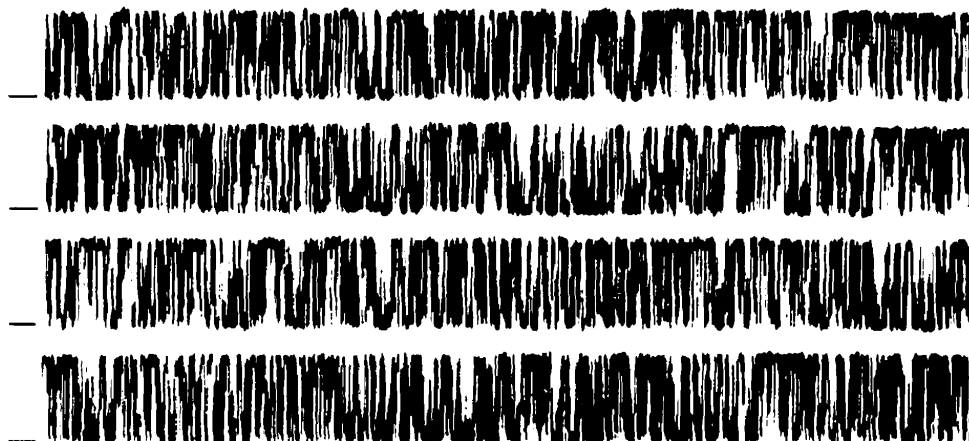


(Fig.4.5D). After the addition of caffeine, the average  $P_o$  was increased  $12.6 \pm 5.7$  fold ( $P < 0.005$ ), the average mean open time was increased  $1.94 \pm 0.8$  fold ( $P < 0.02$ ) and the average mean closed time was decreased to  $12 \pm 8\%$  ( $P < 0.04$ ) ( $n=6$ ) compared with those before the addition of caffeine. The channel kinetics and conductance were dramatically altered upon the addition of  $10 \mu\text{M}$  ryanodine (Fig. 4.5E). Conductance was reduced to  $59.76 \pm 2.44\%$  of the unmodified channel, from  $645.62 \pm 60.43$  pS to  $384.75 \pm 22.14$  pS. The ryanodine-modified channel was blocked by  $30 \mu\text{M}$  ruthenium red (Fig. 4.5F). These data clearly demonstrate that the recombinant  $\text{Ca}^{2+}$  release channels are modulated by various ligands with patterns similar to those observed with the native  $\text{Ca}^{2+}$  release channel (Coronado et al., 1994).

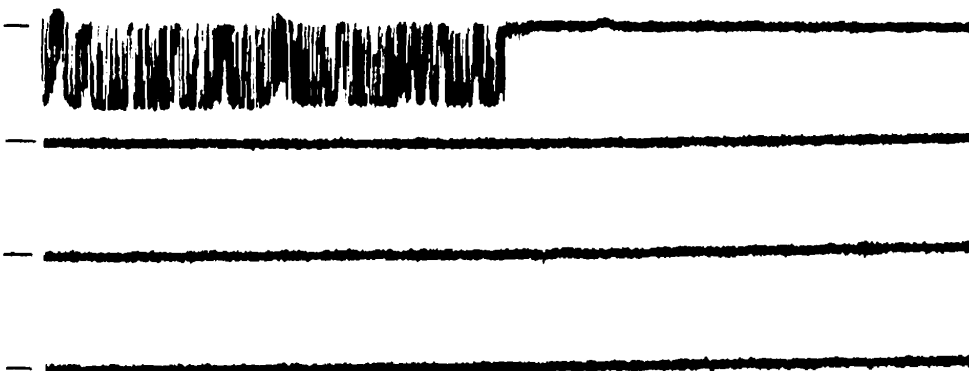
**Blockade of the recombinant single  $\text{Ca}^{2+}$  release channel.** Long closed events were often observed in current records of most recombinant  $\text{Ca}^{2+}$  release channels, particularly those in which current flowed from the cytoplasmic to the luminal side of the channel. In experiments described above, the current records show luminal to cytoplasmic current, which represents the direction of  $\text{Ca}^{2+}$  flow during  $\text{Ca}^{2+}$  release from the sarcoplasmic reticulum. The cytoplasmic to luminal current was often blocked in these cases. Fig. 4.6 illustrates one of these asymmetrically blocked channels. At  $+30$  mV (luminal), the channel was conducting a

**Figure 4.6. Asymmetrical blockade of recombinant single  $\text{Ca}^{2+}$  release channels.** A spontaneous channel activity was inactivated by *cis* 0.21 mM EGTA, reactivated by *cis* 0.21 mM  $\text{CaCl}_2$  and further activated by *cis* 2.0 mM ATP, indicating that the cytoplasmic face of the channel lies in the *cis* chamber. In this experiment, the luminal (*trans*) potentials were varied and reported. Panel A shows single channel currents recorded at +30 mV in symmetrical 250 mM KCl. Openings are upward and base lines are indicated by lines on the left of each current trace. Under these conditions, the direction of the current flow was from the luminal to the cytoplasmic side of the channel. Long-lived closed events were rare under these conditions. Panel B shows single channel currents shortly after changing the voltage from +30 mV to -30 mV. Openings are downward and base lines are marked. At -30 mV, current flowed from the cytoplasmic to the luminal side. Note that the channel was completely closed after opening for several seconds at -30 mV. Single channel currents recorded after changing the voltage from -30 mV back to +30 mV are shown in panel C. Openings are shown as upward deflections. Note that the channel was reactivated at +30 mV. A 16 s continuous recording is shown in each panel and all recordings are from the same channel.

A +30 mV (luminal to cytoplasmic current)

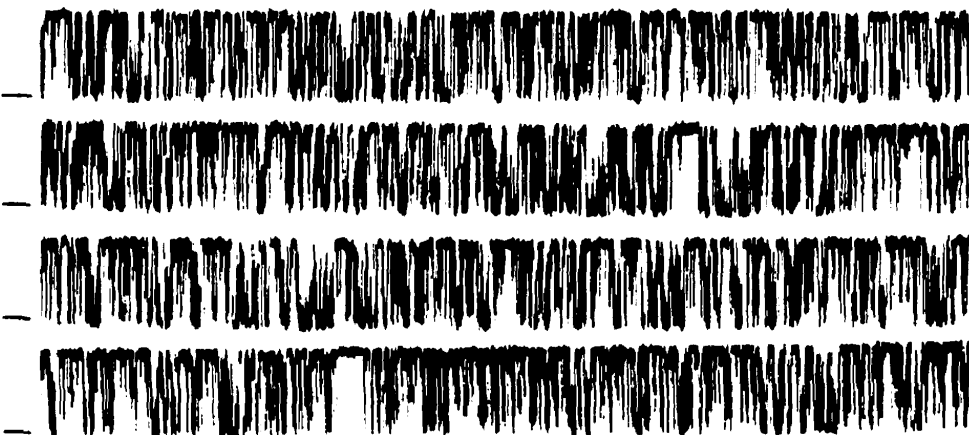


B -30 mV (cytoplasmic to luminal current)



400 ms  
20 pA

C +30 mV (luminal to cytoplasmic current)



luminal to cytoplasmic current with properties similar to those described earlier (Fig. 4.6A). At  $-30$  mV (luminal), however, the channel, began conducting in the cytoplasmic to luminal direction, but closed a few seconds after the direction of voltage was switched (Fig. 4.6B). The channel reactivated only after the voltage was changed from  $-30$  back to  $+30$  mV (Fig. 4.6C). Asymmetrical blockade of single channel currents was observed in most of the single recombinant channels that we detected.

## DISCUSSION

In this study, we describe the expression of a full length cDNA encoding the rabbit skeletal muscle sarcoplasmic reticulum  $\text{Ca}^{2+}$  release channel (the ryanodine receptor) and the functional characterization of the expressed protein. The  $\text{Ca}^{2+}$  release channel expressed in HEK-293 cells was characterized by immunochemical assays and by single channel recordings in planar lipid bilayers. The expressed protein was recognized specifically by an anti-rabbit ryanodine receptor antibody (Fig. 4.1) and exhibited mobilities in SDS-polyacrylamide gels and in sucrose-density gradients that were identical to those of the native channel (not shown). The recombinant ryanodine receptor formed a large conductance channel with a slope conductance of about 780 pS in 250 mM KCl and 116 pS in 50 mM  $\text{Ca}^{2+}$  and displayed fast gating kinetics with an open time constant of about 0.22 ms (Figs. 4.2 and 4.3). Like the native  $\text{Ca}^{2+}$  release channel, the recombinant  $\text{Ca}^{2+}$  release channel was more permeable to  $\text{Ca}^{2+}$  than to  $\text{K}^+$ . The permeation ratio,  $\text{pCa}^{2+}/\text{pK}^+$ , was about 6.8 (Fig. 4.3). Furthermore, the open probability of the recombinant channel was regulated by cytoplasmic  $\text{Ca}^{2+}$  in a typical bell-curve fashion in which the channel was activated by  $\text{Ca}^{2+}$  at micromolar concentrations and inhibited by millimolar  $\text{Ca}^{2+}$  (Fig. 4.4). The recombinant  $\text{Ca}^{2+}$  release channels were also modulated by ATP,  $\text{Mg}^{2+}$ , caffeine, ryanodine and ruthenium red with patterns similar to those observed with the native

channels (Fig. 4.5). These results demonstrate that the  $\text{Ca}^{2+}$  release channel expressed in HEK-293 cells possesses all of the major characteristics of the native single  $\text{Ca}^{2+}$  release channel of skeletal muscle sarcoplasmic reticulum.

Functional expression of the rabbit skeletal muscle ryanodine receptor cDNA in a heterologous cell culture system has been the subject of previous investigations. Penner *et al.* (Penner et al., 1989), Otsu *et al.* (Otsu et al., 1994) and Treves *et al.* (Treves et al., 1994) reported the expression of skeletal muscle ryanodine receptor cDNAs in CHO cells, C2C12 cells and COS-7 cells, respectively. In these studies, the expressed ryanodine receptor appeared to function as an intracellular  $\text{Ca}^{2+}$  release channel at the whole cell level. However, gating kinetics, channel permeation and conductance, response to cytoplasmic  $\text{Ca}^{2+}$  and modulation by ATP,  $\text{Mg}^{2+}$  and ruthenium red of the recombinant  $\text{Ca}^{2+}$  release channel have not been reported.

We have described the expression of the ryanodine receptor cDNA in COS-1 cells (Chen et al., 1993b). The  $\text{Ca}^{2+}$  release channel expressed in COS-1 cells displayed anomalous single channel conductances. The reason for these differences between recombinant and native channels is not clear, but the abnormal conductance states of the expressed channel may have been artifacts induced by channel purification and manipulation. For instance, sucrose gradient fractions containing the CHAPS-solubilized expressed channel were concentrated up to 30-fold in order to enrich the expressed



channel protein, which was expressed at a very low level in COS-1 cells. This concentrating step may have resulted in channel aggregation or partial denaturation. Alternatively, COS-1 cells may have lacked specific components that are essential for the proper function and regulation of the skeletal muscle  $\text{Ca}^{2+}$  release channel.

Coexpression of FKBP12 cDNA improved the stability and conductance of the  $\text{Ca}^{2+}$  release channel expressed in insect cells (Brillantes et al., 1994), suggesting that FKBP12 is an important component for the proper function of the  $\text{Ca}^{2+}$  release channel. Since the  $\text{Ca}^{2+}$  release channel expressed in HEK-293 cells exhibits properties very similar to those of the native channel, it is likely that FKBP12 is expressed endogenously in HEK-293 cells and associates with the  $\text{Ca}^{2+}$  release channel. The presence of FKBP12 message in HEK-293 cells was confirmed by RT-PCR and sequence analysis of the amplified cDNA (not shown). The deduced amino acid sequence of the FKBP12 cDNA, expressed in the HEK-293 human cell line, was identical to the sequence previously reported for human FKBP12 (Standaert et al., 1990). The presence of FKBP12 in whole cells was confirmed by immunocytochemical staining and the presence of FKBP12 in fractions containing the expressed  $\text{Ca}^{2+}$  release channel was confirmed by immunoblotting. The presence of endogenous FKBP12 in HEK-293 cells may be one of the factors that contributes to the high level of expression and the

highly conserved function of the recombinant skeletal muscle  $\text{Ca}^{2+}$  release channel.

The physiological role of FKBP12 is not fully understood. It may have multiple functions in the regulation of the  $\text{Ca}^{2+}$  release channel. We found that excess FKBP12 added to the cytoplasmic face of the CHAPS-solubilized native  $\text{Ca}^{2+}$  release channel blocked the channel asymmetrically, allowing current to flow only from the luminal side to the cytoplasmic side, but not in the reverse direction (Chen et al., 1994). Removal of excess added FKBP12 after the onset of asymmetrical blockade did not relieve the inhibition, suggesting that the binding of FKBP12 to the  $\text{Ca}^{2+}$  release channel, which leads to asymmetrical blockade, is tight. In the absence of added FKBP12, asymmetrical blockade was occasionally observed in native  $\text{Ca}^{2+}$  release channels. By contrast, most recombinant  $\text{Ca}^{2+}$  release channels from HEK-293 cells displayed asymmetrical blockade, conducting current unidirectionally from the luminal to the cytoplasmic side (Fig. 4.6). When we observed bidirectional current, the currents in both directions were modulated by the same ligands. The asymmetrical blockade of the  $\text{Ca}^{2+}$  release channels expressed in HEK-293 cells appeared to be similar to that observed when excess FKBP12 was added to native channels. However, further investigation is required to determine whether the endogenous FKBP12 in HEK-293 cells is involved in asymmetrical blockade of the

recombinant channels. A similar asymmetrical blockade has also been observed in rabbit (Ma et al., 1995) and chicken (Percival et al., 1994) skeletal muscle ryanodine receptor isoforms.

Although most recombinant channels exhibited similar gating kinetics and sensitivity to  $\text{Ca}^{2+}$  activation and  $\text{Ca}^{2+}$  inactivation, the extent of maximal activation by  $\text{Ca}^{2+}$  varied from channel to channel. Of ten single recombinant channels analyzed, seven showed maximal  $P_o$  of about 0.2, while three channels displayed maximal  $P_o$  of about 0.6. Different levels of maximal activation of the  $\alpha$ -ryanodine receptor of chicken skeletal muscle by  $\text{Ca}^{2+}$  have also been reported (Percival et al., 1994). In this system, the difference in maximal  $P_o$  was believed to result from gating mode switching between a low and a high activity mode. We do not know whether variation in maximal  $P_o$  of the recombinant channels result from gating mode switching, since we have not observed channels that switch between low and high activity spontaneously. Considering the high degree of retention of native channel function, the recombinant channel expressed in HEK-293 cells should be useful for studying the effects of mutation on conduction, permeation, gating kinetics,  $\text{Ca}^{2+}$  activation and inactivation, and modulation by ATP,  $\text{Mg}^{2+}$ , caffeine, ryanodine and ruthenium red.

## **CHAPTER 5**

### **Summary and Future Directions**

## 1 Summary

The interaction between RyR1 and DHPR has been shown to be critical for skeletal-type E-C coupling in studies of mice with a targeted mutation in RyR1 or DHPR (Tanabe et al., 1988; Takeshima et al., 1994). Accumulating biochemical evidence suggests that the interaction between RyR and DHPR leading to sarcoplasmic reticulum  $\text{Ca}^{2+}$  release is direct (Cadwell and Caswell, 1982; Marty et al., 1994a; Murray and Ohlendieck, 1997). The first goal of this project was to demonstrate that one or more linear amino acid sequences in the cytoplasmic domain of the RyR1 interacts directly with one or more cytoplasmic loops of DHPR. The cytoplasmic domain of RyR forms a structural domain or foot which extends across the gap between the sarcoplasmic reticulum membrane and the transverse tubule membrane to interact with DHPR (Franzini-Armstrong, 1970; Block et al., 1988). The cytoplasmic loop linking DHPR II-III has been shown to be critical for skeletal-type E-C coupling by studies of skeletal and cardiac DPR chimeras (Tanabe et al., 1990a). *In vitro* assays have shown that the DHPR II-III loop can activate RyR1 opening (Lu et al., 1995; Lu et al., 1994; el-Hayek et al., 1995). In Chapter 2, I describe the use of a purified fusion protein containing the DHPR II-III loop fused to GST- or His-peptide- as a protein affinity column for  $^{35}\text{S}$ -labeled *in vitro* translated fragments from the N-terminal three-fourths of RyR1 (Leong and MacLennan, 1998b). This study provides

strong evidence for a direct interaction between RyR1 and DHPR. These studies define a 37 amino acid sequence in RyR1, Arg<sup>1076</sup> to Asp<sup>1112</sup>, which interacts with the DHPR II-III loop. The interaction is specific for RyR1 *vs* RyR2, and skeletal DHPR *vs* cardiac DHPR. Comparison of skeletal and cardiac DHPRs and Na<sup>+</sup> channel sequence in this region identified two lysines in DHPR which are important for RyR1/DHPR interaction. Mutation of the two lysines to glutamic acid resulted in loss of most of the capacity of the DHPR II-III loop to interact with RyR1.

Mutations in RyR1 have been shown to cause malignant hyperthermia (MH) (Loke and MacLennan, 1998). Recently, the mutation A1086H in the DHPR III-IV loop has been linked to MH (Monnier et al., 1997). Since MH is a defect in Ca<sup>2+</sup> regulation, and the DHPR interacts with RyR1, leading to the release of Ca<sup>2+</sup>, I proposed that the DHPR III-IV loop may also interact in a functionally important manner with RyR1. In chapter 3, I identified the domain of RyR1 that specifically interacts with the DHPR III-IV loop. I used the same affinity chromatography approach described in Chapter 2, to purify DHPR III-IV loop fused to GST- or His-peptide- as a protein affinity column for <sup>35</sup>S-labeled *in vitro* translated fragments from the N-terminal three-fourths of RyR1. The same 37 amino acid sequence in RyR1, Arg<sup>1076</sup> to Asp<sup>1112</sup>, which interacted with the DHPR II-III loop also contributed to the binding site of the DHPR III-IV loop (Leong and MacLennan, 1998a). The

RyR/DHPR III-IV loop interaction was also specific for RyR1 *vs* RyR2. Both skeletal and cardiac isoforms of the DHPR III-IV loop bound to RyR1, probably because of the high sequence identity between skeletal and cardiac DHPR III-IV loop. The N-type  $\text{Ca}^{2+}$  channel III-IV loop did not interact with RyR1. Thus DHPR II-III and III-IV loops interact with a contiguous sequence on RyR1 between RyR, Lys<sup>954</sup> to Arg<sup>1112</sup>. They could have the potential for opening and closing the  $\text{Ca}^{2+}$  release channel.

In chapter 3, I used a competition binding assay to show that RyR Leu<sup>922</sup> to Asp<sup>1112</sup> fragment binding to GST-DHPR loop affinity columns was inhibited by free His-peptide DHPR loops. Binding to GST- DHPR II-III affinity columns was inhibited by the addition of free His-peptide DHPR III-IV and, similarly, RyR fragment Leu<sup>922</sup> to Asp<sup>1112</sup> binding to GST- DHPR III-IV affinity columns was inhibited in the presence of free His-peptide DHPR II-III. This study suggests that the Leu<sup>922</sup> to Asp<sup>1112</sup> fragment of RyR1 forms complexes in solution with DHPR II-III and with DHPR III-IV loops. These complexes no longer bind to DHPR affinity columns and can be found in the flow-through. Complexes between His-peptide DHPR loops and RyR1, Leu<sup>922</sup>-Asp<sup>1112</sup> , can be purified by Ni-NTA resin. The concentration of DHPR loops required for half maximal co-purification of RyR1 fragment allowed me to estimate that the affinity of the interaction is approximately 5

$\mu\text{M}$ . Thus, RyR-His-peptide DHPR complexes purified in this manner have the potential to be used for high resolution structural analysis.

A second goal of this project was to develop an alternative expression system which would facilitate studies of a fully functional RyR1. When this project was initiated, the  $\text{Ca}^{2+}$  release channel of rabbit skeletal muscle sarcoplasmic reticulum or ryanodine receptor (RyR1) had already been cloned and sequenced (Takasawa et al., 1995; Zorzato et al., 1990). The cDNA for RyR1 is 15265 nucleotides long and encodes a protein of 565 kDa molecular weight and 5037 amino acids. The expression from cDNA of the sarcoplasmic reticulum  $\text{Ca}^{2+}$  ATPase (SERCA) has facilitated investigation of the effects of mutagenesis on function which has led to many insights into the structure of SERCA and the mechanism of  $\text{Ca}^{2+}$  transport. Dr. D. H. MacLennan proposed that the development of a heterologous expression system for RyR1 would facilitate similar studies of structure and function of the  $\text{Ca}^{2+}$  release channel. Chen *et al.* (Chen et al., 1993b) expressed RyR1 from its cDNA in COS-1 cells and the recombinant channel responds to modulators such as  $\text{Ca}^{2+}$ , ATP,  $\text{Mg}^{2+}$ , ruthenium red, and ryanodine. However, the channels expressed in COS-1 cells displayed multiple, anomalous conductances. The occurrence of multiple conductance states made it difficult to contemplate further studies of kinetics, conductance, and ligand gating properties of the  $\text{Ca}^{2+}$  release channel.



The fourth chapter in this thesis describes the expression of RyR1 from its cDNA in HEK-293 cells (Chen et al., 1997a). This study confirmed that the cDNA clone encodes a functional ryanodine receptor. The recombinant RyR1 expressed in HEK-293 cells and studied in planar lipid bilayer have conductance, kinetics of opening, current-voltage relationship,  $\text{Ca}^{2+}$  permeability, and modulation by physiological ligands identical to those of the native rabbit skeletal muscle  $\text{Ca}^{2+}$  release channel. Considering the high degree of retention of native channel function, the recombinant channel expressed in HEK-293 cells should be useful for studies of the effects of mutations on conduction, permeation, gating kinetics,  $\text{Ca}^{2+}$  activation and inactivation, and modulation by ATP,  $\text{Mg}^{2+}$ , caffeine, ryanodine, and ruthenium red. The characterization of the recombinant RyR1 and establishment of the HEK-293 cell expression system is a significant advance and provides the opportunity to study many aspects of RyR1 structure and function. These advances have been exploited in a variety of studies from our laboratory (Tong et al., 1997; Tong and MacLennan, 1998; Du and MacLennan, 1998).

## **2 Future Directions**

A longterm goal in the study of RyRs is to identify functional domains and regulatory sites. Amino acid sequences which are candidates for the

regulation of the  $\text{Ca}^{2+}$  channel by  $\text{Ca}^{2+}$ , calmodulin, ATP, ruthenium red, and ryanodine have been proposed, based on predictions from consensus binding sequences (Takeshima et al., 1989; Zorzato et al., 1990; Otsu et al., 1990; Nakai et al., 1990; Hakamata et al., 1992; Tunwell et al., 1996), overlay assays (Chen et al., 1992; Chen and MacLennan, 1994; Menegazzi et al., 1994), and labeling by photoactivated analogs (Brandt et al., 1992; Zarka and Shoshan-Barmatz, 1993; Callaway et al., 1994; Witcher et al., 1994).

Antibodies have been used as probes to assay the functional effects of antibody binding to proposed modulatory domains (Fill et al., 1991; Chen et al., 1992; Chen et al., 1993c; Treves et al., 1993). A site-directed mutagenesis approach and single channel recordings of recombinant channel purified from HEK 293 can then be used to identify specific residues which are involved. A site for  $\text{Ca}^{2+}$  activation of RyR3 has been identified by mutagenesis (Chen et al., 1998). The three RyR isoforms can be distinguished by their kinetics of opening,  $\text{Ca}^{2+}$  permeability, and modulation by physiological ligands (Coronado et al., 1994; Chen et al., 1997b). Chimeric molecules among RyR1, RyR2, and RyR3 should yield definitive information on the sequences important for channel characteristics and regulation.

The  $\text{Ca}^{2+}$  conducting pore of RyR1 must lie in the region containing transmembrane sequences. The membrane topology of RyR1 has been predicted from primary sequence by hydropathy analysis. Four transmembrane sequences in the C-terminal end of the ryanodine receptor

were proposed by Takeshima *et al.* (Takeshima et al., 1989). Upon considering that transmembrane sequences in channel forming molecules often have hydrophilic residues facing the pore, a model with 8 additional transmembrane sequences was proposed by Zorzato *et al.* (Zorzato et al., 1990). All of the predicted transmembrane sequences lie in the C-terminal fifth of RyR1. RyR1 cDNA can be truncated and transfected into HEK-293, the truncated RyR1 purified, and single channel studies in planar lipid bilayer can be carried out to define a channel-forming domain. This strategy has already been used to identify a 130 kDa fragment from the C-terminus which forms a cation-selective channel which is activated by  $\text{Ca}^{2+}$  and regulated by ryanodine (Bhat et al., 1997a). It is likely that the RyR1 cDNA can be truncated further for better definition of the channel-forming domain since trypsin proteolysis studies have identified a 76 kDa fragment from the C-terminal of RyR1 which binds ryanodine (Callaway et al., 1994) and ATP (Zarka and Shoshan-Barmatz, 1993). A transcript encoding the 76 kDa fragment has been identified in brain (Takeshima et al., 1993). The 130 kDa fragment can be truncated further in order to delineate ryanodine binding and  $\text{Ca}^{2+}$  activation sites. More detailed study of the channel pore by site-directed mutagenesis of predicted transmembrane sequences will yield important information about residues which line the channel pore, and secondary structure important for  $\text{Ca}^{2+}$  conduction and selectivity.

Genetic linkage analysis has identified amino acid changes which are associated with malignant hyperthermia and central core disease and which may be located in regulatory domains of RyR1 (Loke and MacLennan, 1998). The role that these residues play in channel function has been studied by introduction of these mutations into the RyR1 cDNA and expression in HEK 293 (Tong et al., 1997; Tong and MacLennan, 1998). The continued characterization of mutant forms of RyR1 in HEK-293 cells should lead to increased understanding of diseases associated with RyR.

Alignment of IP<sub>3</sub> and ryanodine receptor sequences reveals that the Ca<sup>2+</sup> channel forming domain and some domains important for regulation of channel opening are conserved between IP<sub>3</sub> Receptors and RyR (Furuichi et al., 1989; Loke and MacLennan, 1998). The region identified in RyR1 which interacts with both DHPR II-III and DHPR III-IV loops sequences, however, is not present in IP<sub>3</sub> receptors. Thus, the insertion of the RyR E-C coupling domain into the IP<sub>3</sub> receptor may give the IP<sub>3</sub> receptor the added ability to interact with DHPR in E-C coupling events. This domain swapping study can be done by injecting RyR/IP<sub>3</sub> receptor chimeras into myotubes from RyR1 knockout mice. These types of RyR/IP<sub>3</sub> receptor chimeras will provide insight into interactions between structural and functional domains of RyR. The isolation of an E-C coupling domain within an IP<sub>3</sub> receptor background might yield important information on the intramolecular interactions which are

important for regulation of the channel forming domain by the E-C coupling domain.

Based on the studies presented in this thesis and others which have been published through the course of these studies, I propose a plausible model for the mechanism of E-C coupling in skeletal muscle that is consistent with current evidence. Muscle depolarization is the first step in a series of events leading to muscle contraction. In response to depolarization, conformation changes in the DHPR of the transverse (T)-tubule lead to the activation of RyR1 channel opening by interactions of the DHPR II-III loop with RyR1, Arg<sup>1076</sup>-Asp<sup>1112</sup> (Leong and MacLennan, 1998b). The interaction of RyR1 with DHPR II-III upon depolarization may cause a conformation change in RyR1 (Orlova, E et al, 1996, Yano, M. 1995) which acts through the RyR1 (1635-2636) sequence identified as being crucial for skeletal muscle-type E-C coupling (Nakai et al., 1998). The DHPR II-III loop may exert its effect by modulating the RyR1 Ca<sup>2+</sup> sensor (Chen et al., 1998) to increase the sensitivity of RyR1 to activation by Ca<sup>2+</sup> to release Ca<sup>2+</sup>, thus increasing the RyR1 channel open probability at resting Ca<sup>2+</sup> levels. Depolarization-induced RyR1 channel opening would thus result in microscopic elevations in intracellular Ca<sup>2+</sup> at the site of RyR which are coupled to DHPR. Through Ca<sup>2+</sup>-activation of Ca<sup>2+</sup> release further microscopic Ca<sup>2+</sup> release events occur, that give rise to activation of sarcoplasmic reticulum Ca<sup>2+</sup> release from the whole muscle. The fast Ca<sup>2+</sup> rise in

**Figure 5.1: Model of Interactions Between Ryanodine and Dihydropyridine Receptors During Excitation-Contraction Coupling.**

The  $\text{Ca}^{2+}$  release channels of skeletal muscle sarcoplasmic reticulum and the L-type  $\text{Ca}^{2+}$  channels of the transverse tubule (the dihydropyridine receptor or DHPR) appear to be in physical contact (Block et al., 1988). **A. Resting State.** In the relaxed muscle,  $\text{Ca}^{2+}$  release channels are closed and a potential difference is generated across the transverse tubular membrane (positive outside; negative inside) by the  $\text{Na}^+/\text{K}^+$  ATPase. The membrane potential difference is likely to stabilize a positively charged S4 transmembrane helix in each of the 4 domains of the  $\alpha$ -subunit of the DHPR. The  $\text{Ca}^{2+}$  release channels are closed (Meissner et al., 1986; Lamb and Stephenson, 1992). **B. Depolarized State.** The entry of  $\text{Na}^+$  following stimulatory events at the neuromuscular junction initiates a wave of depolarization across the transverse tubular membrane. Depolarization is proposed to destabilize S4 transmembrane helices, leading to the movement of positively charged helices towards the more negative exterior and to a probable shift in the position of these helices in the lipid bilayer. This proposed shift is the most likely source of a charge movement (Schneider and Chandler, 1973). As a result of the change in conformation of the DHPR, the DHPR II-III loop is proposed to activate the  $\text{Ca}^{2+}$  release channel to release  $\text{Ca}^{2+}$  through a direct interaction between the two proteins (Tanabe et al., 1990a; Meissner and Lu, 1995; Leong and MacLennan, 1998b). The sites of interaction between the  $\text{Ca}^{2+}$  release channel and the DHPR are being defined (Tanabe et al., 1990a; Lu et al., 1994; Lu et al., 1995; el-Hayek et al., 1995; Leong and MacLennan, 1998b; Leong and MacLennan, 1998a). Upon repolarization,  $\text{Ca}^{2+}$  release is terminated (Suda, 1995), possibly as a result of interactions between RyR1 and the DHPR III-IV loop (Leong and MacLennan, 1998a).

## A. Resting State

DHP Receptor  
( $\alpha 1$ ,  $\alpha 2/\delta$ ,  $\beta$ ,  $\gamma$  subunits)

Extracellular Space

S4 transmembrane

T-Tubule membrane

Sarcoplasm

FK506 Binding Protein

Calmodulin

$\text{Ca}^{2+}$

Sarcoplasmic Reticulum Lumen

Sarcoplasmic Reticulum Membrane

## B. Depolarized State

DHP loops activate opening and closing of the  $\text{Ca}^{2+}$  release channel

$\text{Ca}^{2+}$  Release Channel  
(Tetramer)

$\text{Ca}^{2+}$

concentration is due to  $\text{Ca}^{2+}$  released from sarcoplasmic reticulum induced first by depolarization and then  $\text{Ca}^{2+}$  release as a result of  $\text{Ca}^{2+}$ -induced  $\text{Ca}^{2+}$  release. The fast component of the decay in the rate of  $\text{Ca}^{2+}$  release occurs as a result of  $\text{Ca}^{2+}$ -induced inactivation of  $\text{Ca}^{2+}$  release.

Calmodulin in the muscle at elevated  $\text{Ca}^{2+}$  levels during contraction may aid in decreasing the open probability of RyR1 (Tripathy et al., 1995; Ikemoto et al., 1995).  $\text{Ca}^{2+}$  levels remain elevated following the initial  $\text{Ca}^{2+}$  peak during the depolarizing pulse due to  $\text{Ca}^{2+}$  release from sarcoplasmic reticulum through channels in direct contact with the DHPR.

The termination of sarcoplasmic reticulum  $\text{Ca}^{2+}$  release through RyR1 upon repolarization (Melzer et al., 1987, Schneider & Simon, 1988, Rios & Pizarro, 1991, Suda, 1995) is another physiologically important function of the RyR-DHPR interaction. Repolarization results in restoration of the DHPR to its resting conformation whereby the DHPR III-IV loop is then postulated to stop  $\text{Ca}^{2+}$  release through its interactions with RyR1. The interaction of DHPR III-IV with RyR1 Leu<sup>954</sup>-Asp<sup>1112</sup> may relieve the  $\text{Ca}^{2+}$ -release inducing effects of DHPR II-III on RyR1 returning RyR1 to its resting sensitivity to  $\text{Ca}^{2+}$ -induced  $\text{Ca}^{2+}$  release.

The ability to express RyR1 from cDNA described in Chapter 4 of this thesis provides a method for testing the mechanism of E-C coupling in skeletal muscle. Studies replacing the RyR1 sequence, Leu<sup>922</sup>-Asp<sup>1112</sup>, with



the corresponding RyR2 sequence in chimeras between RyR1 and RyR2 will elucidate the functional importance of this sequence in E-C coupling. This chimeric molecule can be expressed in RyR1 knockout mice. Myotubes from these mice can be assayed to determine if the chimeric molecule restores the structure of the triad junction, depolarization-induced activation of RyR1, enhancement of DHPR channel activity or repolarization-induced inhibition of RyR1. Only 10 residues between Arg<sup>1076</sup> and Asp<sup>1112</sup> differ in RyR1 and RyR2 and several of these residues are likely to form part of the interaction site between the two proteins. Site-directed mutagenesis of these residues should yield detailed information on the interactions between RyR1 and DHPR important for E-C coupling.

In Chapter 3, I described the purification of RyR-His-peptide DHPR complexes which have the potential to be used for high resolution structural analysis. The elucidation of these structures should be helpful for predicting local conformational changes in RyR and DHPR which occur during E-C coupling and provide information on how interactions on multiple sites on RyR and DHPR lead to the regulation of Ca<sup>2+</sup> release.

Additional proteins are present at the junction between the transverse tubule and the sarcoplasmic reticulum and these proteins may play a role in the regulation of E-C coupling. Antisense oligonucleotides can be introduced into myotubes to inhibit the translation of specific proteins (Bulteau et al., 1998). The role that these proteins play in the regulation of Ca<sup>2+</sup> release can

be deduced by the consequences of their absence through the use of *in vivo* assays to study the effect of these functional knockouts on tension development (Tanabe et al., 1988) and  $\text{Ca}^{2+}$  release (Nakai et al., 1996).

## References

- Abramson, J. J., E. Buck, G. Salama, J. E. Casida, and I. N. Pessah. 1988a. Mechanism of anthraquinone-induced calcium release from skeletal muscle sarcoplasmic reticulum. *J Biol Chem.* 263:18750-18758.
- Abramson, J. J., J. R. Cronin, and G. Salama. 1988b. Oxidation induced by phthalocyanine dyes causes rapid calcium release from sarcoplasmic reticulum vesicles. *Arch Biochem Biophys.* 263:245-255.
- Abramson, J. J., S. Milne, E. Buck, and I. N. Pessah. 1993. Porphyrin induced calcium release from skeletal muscle sarcoplasmic reticulum. *Arch Biochem Biophys.* 301:396-403.
- Abramson, J. J., J. L. Trimm, L. Weden, and G. Salama. 1983. Heavy metals induce rapid calcium release from sarcoplasmic reticulum vesicles isolated from skeletal muscle. *Proc Natl Acad Sci U S A.* 80:1526-1530.
- Abramson, J. J., A. C. Zable, T. G. Favero, and G. Salama. 1995. Thimerosal interacts with the Ca<sup>2+</sup> release channel ryanodine receptor from skeletal muscle sarcoplasmic reticulum. *J Biol Chem.* 270:29644-29647.
- Adams, B. A., T. Tanabe, A. Mikami, S. Numa, and K. G. Beam. 1990. Intramembrane charge movement restored in dysgenic skeletal muscle by injection of dihydropyridine receptor cDNAs. *Nature.* 346:569-572.
- Ahern, G. P., P. R. Junankar, and A. F. Dulhunty. 1994. Single channel activity of the ryanodine receptor calcium release channel is modulated by FK-506. *FEBS Lett.* 352:369-374.
- Ausubel, F., M., R. Brent, R. Kingston, E., D. Moore, D., J. Seidman, G., J. Smith, A. , and K. Struhl. 1997. Current Protocols in Molecular Biology. John Wiley & Sons, Inc.

- Berridge, M. J. 1993. Cell signalling. A tale of two messengers [news; comment]. *Nature*. 365:388-389.
- Bhat, M. B., J. Zhao, H. Takeshima, and J. Ma. 1997a. Functional calcium release channel formed by the carboxyl-terminal portion of ryanodine receptor. *Biophys J*. 73:1329-1336.
- Bhat, M. B., J. Zhao, W. Zang, C. W. Balke, H. Takeshima, W. G. Wier, and J. Ma. 1997b. Caffeine-induced release of intracellular  $\text{Ca}^{2+}$  from Chinese hamster ovary cells expressing skeletal muscle ryanodine receptor. Effects on full-length and carboxyl-terminal portion of  $\text{Ca}^{2+}$  release channels. *J Gen Physiol*. 110:749-762.
- Block, B. A., T. Imagawa, K. P. Campbell, and C. Franzini-Armstrong. 1988. Structural evidence for direct interaction between the molecular components of the transverse tubule/sarcoplasmic reticulum junction in skeletal muscle. *J Cell Biol*. 107:2587-2600.
- Brandt, N. R., A. H. Caswell, T. Brandt, K. Brew, and R. L. Mellgren. 1992. Mapping of the calpain proteolysis products of the junctional foot protein of the skeletal muscle triad junction. *J Membr Biol*. 127:35-47.
- Brandt, N. R., A. H. Caswell, S. R. Wen, and J. A. Talvenheimo. 1990. Molecular interactions of the junctional foot protein and dihydropyridine receptor in skeletal muscle triads. *J Membr Biol*. 113:237-251.
- Brillantes, A. B., K. Ondrias, A. Scott, E. Kobrinsky, E. Ondriasova, M. C. Moschella, T. Jayaraman, M. Landers, B. E. Ehrlich, and A. R. Marks. 1994. Stabilization of calcium release channel (ryanodine receptor) function by FK506-binding protein. *Cell*. 77:513-523.
- Britt, B. A., and W. Kalow. 1970. Malignant hyperthermia: a statistical review. *Can Anaesth Soc J*. 17:293-315.

- Brostrom, C. O., J. D. Corbin, C. A. King, and E. G. Krebs. 1971. Interaction of the subunits of adenosine 3':5'-cyclic monophosphate- dependent protein kinase of muscle. *Proc Natl Acad Sci U S A*. 68:2444-2447.
- Bull, R., and J. J. Marengo. 1993. Sarcoplasmic reticulum release channels from frog skeletal muscle display two types of calcium dependence [published erratum appears in FEBS Lett 1994 Jan 3;337(1):121]. *FEBS Lett*. 331:223-227.
- Bulteau, L., G. Raymond, and C. Cognard. 1998. Antisense oligonucleotides against 'cardiac' and 'skeletal' DHP-receptors reveal a dual role for the 'skeletal' isoform in EC coupling of skeletal muscle cells in primary culture. *J. Cell Sci*. 111:2149-2158.
- Buratti, R., G. Prestipino, P. Menegazzi, S. Treves, and F. Zorzato. 1995. Calcium dependent activation of skeletal muscle  $\text{Ca}^{2+}$  release channel (ryanodine receptor) by calmodulin. *Biochem Biophys Res Commun*. 213:1082-1090.
- Cadwell, J. J., and A. H. Caswell. 1982. Identification of a constituent of the junctional feet linking terminal cisternae to transverse tubules in skeletal muscle. *J Cell Biol*. 93:543-550.
- Callaway, C., A. Seryshev, J. P. Wang, K. J. Slavik, D. H. Needleman, C. Cantu, 3rd, Y. Wu, T. Jayaraman, A. R. Marks, and S. L. Hamilton. 1994. Localization of the high and low affinity [3H]ryanodine binding sites on the skeletal muscle  $\text{Ca}^{2+}$  release channel. *J Biol Chem*. 269:15876-15884.
- Campbell, K. P., C. Franzini-Armstrong, and A. E. Shamo. 1980. Further characterization of light and heavy sarcoplasmic reticulum vesicles. Identification of the 'sarcoplasmic reticulum feet' associated with

- heavy sarcoplasmic reticulum vesicles. *Biochim Biophys Acta*. 602:97-116.
- Campbell, K. P., C. M. Knudson, T. Imagawa, A. T. Leung, J. L. Sutko, S. D. Kahl, C. R. Raab, and L. Madson. 1987. Identification and characterization of the high affinity [3H]ryanodine receptor of the junctional sarcoplasmic reticulum Ca<sup>2+</sup> release channel. *J Biol Chem*. 262:6460-6463.
- Campbell, K. P., and D. H. MacLennan. 1981. Purification and characterization of the 53,000-dalton glycoprotein from the sarcoplasmic reticulum. *J Biol Chem*. 256:4626-4632.
- Caswell, A. H., N. R. Brandt, J. P. Brunschwig, and S. Purkerson. 1991. Localization and partial characterization of the oligomeric disulfide-linked molecular weight 95,000 protein (triadin) which binds the ryanodine and dihydropyridine receptors in skeletal muscle triadic vesicles. *Biochemistry*. 30:7507-7513.
- Caswell, A. H., Y. H. Lau, and J. P. Brunschwig. 1976. Ouabain-binding vesicles from skeletal muscle. *Arch Biochem Biophys*. 176:417-430.
- Caswell, A. H., Y. H. Lau, M. Garcia, and J. P. Brunschwig. 1979. Recognition and junction formation by isolated transverse tubules and terminal cisternae of skeletal muscle. *J Biol Chem*. 254:202-208.
- Catterall, W. A. 1991. Excitation-contraction coupling in vertebrate skeletal muscle: a tale of two calcium channels. *Cell*. 64:871-874.
- Catterall, W. A. 1996. Molecular properties of sodium and calcium channels. *J Bioenerg Biomembr*. 28:219-230.
- Chavis, P., L. Fagni, J. B. Lansman, and J. Bockaert. 1996. Functional coupling between ryanodine receptors and L-type calcium channels in neurons. *Nature*. 382:719-722.

- Chen, S. R., J. A. Airey, and D. H. MacLennan. 1993a. Positioning of major tryptic fragments in the  $\text{Ca}^{2+}$  release channel (ryanodine receptor) resulting from partial digestion of rabbit skeletal muscle sarcoplasmic reticulum. *J Biol Chem.* 268:22642-22649.
- Chen, S. R., P. Leong, J. P. Imredy, C. Bartlett, L. Zhang, and D. H. MacLennan. 1997a. Single-channel properties of the recombinant skeletal muscle  $\text{Ca}^{2+}$  release channel (ryanodine receptor). *Biophys J.* 73:1904-1912.
- Chen, S. R., and D. H. MacLennan. 1994. Identification of calmodulin-,  $\text{Ca}(2+)$ -, and ruthenium red-binding domains in the  $\text{Ca}^{2+}$  release channel (ryanodine receptor) of rabbit skeletal muscle sarcoplasmic reticulum. *J Biol Chem.* 269:22698-22704.
- Chen, S. R., D. M. Vaughan, J. A. Airey, R. Coronado, and D. H. MacLennan. 1993b. Functional expression of cDNA encoding the  $\text{Ca}^{2+}$  release channel (ryanodine receptor) of rabbit skeletal muscle sarcoplasmic reticulum in COS-1 cells. *Biochemistry.* 32:3743-3753.
- Chen, S. R., L. Zhang, and D. H. MacLennan. 1992. Characterization of a  $\text{Ca}^{2+}$  binding and regulatory site in the  $\text{Ca}^{2+}$  release channel (ryanodine receptor) of rabbit skeletal muscle sarcoplasmic reticulum. *J Biol Chem.* 267:23318-23326.
- Chen, S. R., L. Zhang, and D. H. MacLennan. 1993c. Antibodies as probes for  $\text{Ca}^{2+}$  activation sites in the  $\text{Ca}^{2+}$  release channel (ryanodine receptor) of rabbit skeletal muscle sarcoplasmic reticulum. *J Biol Chem.* 268:13414-13421.
- Chen, S. R., L. Zhang, and D. H. MacLennan. 1994. Asymmetrical blockade of the  $\text{Ca}^{2+}$  release channel (ryanodine receptor) by 12-kDa FK506 binding protein. *Proc Natl Acad Sci U S A.* 91:11953-11957.



- Chen, S. R. W., K. Ebisawa, X. Li, and L. Zhang. 1998. Molecular identification of the ryanodine receptor  $\text{Ca}^{2+}$  sensor [In Process Citation]. *J Biol Chem.* 273:14675-14678.
- Chen, S. R. W., X. Li, K. Ebisawa, and L. Zhang. 1997b. Functional characterization of the recombinant type 3  $\text{Ca}^{2+}$  release channel (ryanodine receptor) expressed in HEK293 cells. *J Biol Chem.* 272:24234-24246.
- Coronado, R., J. Morrisette, M. Sukhareva, and D. M. Vaughan. 1994. Structure and function of ryanodine receptors. *Am J Physiol.* 266:C1485-1504.
- Curtis, B. M., and W. A. Catterall. 1986. Reconstitution of the voltage-sensitive calcium channel purified from skeletal muscle transverse tubules. *Biochemistry.* 25:3077-3083.
- Damiani, E., G. Tobaldin, E. Bortoloso, and A. Margreth. 1997. Functional behaviour of the ryanodine receptor/ $\text{Ca}^{2+}$ -release channel in vesiculated derivatives of the junctional membrane of terminal cisternae of rabbit fast muscle sarcoplasmic reticulum. *Cell Calcium.* 22:129-150.
- De Waard, M., and K. P. Campbell. 1995. Subunit regulation of the neuronal  $\alpha$  1A  $\text{Ca}^{2+}$  channel expressed in *Xenopus* oocytes. *J Physiol (Lond).* 485:619-634.
- De Waard, M., C. A. Gurnett, and K. P. Campbell. 1996. Structural and functional diversity of voltage-activated calcium channels. *Ion Channels.* 4:41-87.
- De Waard, M., D. R. Witcher, M. Pragnell, H. Liu, and K. P. Campbell. 1995. Properties of the  $\alpha$  1-beta anchoring site in voltage-dependent  $\text{Ca}^{2+}$  channels. *J Biol Chem.* 270:12056-12064.

- Desmedt, J. E., and K. Hainaut. 1977. Inhibition of the intracellular release of calcium by Dantrolene in barnacle giant muscle fibres. *J Physiol (Lond)*. 265:565-585.
- Donoso, P., M. Beltran, and C. Hidalgo. 1996. Luminal pH regulated calcium release kinetics in sarcoplasmic reticulum vesicles. *Biochemistry*. 35:13419-13425.
- Du, G.-G., and D. H. MacLennan. 1998. *submitted*.
- Dubowitz, V., and M. Platts. 1965. Central core disease of muscle with focal wasting. *J Neurol Neurosurg Psychiatry*. 28:432-437.
- el-Hayek, R., B. Antoniu, J. Wang, S. L. Hamilton, and N. Ikemoto. 1995. Identification of calcium release-triggering and blocking regions of the II-III loop of the skeletal muscle dihydropyridine receptor. *J Biol Chem*. 270:22116-22118.
- el-Hayek, R., C. Valdivia, H. H. Valdivia, K. Hogan, and R. Coronado. 1993. Activation of the Ca<sup>2+</sup> release channel of skeletal muscle sarcoplasmic reticulum by palmitoyl carnitine. *Biophys J*. 65:779-789.
- Ellis, F. R., N. P. Keaney, D. G. Harriman, D. W. Sumner, K. Kyei-Mensah, J. H. Tyrrell, J. B. Hargreaves, R. K. Parikh, and P. L. Mulrooney. 1972. Screening for malignant hyperpyrexia. *Br Med J*. 3:559-561.
- Ellis, K. O., A. W. Castellion, L. J. Honkomp, F. L. Wessels, J. E. Carpenter, and R. P. Halliday. 1973. Dantrolene, a direct acting skeletal muscle relaxant. *J Pharm Sci*. 62:948-951.
- Empson, R. M., and A. Galione. 1997. Cyclic ADP-ribose enhances coupling between voltage-gated Ca<sup>2+</sup> entry and intracellular Ca<sup>2+</sup> release. *J Biol Chem*. 272:20967-20970.

- Endo, M., M. Tanaka, and Y. Ogawa. 1970. Calcium induced release of calcium from the sarcoplasmic reticulum of skinned skeletal muscle fibres. *Nature*. 228:34-36.
- Fabiato, A. 1982. Calcium release in skinned cardiac cells: variations with species, tissues, and development. *Fed Proc*. 41:2238-2244.
- Fabiato, A. 1985. Simulated calcium current can both cause calcium loading in and trigger calcium release from the sarcoplasmic reticulum of a skinned canine cardiac Purkinje cell. *J Gen Physiol*. 85:291-320.
- Fatt, P., and B. Ginsborg, L. 1958. The ionic requirements for the production of action potentials in crustacean muscle fibres. *J. Physiol. (Lond.)*. 142:516-543.
- Favero, T. G., A. C. Zable, and J. J. Abramson. 1995a. Hydrogen peroxide stimulates the  $\text{Ca}^{2+}$  release channel from skeletal muscle sarcoplasmic reticulum. *J Biol Chem*. 270:25557-25563.
- Favero, T. G., A. C. Zable, M. B. Bowman, A. Thompson, and J. J. Abramson. 1995b. Metabolic end products inhibit sarcoplasmic reticulum  $\text{Ca}^{2+}$  release and [3H]ryanodine binding. *J Appl Physiol*. 78:1665-1672.
- Fill, M., R. Mejia-Alvarez, F. Zorzato, P. Volpe, and E. Stefani. 1991. Antibodies as probes for ligand gating of single sarcoplasmic reticulum  $\text{Ca}^{2+}$ -release channels. *Biochem J*. 273:449-457.
- Fliegel, L., M. Ohnishi, M. R. Carpenter, V. K. Khanna, R. A. Reithmeier, and D. H. MacLennan. 1987. Amino acid sequence of rabbit fast-twitch skeletal muscle calsequestrin deduced from cDNA and peptide sequencing. *Proc Natl Acad Sci U S A*. 84:1167-1171.
- Flucher, B. E., and C. Franzini-Armstrong. 1996. Formation of junctions involved in excitation-contraction coupling in skeletal and cardiac muscle. *Proc Natl Acad Sci U S A*. 93:8101-8106.

- Flucher, B. E., J. L. Phillips, J. A. Powell, S. B. Andrews, and M. P. Daniels. 1992. Coordinated development of myofibrils, sarcoplasmic reticulum and transverse tubules in normal and dysgenic mouse skeletal muscle, in vivo and in vitro. *Dev Biol.* 150:266-280.
- Ford, L. E., and R. J. Podolsky. 1970. Regenerative calcium release within muscle cells. *Science.* 167:58-59.
- Franzini-Armstrong, C. 1970. Studies of the triad. I. Structure of the junction in frog twitch fibres. *J. Cell Biol.* 47:488-499.
- Franzini-Armstrong, C., and F. Protasi. 1997. Ryanodine receptors of striated muscles: a complex channel capable of multiple interactions. *Physiol Rev.* 77:699-729.
- Fruen, B. R., J. R. Mickelson, and C. F. Louis. 1997. Dantrolene inhibition of sarcoplasmic reticulum  $Ca^{2+}$  release by direct and specific action at skeletal muscle ryanodine receptors. *J Biol Chem.* 272:26965-26971.
- Fruen, B. R., J. R. Mickelson, N. H. Shomer, P. Velez, and C. F. Louis. 1994. Cyclic ADP-ribose does not affect cardiac or skeletal muscle ryanodine receptors. *FEBS Lett.* 352:123-126.
- Fujii, J., K. Otsu, F. Zorzato, S. de Leon, V. K. Khanna, J. E. Weiler, P. J. O'Brien, and D. H. MacLennan. 1991. Identification of a mutation in porcine ryanodine receptor associated with malignant hyperthermia. *Science.* 253:448-451.
- Furuichi, T., D. Furutama, Y. Hakamata, J. Nakai, H. Takeshima, and K. Mikoshiba. 1994. Multiple types of ryanodine receptor/ $Ca^{2+}$  release channels are differentially expressed in rabbit brain. *J Neurosci.* 14:4794-4805.

- Furuichi, T., S. Yoshikawa, A. Miyawaki, K. Wada, N. Maeda, and K. Mikoshiba. 1989. Primary structure and functional expression of the inositol 1,4,5- trisphosphate-binding protein P400. *Nature*. 342:32-38.
- Garcia, J., J. Nakai, K. Imoto, and K. G. Beam. 1997. Role of S4 segments and the leucine heptad motif in the activation of an L-type calcium channel. *Biophys J*. 72:2515-2523.
- Giannini, G., E. Clementi, R. Ceci, G. Marziali, and V. Sorrentino. 1992. Expression of a ryanodine receptor-Ca<sup>2+</sup> channel that is regulated by TGF-beta. *Science*. 257:91-94.
- Giannini, G., A. Conti, S. Mammarella, M. Scrobogna, and V. Sorrentino. 1995. The ryanodine receptor/calcium channel genes are widely and differentially expressed in murine brain and peripheral tissues. *J Cell Biol*. 128:893-904.
- Grunwald, R., and G. Meissner. 1995. Lumenal sites and C terminus accessibility of the skeletal muscle calcium release channel (ryanodine receptor). *J Biol Chem*. 270:11338-11347.
- Guerrini, R., P. Menegazzi, R. Anacardio, M. Marastoni, R. Tomatis, F. Zorzato, and S. Treves. 1995. Calmodulin binding sites of the skeletal, cardiac, and brain ryanodine receptor Ca<sup>2+</sup> channels: modulation by the catalytic subunit of cAMP- dependent protein kinase? *Biochemistry*. 34:5120-5129.
- Guo, W., and K. P. Campbell. 1995. Association of triadin with the ryanodine receptor and calsequestrin in the lumen of the sarcoplasmic reticulum. *J Biol Chem*. 270:9027-9030.
- Guo, W., A. O. Jorgensen, and K. P. Campbell. 1996. Triadin, a linker for calsequestrin and the ryanodine receptor. *Soc Gen Physiol Ser*. 51:19-28.

- Hain, J., H. Onoue, M. Mayrleitner, S. Fleischer, and H. Schindler. 1995. Phosphorylation modulates the function of the calcium release channel of sarcoplasmic reticulum from cardiac muscle. *J Biol Chem.* 270:2074-2081.
- Hakamata, Y., J. Nakai, H. Takeshima, and K. Imoto. 1992. Primary structure and distribution of a novel ryanodine receptor/calcium release channel from rabbit brain. *FEBS Lett.* 312:229-235.
- Han, J. W., R. Thieleczek, M. Varsanyi, and L. M. Heilmeyer, Jr. 1992. Compartmentalized ATP synthesis in skeletal muscle triads. *Biochemistry.* 31:377-384.
- Harrison, G. G. 1975. Control of the malignant hyperpyrexia syndrome in MHS swine by dantrolene sodium. *Br J Anaesth.* 47:62-65.
- Henkart, M., D. M. Landis, and T. S. Reese. 1976. Similarity of junctions between plasma membranes and endoplasmic reticulum in muscle and neurons. *J Cell Biol.* 70:338-347.
- Huxley, A. F., and R. E. Taylor. 1958. Local activation of skeletal muscle fibers. *Journal of Physiology (London).*
- Hymel, L., M. Inui, S. Fleischer, and H. Schindler. 1988. Purified ryanodine receptor of skeletal muscle sarcoplasmic reticulum forms  $\text{Ca}^{2+}$ -activated oligomeric  $\text{Ca}^{2+}$  channels in planar bilayers. *Proc Natl Acad Sci U S A.* 85:441-445.
- Ikemoto, N., B. Antoniu, J. J. Kang, L. G. Meszaros, and M. Ronjat. 1991. Intravesicular calcium transient during calcium release from sarcoplasmic reticulum. *Biochemistry.* 30:5230-5237.
- Ikemoto, N., M. Ronjat, L. G. Meszaros, and M. Koshita. 1989. Postulated role of calsequestrin in the regulation of calcium release from sarcoplasmic reticulum. *Biochemistry.* 28:6764-6771.

- Ikemoto, T., M. Iino, and M. Endo. 1995. Enhancing effect of calmodulin on  $\text{Ca}^{2+}$ -induced  $\text{Ca}^{2+}$  release in the sarcoplasmic reticulum of rabbit skeletal muscle fibres. *J Physiol (Lond)*. 487:573-582.
- Imagawa, T., J. S. Smith, R. Coronado, and K. P. Campbell. 1987. Purified ryanodine receptor from skeletal muscle sarcoplasmic reticulum is the  $\text{Ca}^{2+}$ -permeable pore of the calcium release channel. *J Biol Chem*. 262:16636-16643.
- Inui, M., A. Saito, and S. Fleischer. 1987a. Isolation of the ryanodine receptor from cardiac sarcoplasmic reticulum and identity with the feet structures. *J Biol Chem*. 262:15637-15642.
- Inui, M., A. Saito, and S. Fleischer. 1987b. Purification of the ryanodine receptor and identity with feet structures of junctional terminal cisternae of sarcoplasmic reticulum from fast skeletal muscle. *J Biol Chem*. 262:1740-1747.
- Jacquemond, V., L. Csernoch, M. G. Klein, and M. F. Schneider. 1991. Voltage-gated and calcium-gated calcium release during depolarization of skeletal muscle fibers. *Biophys J*. 60:867-873.
- Jenden, D. J., and A. S. Fairhurst. 1969. The pharmacology of ryanodine. *Pharmacol Rev*. 21:1-25.
- Jones, L. R., L. Zhang, K. Sanborn, A. O. Jorgensen, and J. Kelley. 1995. Purification, primary structure, and immunological characterization of the 26-kDa calsequestrin binding protein (junctin) from cardiac junctional sarcoplasmic reticulum. *J Biol Chem*. 270:30787-30796.
- Jong, D. S., P. C. Pape, S. M. Baylor, and W. K. Chandler. 1995. Calcium inactivation of calcium release in frog cut muscle fibers that contain millimolar EGTA or Fura-2. *J Gen Physiol*. 106:337-388.

- Jong, D. S., P. C. Pape, W. K. Chandler, and S. M. Baylor. 1993. Reduction of calcium inactivation of sarcoplasmic reticulum calcium release by fura-2 in voltage-clamped cut twitch fibers from frog muscle. *J Gen Physiol.* 102:333-370.
- Jorgensen, A. O., A. C. Shen, W. Arnold, A. T. Leung, and K. P. Campbell. 1989. Subcellular distribution of the 1,4-dihydropyridine receptor in rabbit skeletal muscle in situ: an immunofluorescence and immunocolloidal gold- labeling study. *J Cell Biol.* 109:135-147.
- Jorgensen, A. O., A. C. Shen, W. Arnold, P. S. McPherson, and K. P. Campbell. 1993. The Ca<sup>2+</sup>-release channel/ryanodine receptor is localized in junctional and corbular sarcoplasmic reticulum in cardiac muscle. *J Cell Biol.* 120:969-980.
- Kalow, W., B. A. Britt, M. E. Terreau, and C. Haist. 1970. Metabolic error of muscle metabolism after recovery from malignant hyperthermia. *Lancet.* 2:895-898.
- Kang, J. J., A. Tarcsafalvi, A. D. Carlos, E. Fujimoto, Z. Shahrokh, B. J. Thevenin, S. B. Shohet, and N. Ikemoto. 1992. Conformational changes in the foot protein of the sarcoplasmic reticulum assessed by site-directed fluorescent labeling [published erratum appears in *Biochemistry* 1992 May 26;31(20):4922]. *Biochemistry.* 31:3288-3293.
- Kawamoto, R. M., J. P. Brunschwig, K. C. Kim, and A. H. Caswell. 1986. Isolation, characterization, and localization of the spanning protein from skeletal muscle triads. *J Cell Biol.* 103:1405-1414.
- Kawasaki, T., and M. Kasai. 1994. Regulation of calcium channel in sarcoplasmic reticulum by calsequestrin. *Biochem Biophys Res Commun.* 199:1120-1127.



- Kim, K. C., A. H. Caswell, J. P. Brunschwig, and N. R. Brandt. 1990a. Identification of a new subpopulation of triad junctions isolated from skeletal muscle; morphological correlations with intact muscle. *J Membr Biol.* 113:221-235.
- Kim, K. C., A. H. Caswell, J. A. Talvenheimo, and N. R. Brandt. 1990b. Isolation of a terminal cisterna protein which may link the dihydropyridine receptor to the junctional foot protein in skeletal muscle. *Biochemistry.* 29:9281-9289.
- Kirino, Y., M. Osakabe, and H. Shimizu. 1983.  $\text{Ca}^{2+}$ -induced  $\text{Ca}^{2+}$  release from fragmented sarcoplasmic reticulum:  $\text{Ca}^{2+}$ - dependent passive  $\text{Ca}^{2+}$  efflux. *J Biochem (Tokyo).* 94:1111-1118.
- Klein, M. G., H. Cheng, L. F. Santana, Y. H. Jiang, W. J. Lederer, and M. F. Schneider. 1996. Two mechanisms of quantized calcium release in skeletal muscle. *Nature.* 379:455-458.
- Knudson, C. M., K. K. Stang, A. O. Jorgensen, and K. P. Campbell. 1993a. Biochemical characterization of ultrastructural localization of a major junctional sarcoplasmic reticulum glycoprotein (triadin). *J Biol Chem.* 268:12637-12645.
- Knudson, C. M., K. K. Stang, C. R. Moomaw, C. A. Slaughter, and K. P. Campbell. 1993b. Primary structure and topological analysis of a skeletal muscle- specific junctional sarcoplasmic reticulum glycoprotein (triadin). *J Biol Chem.* 268:12646-12654.
- Kozak, M., and A. J. Shatkin. 1979. Characterization of translational initiation regions from eukaryotic messenger RNAs. *Methods Enzymol.* 60:360-375.
- Lacerda, A. E., H. S. Kim, P. Ruth, E. Perez-Reyes, V. Flockerzi, F. Hofmann, L. Birnbaumer, and A. M. Brown. 1991. Normalization of current

- kinetics by interaction between the alpha 1 and beta subunits of the skeletal muscle dihydropyridine-sensitive  $\text{Ca}^{2+}$  channel. *Nature*. 352:527-530.
- Lai, F. A., H. Erickson, B. A. Block, and G. Meissner. 1987. Evidence for a junctional feet-ryanodine receptor complex from sarcoplasmic reticulum. *Biochem Biophys Res Commun*. 143:704-709.
- Lai, F. A., H. P. Erickson, E. Rousseau, Q. Y. Liu, and G. Meissner. 1988. Purification and reconstitution of the calcium release channel from skeletal muscle. *Nature*. 331:315-319.
- Lamb, G., D., and D. Stephenson, G. 1992. Importance of  $\text{Mg}^{2+}$  in Excitation-Contraction Coupling in Skeletal Muscle. *News Physiol. Sci.* 7:270-274.
- Laver, D. R., T. M. Baynes, and A. F. Dulhunty. 1997. Magnesium inhibition of ryanodine-receptor calcium channels: evidence for two independent mechanisms. *J Membr Biol*. 156:213-229.
- Lee, H. C., R. Aarhus, R. Graeff, M. E. Gurnack, and T. F. Walseth. 1994. Cyclic ADP ribose activation of the ryanodine receptor is mediated by calmodulin. *Nature*. 370:307-309.
- Leong, P., and D. MacLennan, H. 1998a. The Cytoplasmic Loops between Domains II and III and Domains III and IV in the Skeletal Muscle Dihydropyridine Receptor Bind to a Contiguous Site in the Skeletal Muscle Ryanodine Receptor. *J. Biol. Chem.* 273:24983-24986.
- Leong, P., and D. H. MacLennan. 1998b. A 37-amino acid sequence in the skeletal muscle ryanodine receptor interacts with the cytoplasmic loop between domains II and III in the skeletal muscle dihydropyridine receptor. *J Biol Chem*. 273:7791-7794.

- Loke, J., and D. H. MacLennan. 1998. Malignant hyperthermia and central core disease: disorders of Ca<sup>2+</sup> release channels. *Am J Med.* 104:470-486.
- Lomant, A. J., and G. Fairbanks. 1976. Chemical Probes of Extended Biological Structures: Synthesis and Properties of the Cleavable Protein Cross-linking Reagent [<sup>35</sup>S]Dithiobis(succinimidyl propionate). *J. Mol. Biol.* 104:243-261.
- Lu, X., L. Xu, and G. Meissner. 1994. Activation of the skeletal muscle calcium release channel by a cytoplasmic loop of the dihydropyridine receptor. *J Biol Chem.* 269:6511-6516.
- Lu, X., L. Xu, and G. Meissner. 1995. Phosphorylation of dihydropyridine receptor II-III loop peptide regulates skeletal muscle calcium release channel function. Evidence for an essential role of the beta-OH group of Ser687. *J Biol Chem.* 270:18459-18464.
- Lytton, J., and D. H. MacLennan. 1992. Sarcoplasmic Reticulum. *In* The heart and Cardiovascular System:Scientific Foundations. H. A. Fozzard, E. Haber, R. B. Jennings, A. M. Katz, and H. E. Morgan, editors. Raven Press, New York. 1203-1222.
- Ma, J., M. B. Bhat, and J. Zhao. 1995. Rectification of skeletal muscle ryanodine receptor mediated by FK506 binding protein. *Biophys J.* 69:2398-2404.
- MacKenzie, A. E., R. G. Korneluk, F. Zorzato, J. Fujii, M. Phillips, D. Iles, B. Wieringa, S. Leblond, J. Bailly, H. F. Willard, and et al. 1990. The human ryanodine receptor gene: its mapping to 19q13.1, placement in a chromosome 19 linkage group, and exclusion as the gene causing myotonic dystrophy. *Am J Hum Genet.* 46:1082-1089.

- MacLennan, D. H., C. Duff, F. Zorzato, J. Fujii, M. Phillips, R. G. Korneluk, W. Frodis, B. A. Britt, and R. G. Worton. 1990. Ryanodine receptor gene is a candidate for predisposition to malignant hyperthermia. *Nature*. 343:559-561.
- MacLennan, D. H., and M. S. Phillips. 1992. Malignant hyperthermia. *Science*. 256:789-794.
- MacLennan, D. H., and R. A. Reithmeier. 1998. Ion tamers [news; comment]. *Nat Struct Biol*. 5:409-411.
- MacLennan, D. H., T. Toyofuku, and J. Lytton. 1992. Structure-function relationships in sarcoplasmic or endoplasmic reticulum type  $\text{Ca}^{2+}$  pumps. *Ann N Y Acad Sci*. 671:1-10.
- Marks, A. R., S. Fleischer, and P. Tempst. 1990. Surface topography analysis of the ryanodine receptor/junctional channel complex based on proteolysis sensitivity mapping. *J Biol Chem*. 265:13143-13149.
- Marty, I., M. Robert, M. Villaz, K. De Jongh, Y. Lai, W. A. Catterall, and M. Ronjat. 1994a. Biochemical evidence for a complex involving dihydropyridine receptor and ryanodine receptor in triad junctions of skeletal muscle. *Proc Natl Acad Sci U S A*. 91:2270-2274.
- Marty, I., M. Villaz, G. Arlaud, I. Bally, and M. Ronjat. 1994b. Transmembrane orientation of the N-terminal and C-terminal ends of the ryanodine receptor in the sarcoplasmic reticulum of rabbit skeletal muscle. *Biochem J*. 298 Pt 3:743-749.
- Mayrleitner, M., R. Chandler, H. Schindler, and S. Fleischer. 1995. Phosphorylation with protein kinases modulates calcium loading of terminal cisternae of sarcoplasmic reticulum from skeletal muscle. *Cell Calcium*. 18:197-206.

- McCarthy, T. V., J. M. Healy, J. J. Heffron, M. Lehane, T. Deufel, F. Lehmann-Horn, M. Farrall, and K. Johnson. 1990. Localization of the malignant hyperthermia susceptibility locus to human chromosome 19q12-13.2. *Nature*. 343:562-564.
- McPhee, J. C., D. S. Ragsdale, T. Scheuer, and W. A. Catterall. 1994. A mutation in segment IVS6 disrupts fast inactivation of sodium channels. *Proc Natl Acad Sci U S A*. 91:12346-12350.
- Meissner, G. 1983. Monovalent ion and calcium ion fluxes in sarcoplasmic reticulum. *Mol Cell Biochem*. 55:65-82.
- Meissner, G. 1984. Adenine nucleotide stimulation of  $\text{Ca}^{2+}$ -induced  $\text{Ca}^{2+}$  release in sarcoplasmic reticulum. *J Biol Chem*. 259:2365-2374.
- Meissner, G. 1986. Evidence of a role for calmodulin in the regulation of calcium release from skeletal muscle sarcoplasmic reticulum. *Biochemistry*. 25:244-251.
- Meissner, G., E. Darling, and J. Eveleth. 1986. Kinetics of rapid  $\text{Ca}^{2+}$  release by sarcoplasmic reticulum. Effects of  $\text{Ca}^{2+}$ ,  $\text{Mg}^{2+}$ , and adenine nucleotides. *Biochemistry*. 25:236-244.
- Meissner, G., and J. S. Henderson. 1987. Rapid calcium release from cardiac sarcoplasmic reticulum vesicles is dependent on  $\text{Ca}^{2+}$  and is modulated by  $\text{Mg}^{2+}$ , adenine nucleotide, and calmodulin. *J Biol Chem*. 262:3065-3073.
- Meissner, G., and X. Lu. 1995. Dihydropyridine receptor-ryanodine receptor interactions in skeletal muscle excitation-contraction coupling. *Biosci Rep*. 15:399-408.
- Melzer, W., E. Rios, and M. F. Schneider. 1984. Time course of calcium release and removal in skeletal muscle fibers. *Biophys J*. 45:637-641.

- Melzer, W., E. Rios, and M. F. Schneider. 1987. A general procedure for determining the rate of calcium release from the sarcoplasmic reticulum in skeletal muscle fibers. *Biophys J.* 51:849-863.
- Menegazzi, P., F. Larini, S. Treves, R. Guerrini, M. Quadroni, and F. Zorzato. 1994. Identification and characterization of three calmodulin binding sites of the skeletal muscle ryanodine receptor. *Biochemistry.* 33:9078-9084.
- Meszaros, L. G., J. Bak, and A. Chu. 1993. Cyclic ADP-ribose as an endogenous regulator of the non-skeletal type ryanodine receptor  $\text{Ca}^{2+}$  channel. *Nature.* 364:76-79.
- Mickelson, J. R., and C. F. Louis. 1996. Malignant hyperthermia: excitation-contraction coupling,  $\text{Ca}^{2+}$  release channel, and cell  $\text{Ca}^{2+}$  regulation defects. *Physiol Rev.* 76:537-592.
- Mikami, A., K. Imoto, T. Tanabe, T. Niidome, Y. Mori, H. Takeshima, S. Narumiya, and S. Numa. 1989. Primary structure and functional expression of the cardiac dihydropyridine-sensitive calcium channel. *Nature.* 340:230-233.
- Mitchell, R. D., H. K. Simmerman, and L. R. Jones. 1988.  $\text{Ca}^{2+}$  binding effects on protein conformation and protein interactions of canine cardiac calsequestrin. *J Biol Chem.* 263:1376-1381.
- Miyamoto, H., and E. Racker. 1981. Calcium-induced calcium release at terminal cisternae of skeletal sarcoplasmic reticulum. *FEBS Lett.* 133:235-238.
- Monnier, N., V. Procaccio, P. Stieglitz, and J. Lunardi. 1997. Malignant-hyperthermia susceptibility is associated with a mutation of the  $\alpha$ 1-subunit of the human dihydropyridine-sensitive L-type voltage-

- dependent calcium-channel receptor in skeletal muscle [see comments].  
*Am J Hum Genet.* 60:1316-1325.
- Morrisette, J., G. Heisermann, J. Cleary, A. Ruoho, and R. Coronado. 1993.  
Cyclic ADP-ribose induced  $\text{Ca}^{2+}$  release in rabbit skeletal muscle  
sarcoplasmic reticulum. *FEBS Lett.* 330:270-274.
- Mothet, J. P., P. Fossier, F. M. Meunier, J. Stinnakre, L. Tauc, and G. Baux.  
1998. Cyclic ADP-ribose and calcium-induced calcium release regulate  
neurotransmitter release at a cholinergic synapse of *Aplysia*. *J Physiol*  
(*Lond*). 507:405-414.
- Moutin, M. J., and Y. Dupont. 1988. Rapid filtration studies of  $\text{Ca}^{2+}$ -induced  
 $\text{Ca}^{2+}$  release from skeletal sarcoplasmic reticulum. Role of monovalent  
ions. *J Biol Chem.* 263:4228-4235.
- Murayama, T., and Y. Ogawa. 1992. Purification and characterization of two  
ryanodine-binding protein isoforms from sarcoplasmic reticulum of  
bullfrog skeletal muscle. *J Biochem (Tokyo)*. 112:514-522.
- Murray, B. E., and K. Ohlendieck. 1997. Cross-linking analysis of the  
ryanodine receptor and  $\alpha 1$ -dihydropyridine receptor in rabbit  
skeletal muscle triads. *Biochem J.* 324:689-696.
- Nabauer, M., G. Callewaert, L. Cleemann, and M. Morad. 1989. Regulation of  
calcium release is gated by calcium current, not gating charge, in  
cardiac myocytes [see comments]. *Science.* 244:800-803.
- Nakai, J., B. A. Adams, K. Imoto, and K. G. Beam. 1994. Critical roles of the  
S3 segment and S3-S4 linker of repeat I in activation of L-type calcium  
channels. *Proc Natl Acad Sci U S A.* 91:1014-1018.
- Nakai, J., R. T. Dirksen, H. T. Nguyen, I. N. Pessah, K. G. Beam, and P. D.  
Allen. 1996. Enhanced dihydropyridine receptor channel activity in the  
presence of ryanodine receptor. *Nature.* 380:72-75.

- Nakai, J., T. Imagawa, Y. Hakamat, M. Shigekawa, H. Takeshima, and S. Numa. 1990. Primary structure and functional expression from cDNA of the cardiac ryanodine receptor/calcium release channel. *FEBS Lett.* 271:169-177.
- Nakai, J., T. Ogura, F. Protasi, C. Franzini-Armstrong, P. D. Allen, and K. G. Beam. 1997. Functional nonequality of the cardiac and skeletal ryanodine receptors. *Proc Natl Acad Sci U S A.* 94:1019-1022.
- Nakai, J., N. Sekiguchi, T. A. Rando, P. D. Allen, and K. G. Beam. 1998. Two regions of the ryanodine receptor involved in coupling with L-type Ca<sup>2+</sup> channels. *J Biol Chem.* 273:13403-13406.
- Nakanishi, S. 1994. Metabotropic glutamate receptors: synaptic transmission, modulation, and plasticity. *Neuron.* 13:1031-1037.
- Nelson, T. E., M. Lin, G. Zapata-Sudo, and R. T. Sudo. 1996. Dantrolene sodium can increase or attenuate activity of skeletal muscle ryanodine receptor calcium release channel. Clinical implications. *Anesthesiology.* 84:1368-1379.
- Noda, M., T. Ikeda, T. Kayano, H. Suzuki, H. Takeshima, M. Kurasaki, H. Takahashi, and S. Numa. 1986. Existence of distinct sodium channel messenger RNAs in rat brain. *Nature.* 320:188-192.
- Noda, M., S. Shimizu, T. Tanabe, T. Takai, T. Kayano, T. Ikeda, H. Takahashi, H. Nakayama, Y. Kanaoka, N. Minamino, and et al. 1984. Primary structure of *Electrophorus electricus* sodium channel deduced from cDNA sequence. *Nature.* 312:121-127.
- Oba, T., T. Ishikawa, and M. Yamaguchi. 1998. Sulfhydryls associated with H<sub>2</sub>O<sub>2</sub>-induced channel activation are on luminal side of ryanodine receptors. *Am J Physiol.* 274:C914-921.



- Ohta, T., S. Ito, and A. Ohga. 1990. Inhibitory action of dantrolene on Ca<sup>2+</sup>-induced Ca<sup>2+</sup> release from sarcoplasmic reticulum in guinea pig skeletal muscle. *Eur J Pharmacol.* 178:11-19.
- Olcese, R., N. Qin, T. Schneider, A. Neely, X. Wei, E. Stefani, and L. Birnbaumer. 1994. The amino terminus of a calcium channel beta subunit sets rates of channel inactivation independently of the subunit's effect on activation. *Neuron.* 13:1433-1438.
- Orlova, E. V., Serysheva, II, M. van Heel, S. L. Hamilton, and W. Chiu. 1996. Two structural configurations of the skeletal muscle calcium release channel. *Nat Struct Biol.* 3:547-552.
- Otsu, K., V. K. Khanna, A. L. Archibald, and D. H. MacLennan. 1991. Cosegregation of porcine malignant hyperthermia and a probable causal mutation in the skeletal muscle ryanodine receptor gene in backcross families. *Genomics.* 11:744-750.
- Otsu, K., K. Nishida, Y. Kimura, T. Kuzuya, M. Hori, T. Kamada, and M. Tada. 1994. The point mutation Arg615-->Cys in the Ca<sup>2+</sup> release channel of skeletal sarcoplasmic reticulum is responsible for hypersensitivity to caffeine and halothane in malignant hyperthermia. *J Biol Chem.* 269:9413-9415.
- Otsu, K., H. F. Willard, V. K. Khanna, F. Zorzato, N. M. Green, and D. H. MacLennan. 1990. Molecular cloning of cDNA encoding the Ca<sup>2+</sup> release channel (ryanodine receptor) of rabbit cardiac muscle sarcoplasmic reticulum. *J Biol Chem.* 265:13472-13483.
- Palade, P. 1987. Drug-induced Ca<sup>2+</sup> release from isolated sarcoplasmic reticulum. III. Block of Ca<sup>2+</sup>-induced Ca<sup>2+</sup> release by organic polyamines. *J Biol Chem.* 262:6149-6154.

- Pape, P. C., D. S. Jong, W. K. Chandler, and S. M. Baylor. 1993. Effect of fura-2 on action potential-stimulated calcium release in cut twitch fibers from frog muscle. *J Gen Physiol.* 102:295-332.
- Patterson, V. H., T. R. Hill, P. J. Fletcher, and J. R. Heron. 1979. Central core disease: clinical and pathological evidence of progression within a family. *Brain.* 102:581-594.
- Penner, R., E. Neher, H. Takeshima, S. Nishimura, and S. Numa. 1989. Functional expression of the calcium release channel from skeletal muscle ryanodine receptor cDNA. *FEBS Lett.* 259:217-221.
- Percival, A. L., A. J. Williams, J. L. Kenyon, M. M. Grinsell, J. A. Airey, and J. L. Sutko. 1994. Chicken skeletal muscle ryanodine receptor isoforms: ion channel properties. *Biophys J.* 67:1834-1850.
- Perutz, M. 1994. Polar zippers: their role in human disease. *Protein Sci.* 3:1629-1637.
- Pessah, I. N., A. O. Francini, D. J. Scales, A. L. Waterhouse, and J. E. Casida. 1986. Calcium-ryanodine receptor complex. Solubilization and partial characterization from skeletal muscle junctional sarcoplasmic reticulum vesicles. *J Biol Chem.* 261:8643-8648.
- Pessah, I. N., A. L. Waterhouse, and J. E. Casida. 1985. The calcium-ryanodine receptor complex of skeletal and cardiac muscle. *Biochem Biophys Res Commun.* 128:449-456.
- Phillips, M. S., J. Fujii, V. K. Khanna, S. DeLeon, K. Yokobata, P. J. de Jong, and D. H. MacLennan. 1996. The structural organization of the human skeletal muscle ryanodine receptor (RYR1) gene. *Genomics.* 34:24-41.
- Pragnell, M., M. De Waard, Y. Mori, T. Tanabe, T. P. Snutch, and K. P. Campbell. 1994. Calcium channel beta-subunit binds to a conserved

motif in the I-II cytoplasmic linker of the alpha 1-subunit [see comments]. *Nature*. 368:67-70.

Quane, K. A., J. M. Healy, K. E. Keating, B. M. Manning, F. J. Couch, L. M. Palmucci, C. Doriguzzi, T. H. Fagerlund, K. Berg, H. Ording, and et al. 1993. Mutations in the ryanodine receptor gene in central core disease and malignant hyperthermia. *Nat Genet*. 5:51-55.

Quane, K. A., K. E. Keating, J. M. Healy, B. M. Manning, R. Krivosic-Horber, I. Krivosic, N. Monnier, J. Lunardi, and T. V. McCarthy. 1994. Mutation screening of the RYR1 gene in malignant hyperthermia: detection of a novel Tyr to Ser mutation in a pedigree with associated central cores. *Genomics*. 23:236-239.

Realini, C., and M. Rechsteiner. 1995. A proteasome activator subunit binds calcium. *J Biol Chem*. 270:29664-29667.

Realini, C., S. W. Rogers, and M. Rechsteiner. 1994. KEKE motifs. Proposed roles in protein-protein association and presentation of peptides by MHC class I receptors. *FEBS Lett*. 348:109-113.

Rios, E., and G. Brum. 1987. Involvement of dihydropyridine receptors in excitation-contraction coupling in skeletal muscle. *Nature*. 325:717-720.

Rios, E., and G. Pizarro. 1988. Voltage Sensors and Calcium Channels of Excitation-Contraction Coupling. *News in Physiol. Sciences*. 3:223-227.

Rios, E., and G. Pizarro. 1991. Voltage sensor of excitation-contraction coupling in skeletal muscle. *Physiol Rev*. 71:849-908.

Rousseau, E., J. Ladine, Q. Y. Liu, and G. Meissner. 1988. Activation of the Ca<sup>2+</sup> release channel of skeletal muscle sarcoplasmic reticulum by caffeine and related compounds. *Arch Biochem Biophys*. 267:75-86.

- Rousseau, E., J. S. Smith, and G. Meissner. 1987. Ryanodine modifies conductance and gating behavior of single  $\text{Ca}^{2+}$  release channel. *Am J Physiol.* 253:C364-368.
- Sabbadini, R. A., R. Betto, A. Teresi, G. Fachechi-Cassano, and G. Salviati. 1992. The effects of sphingosine on sarcoplasmic reticulum membrane calcium release. *J Biol Chem.* 267:15475-15484.
- Saito, A., C. T. Wang, and S. Fleischer. 1978. Membrane asymmetry and enhanced ultrastructural detail of sarcoplasmic reticulum revealed with use of tannic acid. *J Cell Biol.* 79:601-616.
- Salama, G., and J. Abramson. 1984. Silver ions trigger  $\text{Ca}^{2+}$  release by acting at the apparent physiological release site in sarcoplasmic reticulum. *J Biol Chem.* 259:13363-13369.
- Schneider, M. F., and W. K. Chandler. 1973. Voltage dependent charge movement of skeletal muscle: a possible step in excitation-contraction coupling. *Nature.* 242:244-246.
- Schneider, M. F., and B. J. Simon. 1988. Inactivation of calcium release from the sarcoplasmic reticulum in frog skeletal muscle. *J Physiol (Lond).* 405:727-745.
- Schoepp, D. D., and B. G. Johnson. 1993. Metabotropic glutamate receptor modulation of cAMP accumulation in the neonatal rat hippocampus. *Neuropharmacology.* 32:1359-1365.
- Scott, B. T., H. K. Simmerman, J. H. Collins, B. Nadal-Ginard, and L. R. Jones. 1988. Complete amino acid sequence of canine cardiac calsequestrin deduced by cDNA cloning. *J Biol Chem.* 263:8958-8964.
- Shirokova, N., and E. Rios. 1997. Small event  $\text{Ca}^{2+}$  release: a probable precursor of  $\text{Ca}^{2+}$  sparks in frog skeletal muscle. *J Physiol (Lond).* 502:3-11.

- Shirokova, N., and E. Rios. 1998. Local Calcium Release in Mammalian Skeletal Muscle. *Biophys J. (Abstracts)*. 74:A269.
- Simon, B. J., M. G. Klein, and M. F. Schneider. 1991. Calcium dependence of inactivation of calcium release from the sarcoplasmic reticulum in skeletal muscle fibers. *J Gen Physiol*. 97:437-471.
- Singer, D., M. Biel, I. Lotan, V. Flockerzi, F. Hofmann, and N. Dascal. 1991. The roles of the subunits in the function of the calcium channel. *Science*. 253:1553-1557.
- Slavik, K. J., J. P. Wang, B. Aghdasi, J. Z. Zhang, F. Mandel, N. Malouf, and S. L. Hamilton. 1997. A carboxy-terminal peptide of the alpha 1-subunit of the dihydropyridine receptor inhibits Ca(2+)-release channels. *Am J Physiol*. 272:C1475-1481.
- Smith, J. S., R. Coronado, and G. Meissner. 1986a. Single channel measurements of the calcium release channel from skeletal muscle sarcoplasmic reticulum. Activation by Ca<sup>2+</sup> and ATP and modulation by Mg<sup>2+</sup>. *J Gen Physiol*. 88:573-588.
- Smith, J. S., R. Coronado, and G. Meissner. 1986b. Single-channel calcium and barium currents of large and small conductance from sarcoplasmic reticulum. *Biophys J*. 50:921-928.
- Smith, J. S., T. Imagawa, J. Ma, M. Fill, K. P. Campbell, and R. Coronado. 1988. Purified ryanodine receptor from rabbit skeletal muscle is the calcium-release channel of sarcoplasmic reticulum. *J Gen Physiol*. 92:1-26.
- Smith, J. S., E. Rousseau, and G. Meissner. 1989. Calmodulin modulation of single sarcoplasmic reticulum Ca<sup>2+</sup>-release channels from cardiac and skeletal muscle. *Circ Res*. 64:352-359.

- Sonnleitner, A., A. Conti, F. Bertocchini, H. Schindler, and V. Sorrentino. 1998. Functional properties of the ryanodine receptor type 3 (RyR3)  $\text{Ca}^{2+}$  release channel. *Embo J.* 17:2790-2798.
- Sonnleitner, A., S. Fleischer, and H. Schindler. 1997. Gating of the skeletal calcium release channel by ATP is inhibited by protein phosphatase 1 but not by  $\text{Mg}^{2+}$ . *Cell Calcium.* 21:283-290.
- Sorrentino, V., and P. Volpe. 1993. Ryanodine receptors: how many, where and why? *Trends Pharmacol Sci.* 14:98-103.
- Standaert, R. F., A. Galat, G. L. Verdine, and S. L. Schreiber. 1990. Molecular cloning and overexpression of the human FK506-binding protein FKBP. *Nature.* 346:671-674.
- Strand, M. A., C. F. Louis, and J. R. Mickelson. 1993. Phosphorylation of the porcine skeletal and cardiac muscle sarcoplasmic reticulum ryanodine receptor. *Biochim Biophys Acta.* 1175:319-326.
- Stuhmer, W., F. Conti, H. Suzuki, X. D. Wang, M. Noda, N. Yahagi, H. Kubo, and S. Numa. 1989. Structural parts involved in activation and inactivation of the sodium channel. *Nature.* 339:597-603.
- Suda, N. 1995. Involvement of dihydropyridine receptors in terminating  $\text{Ca}^{2+}$  release in rat skeletal myotubes. *J Physiol (Lond).* 486:105-112.
- Suda, N., and C. Heinemann. 1996. RISC (Repolarization-induced stop of caffeine-contraction) is not due to store depletion in cultured murine skeletal muscle. *Pflugers Arch.* 432:948-951.
- Suda, N., and R. Penner. 1994. Membrane repolarization stops caffeine-induced  $\text{Ca}^{2+}$  release in skeletal muscle cells. *Proc Natl Acad Sci U S A.* 91:5725-5729.
- Suko, J., I. Maurer-Fogy, B. Plank, O. Bertel, W. Wyskovsky, M. Hohenegger, and G. Hellmann. 1993. Phosphorylation of serine 2843 in ryanodine

- receptor-calcium release channel of skeletal muscle by cAMP-, cGMP- and CaM-dependent protein kinase. *Biochim Biophys Acta*. 1175:193-206.
- Sun, X. H., F. Protasi, M. Takahashi, H. Takeshima, D. G. Ferguson, and C. Franzini-Armstrong. 1995. Molecular architecture of membranes involved in excitation-contraction coupling of cardiac muscle. *J Cell Biol*. 129:659-671.
- Takasawa, S., A. Ishida, K. Nata, K. Nakagawa, N. Noguchi, A. Tohgo, I. Kato, H. Yonekura, H. Fujisawa, and H. Okamoto. 1995. Requirement of calmodulin-dependent protein kinase II in cyclic ADP- ribose-mediated intracellular Ca<sup>2+</sup> mobilization. *J Biol Chem*. 270:30257-30259.
- Takekura, H., L. Bennett, T. Tanabe, K. G. Beam, and C. Franzini-Armstrong. 1994. Restoration of junctional tetrads in dysgenic myotubes by dihydropyridine receptor cDNA. *Biophys J*. 67:793-803.
- Takekura, H., M. Nishi, T. Noda, H. Takeshima, and C. Franzini-Armstrong. 1995a. Abnormal junctions between surface membrane and sarcoplasmic reticulum in skeletal muscle with a mutation targeted to the ryanodine receptor. *Proc Natl Acad Sci U S A*. 92:3381-3385.
- Takekura, H., H. Takeshima, S. Nishimura, M. Takahashi, T. Tanabe, V. Flockerzi, F. Hofmann, and C. Franzini-Armstrong. 1995b. Co-expression in CHO cells of two muscle proteins involved in excitation-contraction coupling. *J Muscle Res Cell Motil*. 16:465-480.
- Takeshima, H., M. Iino, H. Takekura, M. Nishi, J. Kuno, O. Minowa, H. Takano, and T. Noda. 1994. Excitation-contraction uncoupling and muscular degeneration in mice lacking functional skeletal muscle ryanodine-receptor gene. *Nature*. 369:556-559.

- Takeshima, H., T. Ikemoto, M. Nishi, N. Nishiyama, M. Shimuta, Y. Sugitani, J. Kuno, I. Saito, H. Saito, M. Endo, M. Iino, and T. Noda. 1996. Generation and characterization of mutant mice lacking ryanodine receptor type 3. *J Biol Chem.* 271:19649-19652.
- Takeshima, H., S. Nishimura, T. Matsumoto, H. Ishida, K. Kangawa, N. Minamino, H. Matsuo, M. Ueda, M. Hanaoka, T. Hirose, and et al. 1989. Primary structure and expression from complementary DNA of skeletal muscle ryanodine receptor. *Nature.* 339:439-445.
- Takeshima, H., S. Nishimura, M. Nishi, M. Ikeda, and T. Sugimoto. 1993. A brain-specific transcript from the 3'-terminal region of the skeletal muscle ryanodine receptor gene. *FEBS Lett.* 322:105-110.
- Takeshima, H., T. Yamazawa, T. Ikemoto, H. Takekura, M. Nishi, T. Noda, and M. Iino. 1995. Ca(2+)-induced Ca<sup>2+</sup> release in myocytes from dyspedic mice lacking the type-1 ryanodine receptor. *Embo J.* 14:2999-3006.
- Tanabe, T., K. G. Beam, B. A. Adams, T. Niidome, and S. Numa. 1990a. Regions of the skeletal muscle dihydropyridine receptor critical for excitation-contraction coupling. *Nature.* 346:567-569.
- Tanabe, T., K. G. Beam, J. A. Powell, and S. Numa. 1988. Restoration of excitation-contraction coupling and slow calcium current in dysgenic muscle by dihydropyridine receptor complementary DNA. *Nature.* 336:134-139.
- Tanabe, T., A. Mikami, S. Numa, and K. G. Beam. 1990b. Cardiac-type excitation-contraction coupling in dysgenic skeletal muscle injected with cardiac dihydropyridine receptor cDNA. *Nature.* 344:451-453.
- Tanaka, Y., and A. H. Tashjian, Jr. 1995. Calmodulin is a selective mediator of Ca(2+)-induced Ca<sup>2+</sup> release via the ryanodine receptor-like Ca<sup>2+</sup>



channel triggered by cyclic ADP-ribose. *Proc Natl Acad Sci U S A*. 92:3244-3248.

- Timerman, A. P., E. Ogunbumni, E. Freund, G. Wiederrecht, A. R. Marks, and S. Fleischer. 1993. The calcium release channel of sarcoplasmic reticulum is modulated by FK-506-binding protein. Dissociation and reconstitution of FKBP-12 to the calcium release channel of skeletal muscle sarcoplasmic reticulum. *J Biol Chem*. 268:22992-22999.
- Tong, J., and D. MacLennan, H. 1998. *submitted*.
- Tong, J., H. Oyamada, N. Demarex, S. Grinstein, T. V. McCarthy, and D. H. MacLennan. 1997. Caffeine and halothane sensitivity of intracellular  $\text{Ca}^{2+}$  release is altered by 15 calcium release channel (ryanodine receptor) mutations associated with malignant hyperthermia and/or central core disease. *J Biol Chem*. 272:26332-26339.
- Toyofuku, T., K. Kurzydowski, M. Tada, and D. H. MacLennan. 1994. Amino acids Glu2 to Ile18 in the cytoplasmic domain of phospholamban are essential for functional association with the  $\text{Ca}^{2+}$ -ATPase of sarcoplasmic reticulum. *J Biol Chem*. 269:3088-3094.
- Treves, S., P. Chiozzi, and F. Zorzato. 1993. Identification of the domain recognized by anti-(ryanodine receptor) antibodies which affect  $\text{Ca}^{2+}$ -induced  $\text{Ca}^{2+}$  release. *Biochem J*. 291:757-763.
- Treves, S., F. Larini, P. Menegazzi, T. H. Steinberg, M. Koval, B. Vilsen, J. P. Andersen, and F. Zorzato. 1994. Alteration of intracellular  $\text{Ca}^{2+}$  transients in COS-7 cells transfected with the cDNA encoding skeletal-muscle ryanodine receptor carrying a mutation associated with malignant hyperthermia. *Biochem J*. 301:661-665.

- Trimm, J. L., G. Salama, and J. J. Abramson. 1986. Sulfhydryl oxidation induces rapid calcium release from sarcoplasmic reticulum vesicles. *J Biol Chem.* 261:16092-16098.
- Trimmer, J. S., S. S. Cooperman, S. A. Tomiko, J. Y. Zhou, S. M. Crean, M. B. Boyle, R. G. Kallen, Z. H. Sheng, R. L. Barchi, F. J. Sigworth, and et al. 1989. Primary structure and functional expression of a mammalian skeletal muscle sodium channel. *Neuron.* 3:33-49.
- Tripathy, A., L. Xu, G. Mann, and G. Meissner. 1995. Calmodulin activation and inhibition of skeletal muscle  $\text{Ca}^{2+}$  release channel (ryanodine receptor). *Biophys J.* 69:106-119.
- Tunwell, R. E., C. Wickenden, B. M. Bertrand, V. I. Shevchenko, M. B. Walsh, P. D. Allen, and F. A. Lai. 1996. The human cardiac muscle ryanodine receptor-calcium release channel: identification, primary structure and topological analysis. *Biochem J.* 318:477-487.
- Ukomadu, C., J. Zhou, F. J. Sigworth, and W. S. Agnew. 1992.  $\mu\text{I Na}^{+}$  channels expressed transiently in human embryonic kidney cells: biochemical and biophysical properties. *Neuron.* 8:663-676.
- Walker, J., P. Crowley, A. D. Moreman, and J. Barrett. 1993. Biochemical properties of cloned glutathione S-transferases from *Schistosoma mansoni* and *Schistosoma japonicum*. *Mol Biochem Parasitol.* 61:255-264.
- Wang, J., and P. M. Best. 1992. Inactivation of the sarcoplasmic reticulum calcium channel by protein kinase. *Nature.* 359:739-741.
- Wang, S., W. R. Trumble, H. Liao, C. R. Wesson, A. K. Dunker, and C. H. Kang. 1998. Crystal structure of calsequestrin from rabbit skeletal muscle sarcoplasmic reticulum [see comments]. *Nat Struct Biol.* 5:476-483.

- Weber, A., and R. Herz. 1968. The relationship between caffeine contracture of intact muscle and the effect of caffeine on reticulum. *J Gen Physiol.* 52:750-759.
- Wei, X., A. Neely, A. E. Lacerda, R. Olcese, E. Stefani, E. Perez-Reyes, and L. Birnbaumer. 1994. Modification of Ca<sup>2+</sup> channel activity by deletions at the carboxyl terminus of the cardiac alpha 1 subunit. *J Biol Chem.* 269:1635-1640.
- Wei, X. Y., E. Perez-Reyes, A. E. Lacerda, G. Schuster, A. M. Brown, and L. Birnbaumer. 1991. Heterologous regulation of the cardiac Ca<sup>2+</sup> channel alpha 1 subunit by skeletal muscle beta and gamma subunits. Implications for the structure of cardiac L-type Ca<sup>2+</sup> channels. *J Biol Chem.* 266:21943-21947.
- Witcher, D. R., R. J. Kovacs, H. Schulman, D. C. Cefali, and L. R. Jones. 1991. Unique phosphorylation site on the cardiac ryanodine receptor regulates calcium channel activity. *J Biol Chem.* 266:11144-11152.
- Witcher, D. R., P. S. McPherson, S. D. Kahl, T. Lewis, P. Bentley, M. J. Mullinnix, J. D. Windass, and K. P. Campbell. 1994. Photoaffinity labeling of the ryanodine receptor/Ca<sup>2+</sup> release channel with an azido derivative of ryanodine. *J Biol Chem.* 269:13076-13079.
- Wu, Y., B. Aghdasi, S. J. Dou, J. Z. Zhang, S. Q. Liu, and S. L. Hamilton. 1997. Functional interactions between cytoplasmic domains of the skeletal muscle Ca<sup>2+</sup> release channel. *J Biol Chem.* 272:25051-25061.
- Xu, L., J. P. Eu, G. Meissner, and J. S. Stamler. 1998. Activation of the cardiac calcium release channel (ryanodine receptor) by poly-S-nitrosylation. *Science.* 279:234-237.
- Yamaguchi, N., and M. Kasai. 1997. Potentiation of depolarization-induced calcium release from skeletal muscle triads by cyclic ADP-ribose and

- inositol 1,4,5-trisphosphate. *Biochem Biophys Res Commun.* 240:772-777.
- Yamazawa, T., H. Takeshima, T. Sakurai, M. Endo, and M. Iino. 1996. Subtype specificity of the ryanodine receptor for  $\text{Ca}^{2+}$  signal amplification in excitation-contraction coupling. *Embo J.* 15:6172-6177.
- Yamazawa, T., H. Takeshima, M. Shimuta, and M. Iino. 1997. A region of the ryanodine receptor critical for excitation-contraction coupling in skeletal muscle. *J Biol Chem.* 272:8161-8164.
- Yano, K., and A. Zarain-Herzberg. 1994. Sarcoplasmic reticulum calsequestrins: structural and functional properties. *Mol Cell Biochem.* 135:61-70.
- Yano, M., R. el-Hayek, and N. Ikemoto. 1995. Conformational changes in the junctional foot protein/ $\text{Ca}^{2+}$  release channel mediate depolarization-induced  $\text{Ca}^{2+}$  release from sarcoplasmic reticulum. *J Biol Chem.* 270:3017-3021.
- Zable, A. C., T. G. Favero, and J. J. Abramson. 1997. Glutathione modulates ryanodine receptor from skeletal muscle sarcoplasmic reticulum. Evidence for redox regulation of the  $\text{Ca}^{2+}$  release mechanism. *J Biol Chem.* 272:7069-7077.
- Zaidi, N. F., C. F. Lagenaur, J. J. Abramson, I. Pessah, and G. Salama. 1989. Reactive disulfides trigger  $\text{Ca}^{2+}$  release from sarcoplasmic reticulum via an oxidation reaction. *J Biol Chem.* 264:21725-21736.
- Zarka, A., and V. Shoshan-Barmatz. 1992. The interaction of spermine with the ryanodine receptor from skeletal muscle. *Biochim Biophys Acta.* 1108:13-20.

- Zarka, A., and V. Shoshan-Barmatz. 1993. Characterization and photoaffinity labeling of the ATP binding site of the ryanodine receptor from skeletal muscle. *Eur J Biochem.* 213:147-154.
- Zhang, J. F., P. T. Ellinor, R. W. Aldrich, and R. W. Tsien. 1994. Molecular determinants of voltage-dependent inactivation in calcium channels. *Nature.* 372:97-100.
- Zhang, L., J. Kelley, G. Schmeisser, Y. M. Kobayashi, and L. R. Jones. 1997. Complex formation between junctin, triadin, calsequestrin, and the ryanodine receptor. Proteins of the cardiac junctional sarcoplasmic reticulum membrane. *J Biol Chem.* 272:23389-23397.
- Zhang, Y., H. S. Chen, V. K. Khanna, S. De Leon, M. S. Phillips, K. Schappert, B. A. Britt, A. K. Browell, and D. H. MacLennan. 1993. A mutation in the human ryanodine receptor gene associated with central core disease. *Nat Genet.* 5:46-50.
- Zorzato, F., J. Fujii, K. Otsu, M. Phillips, N. M. Green, F. A. Lai, G. Meissner, and D. H. MacLennan. 1990. Molecular cloning of cDNA encoding human and rabbit forms of the Ca<sup>2+</sup> release channel (ryanodine receptor) of skeletal muscle sarcoplasmic reticulum. *J Biol Chem.* 265:2244-2256.
- Zot, A. S., and J. D. Potter. 1987. Structural aspects of troponin-tropomyosin regulation of skeletal muscle contraction. *Annu Rev Biophys Biophys Chem.* 16:535-559.